Universidad Miguel Hernández de Elche

ACTIVITY-DEPENDENT REFINEMENT OF THE DEVELOPING VISUAL SYSTEM. A COMPARATIVE STUDY ACROSS RETINAL GANGLION CELL POPULATIONS AND TARGET NUCLEI

Doctoral Thesis presented by

Santiago Negueruela Lázaro

- 2020 -

Thesis Director: Eloísa Herrera González de Molina

Co-director: Mª Cruz Morenilla Palao

PhD Program in Neuroscience

Instituto de Neurociencias – UMH-CSIC

La tesis doctoral titulada “Activity-dependent refinement of the developing visual system. A comparative study across retinal ganglion cell populations and target nuclei” realizada por mí, Santiago Negueruela Lázaro, se presenta en formato convencional incluyendo como indicio de calidad el siguiente trabajo previamente publicado:

Murcia-Belmonte V, Coca Y, Vegar C, ***Negueruela S***, de Juan Romero C, Valiño AJ, Sala S, DaSilva R, Kania A, Borrell V, Martinez LM, Erskine L, Herrera E. Current Biology. **A Retino-retinal Projection Guided by Unc5c Emerged in Species with Retinal Waves. Current Biology**, 2019. doi: 10.1016/j.cub.2019.02.052.

INSTITUTO DE NEUROCIENCIAS

1999 - 2019 AN 20

INSTITUTO DE NEUROCIENCIAS

EXCELENCIA SEVERO OCHOA

Sant Joan d'Alacant, 15 de julio de 2020,

Dña Eloísa Herrera González de Molina, Investigadora Científica del Consejo Superior de Investigaciones Científicas, Directora de esta Tesis Doctoral y Dña Cruz Morenilla-Palao, profesora asociada de la Universidad Miguel Hernández.

AUTORIZAMOS la presentación de la Tesis Doctoral titulada "Activity-dependent refinement of the developing the visual system. A comparative study across retinal ganglion cell populations and target nuclei" y realizada por D. Santiago Negueruela Lázaro, bajo nuestra inmediata dirección y supervisión en el Instituto de Neurociencias (UMH-CSIC) y que presenta para la obtención del grado de Doctor por la Universidad Miguel Hernández.

Y para que conste, a los efectos oportunos, firmamos el presente certificado.

Firmado por ELOISA HERRERA GONZALEZ DE MOLINA - NIF:24252485C el día 16/07/2020 con un certificado emitido por ACCVCA-120

Firmado por MARIA CRUZ MORENILLA PALAO - NIF:48318772G el día 16/07/2020 con un certificado emitido por ACCVCA-120

Dr. Eloísa Herrera González de Molina

Dr. Cruz Morenilla-Palao

Sant Joan d'Alacant, 15 de Julio de 2020,

Miguel Valdeolmillos López, Catedrático y Coordinador del programa de doctorado en Neurociencias del Instituto de Neurociencias de Alicante, centro mixto de la Universidad Miguel Hernández (UMH) y de la Agencia Estatal Consejo Superior de Investigaciones Científicas (CSIC)

CERTIFICO:

Que la Tesis Doctoral titulada "Activity-dependent refinement of the developing the visual system. A comparative study across retinal ganglion cell populations and target nuclei" has sido realizada por D. Santiago Negueruela Lázaro, bajo la dirección de Dr. Eloísa Herrera González de Molina como directora y Dr. Cruz Morenilla-Palao como co-directora, y doy mi conformidad para que sea presentada a la Comisión de Doctorado de la Universidad Miguel Hernández.

Y para que conste, a los efectos oportunos, firmo el presente certificado.

MIGUEL ANGEL| VALDEOLMILLOS|LOPEZ

Firmado digitalmente por MIGUEL ANGEL| VALDEOLMILLOS| LOPEZ
Fecha: 2020.07.16 08:52:42 +02'00'

Dr. Miguel Valdeolmillos López

miguel.valdeolmillos@umh.es

Tel: +34 965 919540

Fax: +34 965 919549

Av Ramón y Cajal s/n, Campus de Sant Joan, 03550 Sant Joan D'Alacant, España

FINANCIACIÓN / SUBVENCIÓN / BECA

European Research Council Starting Grants

Programa Prometeo-Generalitat Valenciana

INDEX

List of abbreviations

AVP: arginine vasopressin

CTB-Alx: Cholera toxin subunit B fused to Alexa fluorophore

DDCSs: Dendro-dendritic chemical synapses

dLGN: dorsal lateral geniculate nucleus of the thalamus

DSGCs: bistratified On-Off direction-selective RGCs

GRP: gastrin-releasing peptide

IGL: intergeniculate leaflet

ipRGCs: intrinsically photosensible retinal ganglion cells

NOT: nucleus of the optic tract

OPN: olivary pretectal nucleus

OPN4: melanopsin photopigment

PN: pretectal nucleus

RGCs: retinal ganglion cells

SACs: starburst amacrine cells

SBEM: block-face scanning electron microscopy

SC: superior colliculus

SCN: suprachiasmatic nucleus

SGS: stratum griseum superficialis

SO: stratum opticum

SRIF: Somatotropin release–inhibiting factor

TTFL: transcription-translation feedback loop

TZ: terminal zone

V1: primary visual cortex

VIP: Vasoactive intestinal peptide

VMH: ventral medial hypothalamus

β2(TG) mice: expression of β2 subunit is restricted to RGCs

$\beta2^{-/-}$ mice: mice lacking the nicotinic acetylcholine receptor subunit β2

RESUMEN

La formación del sistema visual de mamíferos es un complejo proceso que tiene lugar en varias fases e incluye neurogénesis, guía axonal, refinamiento axonal y ensamblaje del circuito. La última etapa ocurre después del nacimiento y antes de la apertura del ojo. Durante este período, los terminales axónicos de las células ganglionares de la retina (CGRs) arborizan primero de forma extensa en los diferentes núcleos visuales para a continuación refinar y establecer las conexiones adecuadas. Se sabe que la actividad espontánea generada en la retina inmadura durante las edades perinatales desempeña un papel importante en este proceso de refinamiento axonal, pero no está claro en qué medida dicha actividad retinal influye de manera diferencial en el refinamiento de las distintas poblaciones de CGRs cuando proyectan a núcleos visuales específicos. Para abordar este tema hemos generado líneas condicionales de ratón para alterar la actividad espontánea en diferentes poblaciones de CGRs y hemos analizado los patrones de proyección de las CRGs en los diferentes núcleos visuales en cada una de estas líneas de ratones. Nuestros resultados muestran que la alteración de la actividad espontánea en las CGRs afecta el refinamiento de sus axones en los núcleos formadores de imagen como son el núcleo geniculado lateral y el colículo superior, apoyando publicaciones previas. Pero además hemos observado que, aunque en menor medida que en los núcleos formadores de imagen, la correlación de la actividad espontánea en la retina es también importante para el refinamiento de los terminales de las CGRs en los núcleos no formadores de imagen como el núcleo olivar pretectal o el núcleo supraquiasmático.

ABSTRACT

The formation of the mammalian visual system is a complex process that takes place in several phases and includes neurogenesis, axon guidance, axonal refinement and circuit assembly. The last stage of this process occurs after birth but before eye opening. During this period, axon terminals from retinal ganglion cells (RGCs) first extensively arborize in the different visual nuclei and then refine and establish appropriate connections. It is known that the spontaneous activity generated in the immature retina during perinatal ages plays an important role in this axonal refinement process but it is not clear to what extent such retinal activity differentially influences the refinement of the distinct populations of RGCs when they project to specific visual nuclei. To address this issue we have generated conditional mouse lines to alter spontaneous activity in different populations of RGCs and we have analyzed the projection patterns of RGCs in different visual nuclei in each of these mouse lines. Our results show that the alteration of spontaneous activity in RGCs affects axon refinement in the image-forming nuclei such as the lateral geniculate nucleus and the superior colliculus, supporting previous publications. Interestingly, we also observed that, although to a lesser extent than in the image-forming nuclei, retinal spontaneous activity correlation is important for the refinement of RGC axons in the non-image-forming nuclei such as the pretectal olive nucleus or the suprachiasmatic nucleus.

1- INTRODUCTION

1.1 GENERAL ANATOMY OF THE VISUAL SYSTEM

Light coming from the outside word is received by 125 millions of photoreceptors in the retina. These photoreceptors, called rods and cones, are specialized in the transmission of electrical signals that are filtered by the three classes of retinal interneurons; horizontal, bipolar and amacrine cells that transmit visual information to retinal ganglion cells (RGCs). Each RGC receives input from many bipolar cells which are fed by a similar number of photoreceptors (Huberman and Niell 2011) (Figure 1.1-A). RGCs are the only retinal cell type that extends axons out of the retina to transmit sensory information to different visual nuclei in the brain. In mammals RGC axons exit the eye through the optic disc. Then, they travel along the base of the ventral diencephalon toward the midline where axons form the optic chiasm. There, a portion of RGC axons cross the midline to project to the contralateral targets in the brain while another population of axons grows away from the midline to project to the visual targets in the ipsilateral side (Figure 1.1-B).

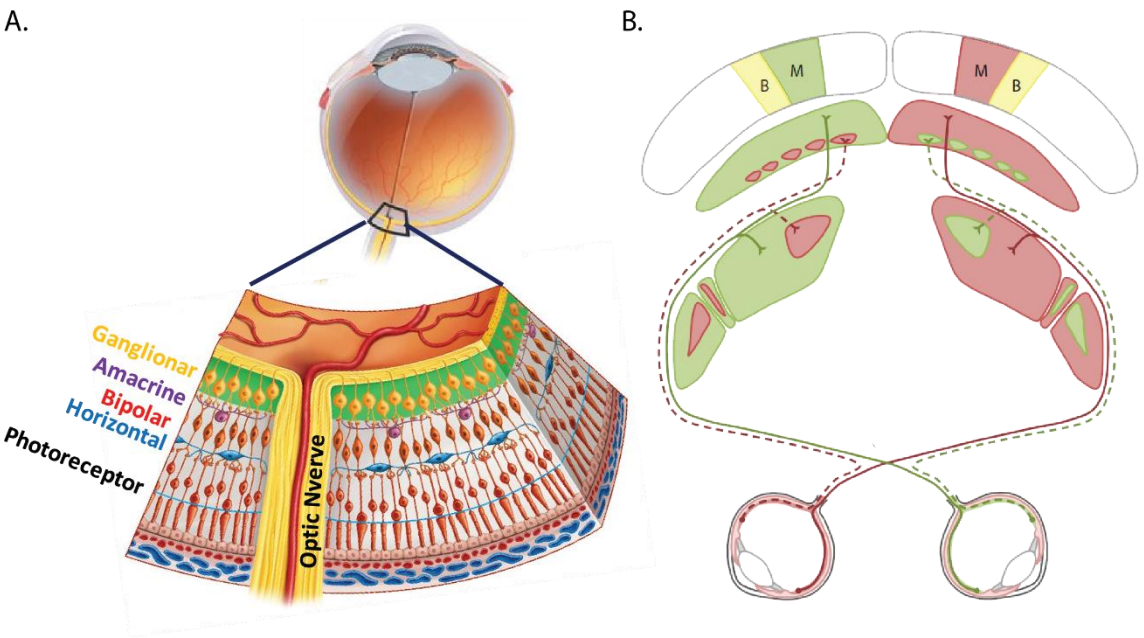

Figure 1.1: Anatomy of the visual system. (A) Scheme showing the cell types, layers and connectivity of the retina. **(B)** Bilateral innervation in the visual circuit. Adapted from *Kenhub.com* (A); Seabrook et al., 2017 (B).

The spatial relationship among RGCs in the retina is maintained at the visual targets as a topographic representation of visual space. This retinotopic representation is imprecise at the beginning but undergoes a refinement process as the system matures. By the time of eye opening, a functional circuit has emerged, though it may be further modulated by visual experience in the following few weeks during a time called critical period (Hooks and Chen 2007). Second-relay thalamic axons growing into the subcortical telencephalon during embryonic development reach the visual cortex and they will assemble with the first segment of the pathway to receive and integrate sensory information from both eyes.

1.2 COMPLEXITY OF THE VISUAL CIRCUIT: LARGE DIVERSITY OF RGC SUBTYPES AND VISUAL TARGETS

RGCs are far from being a homogeneous cell type. Depending on their localization, morphology and function, at least 30 different subtypes of RGCs may be found (Masland 2012; Sanes and Masland 2015). This number can be raised to 40 based on their electrophysiological properties (Baden et al. 2016) (Figure 1.2-C). Each subtype is characterized by a different dendritic arborization in the internal plexiform layer of the retina (Figure 1.2-B) and projects to specific regions and/or layers in their corresponding retinorecipient targets (Figure 1.2-D). Furthermore, each type is related to different visual functions. Recently, single cell RNA-seq approaches have revealed many combinations of transcription factors leading to the differentiation of each RGC subtype (Rheaume et al. 2018). On the other hand, there are more than 40 distinct retinal targets in the brain (Figure 1.2-A), each of them mediating a different set of functions (Morin and Studholme 2014). Such complexity derives from the existence of regulatory mechanisms that precisely connect each population of RGCs with its corresponding nuclei in the brain.

According to their function, there are two main visual pathways. The image-forming pathway, dedicated to transmit images perceived by each eye into the brain, and the non-image forming pathway, that is important to respond to the environmental light.

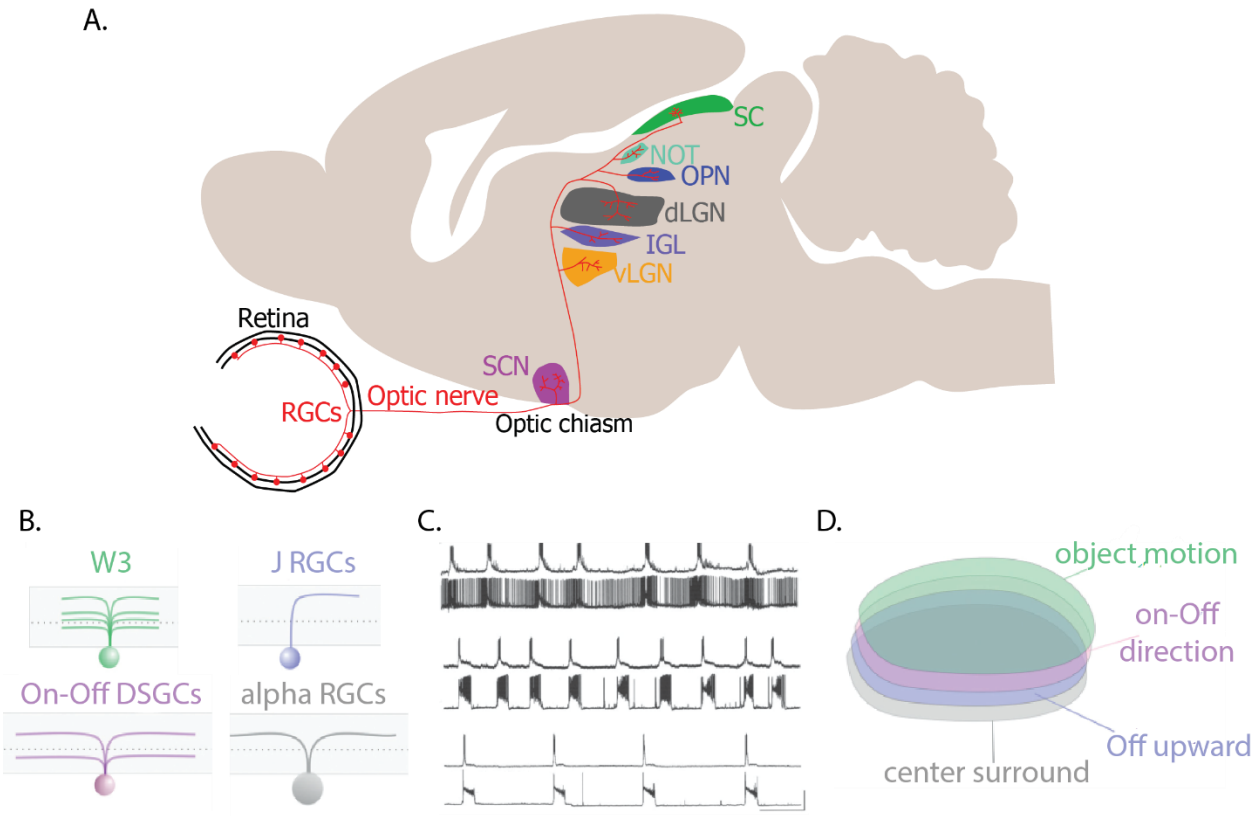

Figure 1.2: The visual system is a complex network that contains a huge diversity of retinorecipient targets (A) and RGC types (B). Adapted from Dhande and Huberman 2014 (B,D); Liets et al., 2003 (C).

1.3 IMAGE-FORMING VISUAL NUCLEI

Image-forming circuits give rise directly to sight. Their main nuclei are the dorsal lateral geniculate nucleus of the thalamus (dLGN) and the superior colliculus (SC). They receive direct retinal input and form a highly interconnected circuit where each nucleus cannot be thought as an independent entity in charge of specific functions. Both of them relay information to the primary visual cortex (V1), which in turn establishes feedback connections. In mice approximately 90% of the RGCs project to the SC (Ellis et al. 2016), a percentage that decreases to 10% in primates (Perry and Cowey 1984). The dLGN receives

input from 30-40% of the RGCs (Martin 1986) and this whole subset of RGCs send collaterals also to the SC (Ellis et al. 2016; Huberman, Manu, et al. 2008). Retinal and cortical innervation of the dLGN is coordinated. It has been recently demonstrated that during development, retinal axons control the entry of cortical projections into the dLGN through the regulation of the repulsive cue aggrecan in the target (Brooks et al. 2013; Seabrook et al. 2013). In addition, mice without visual cortex do not exhibit retinogeniculate projections (Shanks et al. 2016).

The main task of the SC is to direct visually-guided behaviors (Stryker and Schiller 1975). The SC is referred as tectum in non-mammalian vertebrates such as birds, fish and frogs, and is the primary center for visual processing in these species. In mice the SC performs part of the image processing that is carried out by the visual cortex in cats and primates (Prusky and Douglas 2004). The dLGN processes and relays visual information to the cortex for a deeper conscious visual perception. Different subtypes of RGCs project to the dLGN and SC into discrete laminar zones (Dhande and Huberman 2014; Huberman et al. 2009; Huberman, Feller, and Chapman 2008; Kay et al. 2011; Kim et al. 2010; Rivlin-Etzion et al. 2011), and this organization is reproduced in a layer-specific connectivity in the cortex (Bickford et al. 2015; Cruz-Martín et al. 2014).

Retinotopic mapping and eye specificity are the two most widely studied spatial maps in the visual system. But, in addition to spatial location, the circuit needs to represent and process other aspects of the visual stimulus such as orientation, direction and color. This happens possibly thanks to the multitude of RGC subtypes that innervate these image-forming nuclei giving rise to different layers, maps and wiring patterns (Hong, Kim, and Sanes 2011; Kay et al. 2011; Kim et al. 2008, 2010).

1.3.1 Retinotopic maps

To receive and process visual-spatial information, image-forming nuclei contain a topographic representation of the retina known as retinotopic map. RGCs project to the targets according to their

distribution over the retina and the strength of postsynaptic response (axonal convergence). Although RGCs also project to the LGN in a topographic manner, the superior colliculus is the most commonly studied model used to understand the molecular and physiological basis of topographic mapformation. The temporo-nasal (T-N) and dorsal-ventral (D-V) axes of the retina correspond to the antero-posterior (A-P) and lateral-medial (L-M) axes in the SC respectively (Figure 1.3-A) (Triplett 2014).

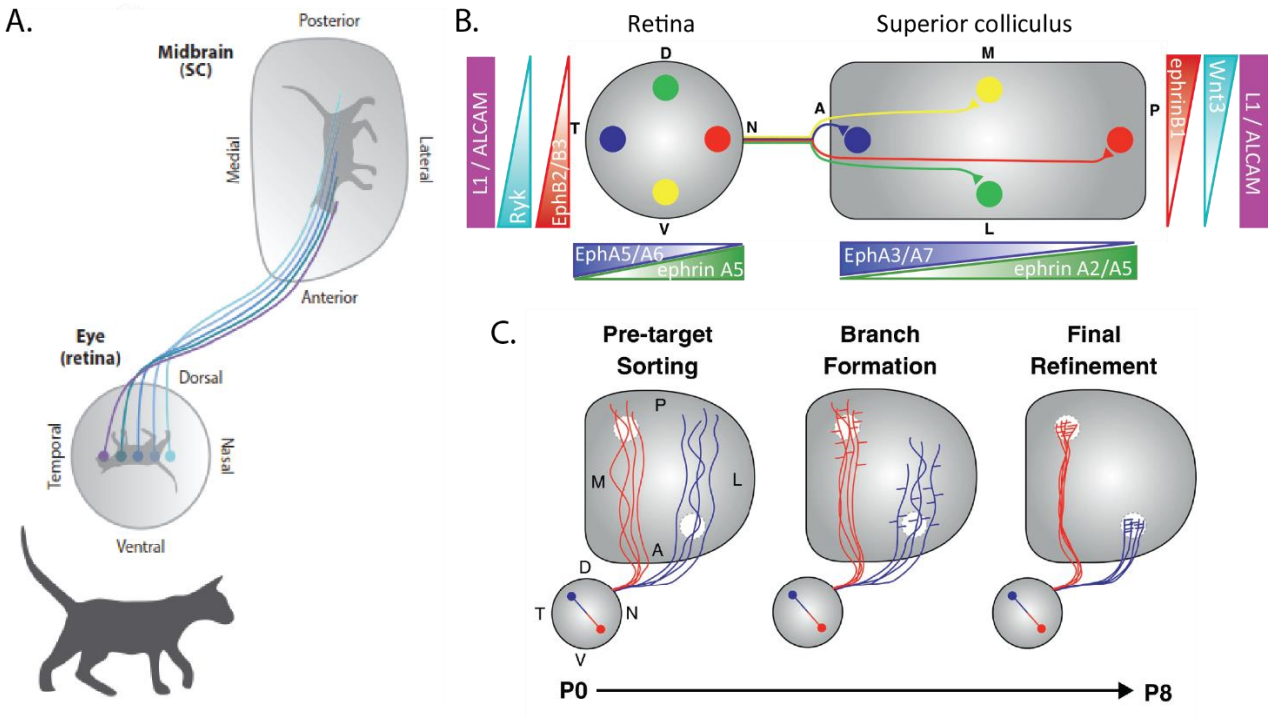

Figure 1.3: Retionotopic maps at the SC. The spatial distribution displayed in the retina is reproduced in the retinorecipient targets. **(A)** Visual information is received in the retina, which is transmitted it to the image-forming visual targets coding the spatial pattern. **(B)** Gradients of guidance cues expressed in both retina and targets govern the formation of a rough retinotopic map. **(C)** During development each axon is directed to its corresponding target zone through branching and pruning. Adapted from Seabrook et al., 2017 (A) and Triplett et al., 2014 (B-C).

When retinocollicular projections reach the SC they first overshoot the zone where they will finally project (terminal zone, TZ), extending to the posterior part of the SC. During the first postnatal week, a precise system of opposing gradients of guidance and adhesion cues defines the target zone for each RGC axon (Figure 1.3-C). Each of these axes is mapped independently (Triplett et al. 2009), using unique molecular strategies to establish topography during the first postnatal week. The main families of guidance molecules driving the formation of the topographic maps are Eph receptors and their ligands

the ephrins. Based on sequence homology and binding affinity there are two main types of Eph receptors (A and B) and two types of ephrin ligands (A and B) (Gale et al. 1996). In general, ephrin-A proteins bind to EphA receptors, while ephrin-Bs bind to EphB receptors, although there are some exceptions to this rule.

RGCs express EphA5 and EphA6 in a high temporal to low nasal gradient (T > N), which interact with a gradient of ephrin-A5 in the SC in order to map along the A-P axis (Carreres et al. 2011; Frisén et al. 1998) (Figure 1.3-B). On the other hand, pre-target sorting and EphB's/ephrinB's interaction with several adhesion molecules define the mapping along the medial-lateral axis (Seabrook et al. 2017; Triplett and Feldheim 2012). EphB1 and EphB2 display a high ventral to low dorsal gradient in the retina while they are more expressed in the medial SC (Hindges et al. 2002; McLaughlin et al. 2014). Apart from the Eph/ephrin family, other molecules also influence retinotopic mapping. For instance, it has been proposed that the secreted molecule Wnt3, expressed in a high medial to low lateral gradient together with one of their receptors, Ryk, expressed in a high ventral to low dorsal gradient on the retina, modulates the directional growing of interstitial branches (Schmitt et al. 2006). The adhesion molecule L1 is expressed in both the retina and SC and, after interaction with EphBs, promotes ALCAM-dependent binding to Ankyrin and regulates branch extension (Buhusi et al. 2009; Dai et al. 2012).

These gradients promote the formation of interstitial branches in the target zone as well as the retraction of the primary axon. BDNF secreted in the SC upregulates the miRNA-132 microRNA in RGC axons to inhibit the GTPase-activating protein p250GAP promoting Rac-mediated branch formation (Marler et al. 2014). This mechanism is antagonized by the interaction of ephrin-As with the BDNF p75 receptor (Lim et al. 2008).

The dLGN also develops a topographic map using similar mechanisms, but following its cytoarchitectonic peculiarities. Gross retinotopic mapping occurs in the early postnatal period (P0-P10, in mouse), when guidance cues such as ephrin-As are present in the nuclei (Huberman et al. 2005), but

later, a further process that refines the projections while strengthening the synapses with the final target cells will give rise to a perfectly functional circuit at the moment of eye opening. This later acting mechanism that refines axon terminals in a fine-tune manner depends on correlated spontaneous neural activity in the retina that is known as “retinal waves”.

1.3.2 Eye-specific segregation

In carnivores and primates, the cell bodies of ipsilateral or contralateral RGCs locate in decussated portions of the retina. In mouse, however, the ipsilateral RGCs (approximately 5%) are scattered throughout the ventrotemporal region and intermingle with contralateral cells (Dräger and Olsen 1980; Herrera et al. 2003; Koch et al. 2011; Petros, Rebsam, and Mason 2008) (Figure 1.4-A). Ipsilateral and contralateral RGCs project to the corresponding areas in the targets according to their topographic location in the retina. As described before, at early postnatal stages the immature axonal arbors overlap and need to be segregated originating eye specific domains (Muscat et al. 2003) (Figure 1.4-C). Retinotopic mapping is mostly governed by guidance and adhesion molecules, but eye-specific segregation rather depends on correlated patterns of retinal spontaneous activity.

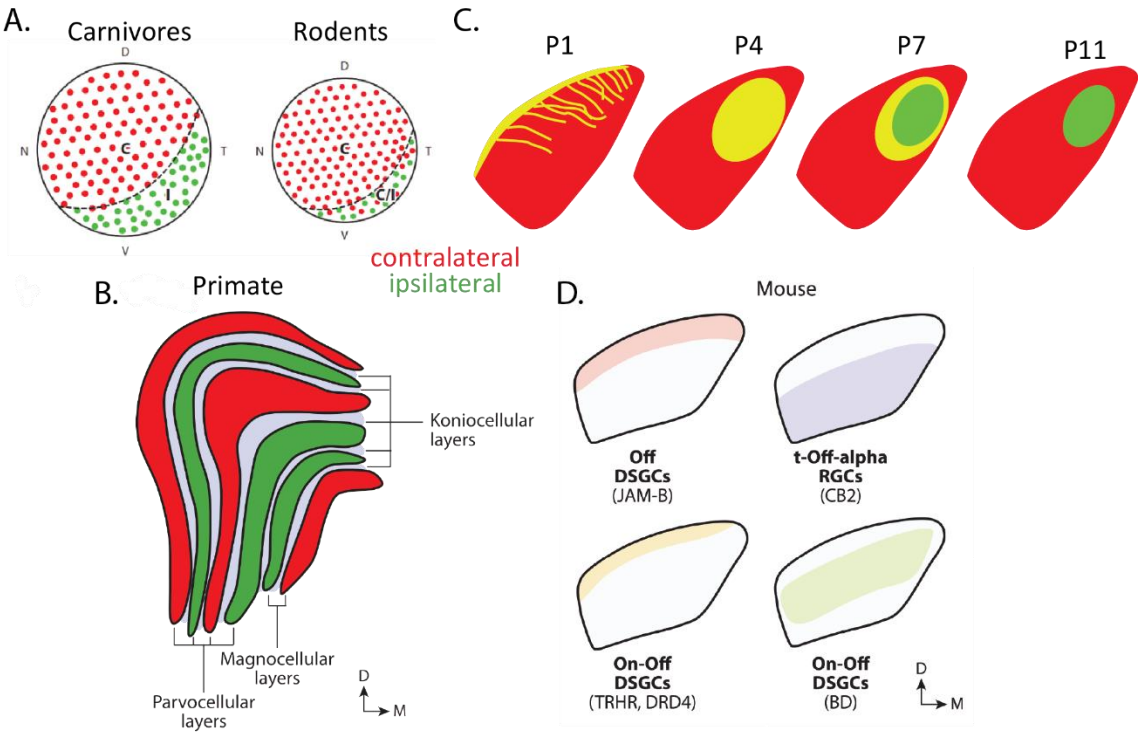

Figure 1.4: Contralateral and ipsilateral retinal projections. (A) Distribution of ipsilateral and contralateral RGCs over the retina. **(B)** The dLGN in primates is organized in eye-specific layers. **(C)** Ipsilateral and contralateral projections to the mouse dLGN during development. **(D)** Functional domains in mouse dLGN. Adapted from Seabrook et al., 2017 (A,C,D).

In the dLGN of carnivores and primates, eye specific territories are found in layers anatomically separated by an interlaminar space (Guillery 1971; Hutchins and Casagrande 1990) (Figure 1.4-B). However, mice and rats do not show such cytoarchitectonic distinction in the LGN. In these species there are functionally distinct layers that relate to the termination patterns of the different RGC subtypes (Martin 1986; Reese n.d.). For instance, alpha-like RGCs connect to the central core region of the dLGN, whereas bistratified On-Off direction-selective RGCs (DSGCs) connect to a shell region that resides adjacent to the optic tract, as do monostratified Off DSGCs known as J RGCs (Ecker et al. 2010; Huberman et al. 2009; Huberman, Manu, et al. 2008; Kay et al. 2011; Kim et al. 2008, 2010; Rivlin-Etzion et al. 2011) (Figure 1.4-D).

It has been thought until recently that eye-specific segregation in mice leads to monocular innervation of LGN cells, as occurs in carnivorous animals and primates because of the interlaminar space (Grubb et al. 2003; Jaubert-Miazza et al. 2005; Zhao et al. 2013). However, three modes of sensory integration by each LGN cells has been found in mice: i/ Relay mode (28%): convergence of a few contralateral RGCs , ii/ Combination mode (32%): numerous and diverse RGCs converge from one eye. iii/ Binocular mode, concurrence of a miscellaneous of ipsilateral and contralateral RGCs (Howarth, Walmsley, and Brown 2014; Rompani et al. 2017). Therefore, the reduced amount of ipsilateral RGC in mouse does not result in a simplification of the circuit. On the contrary, the great diversity in combination of RGC subtypes integrated in dLGN cells is extended to the combination of binocular inputs.

In the SC, there are two retinorecipient layers, where the retinal inputs project and segregate. The stratum griseum superficialis (SGS) contains a representation of the contralateral retina (Dräger and Hubel 1976; Koch et al. 2011). In a deeper layer, we found the stratum opticum (SO), which is innervated

by axons coming from the ventrotemporal portion of the ipsilateral eye (Dräger and Hubel 1975). In comparison with the dLGN, little is known about the function of this binocular representation and the specific mechanisms that mediate segregation in the SC.

1.3.3 Spontaneous activity

1.3.3.1 Presence across the nervous system

Even in the absence of sensory stimulation, the neonatal brain is spontaneously active. Spontaneous network activation has been observed in multiple developing circuits including retina (Galli and Maffei 1988; Meister et al. 1991), spinal cord (Landmesser and O'Donovan 1984), hippocampus (Ben-Ari et al. 1989; Garaschuk, Hanse, and Konnerth 1998), cochlea (Tritsch et al. 2007), cerebellum (Watt et al. 2009), neocortex (Corlew, Bosma, and Moody 2004; Garaschuk et al. 2000), hindbrain (Gust et al. 2003), thalamus (Antón-Bolaños et al. 2019; Moreno-Juan et al. 2017) and midbrain (Rockhill, Kirkman, and Bosma 2009). In the past, this intrinsic activity was considered as noise interfering with brain processing (Faisal, Selen, and Wolpert 2008; Tolhurst D. Movshon and Dean 1983). However it is known today that correlated spontaneous activity emerges early after birth, plays important roles in the fine maturation and integration of different sensory circuits and exhibits spatial patterns matching functional sensory maps (Jetti, Vendrell-Llopis, and Yaksi 2014; Kenet et al. 2003; Romano et al. 2015). Spontaneous activity-mediated mechanisms ruling the development of the visual system also maintain fundamental parallels with refinement and maturation of non-sensory circuits of the brain (Kozorovitskiy et al. 2012).

1.3.3.2 Historical perspective of retinal waves

Retinal waves were recorded for the first time in rabbit retinal preparations in vitro (Masland 1977) and subsequently were visualized in rat pups using single electrodes in vivo (Galli and Maffei 1988).

Correlation between RGCs was later observed in multielectrode recordings (Meister et al. 1991; Wong, Meister, and Shatz 1993). Wave propagation was monitored by calcium imaging. Retinal waves travel across finite regions of the retina called domains (Feller et al. 1996; Wong et al. 1995). Voltage-clamp recordings have shown that both RGCs and amacrine cells receive synaptic input during retinal waves (Butts et al. 1999; Feller et al. 1996; Singer, Mirotznik, and Feller 2001; Zhou 1998). Retinal waves are comprised of large and slow depolarizations crested by bursts of action potentials, that correlate the firing of neighboring RGCs (Demas, Eglen, and Wong 2003; McLaughlin, Hindges, and O'Leary 2003; Wong et al. 1993). Extracellular recordings demonstrated individual RGCs fire 2–3 s-long bursts of action potentials approximately once every minute and then remain silent for 1–2 min, meaning that each cell fires only about 5% of the time (Galli and Maffei 1988; Meister et al. 1991). After a wave has propagated through a region, a second wave cannot enter that region until the refractory period has passed. This time varies between retinas, ranging between 25 and 50 seconds depending on the species (Bansal et al. 2000; Feller et al. 1996, 1997; Syed et al. 2004).

1.3.3.3 Evolutionary differences in the development of the visual system

The developing retina of anamniotes is exposed to light very early through their transparent jelly eyelids. Forward-directed locomotion produces a predominant anterior to posterior optic flow that activates RGCs in a temporal to nasal sequence. In this way, experience-driven-activity governs retinotopic refinement in these phyla. In zebrafish larvae, retinal waves take place only during 2.5–3.5 days post-fertilization, becoming shortly substituted by light input (Zhang et al. 2016). Indeed, rearing animals with an inversed stimulus severely impairs visual refinement (Hiramoto and Cline 2014). In amphibian, retinal spontaneous activity is not present during development although emerges in dark reared individuals without disrupting topographic maps (Demas, Payne, and Cline 2012). However, retinal waves are present in all amniotes

examined. Because amniote development happens in the dark, the current hypothesis proposes that these species adopted retinal waves as a surrogate for visually-evoked activity. Spontaneous activity is originated in the vetrotemporal region of the retina (Ackman, Burbridge, and Crair 2012) and randomly propagates (Feller et al. 1996), resembling the characteristic temporal to nasal axis experience driven activity displayed in embryonic anamniotic retina. Although their pattern and mechanisms of action are conserved across species, there are important timing variations between mammals and non-mammals. In some mammalian species, such as primates or humans, waves occur only prenatally, whereas in other species, such as mice and ferrets, they occur both prenatally and postnatally (Catsicas et al. 1998; Feller 2002; Sernagor, Eglen, and Wong 2001; Warland, Huberman, and Chalupa 2006; Wong 1999; Zhou 2001b). Turtles exhibit spontaneous activity even after eye opening (Sernagor and Grzywacz 1996). In mammals, retinal waves begin way before photoreceptors are capable of transducing light, and they disappear around the time of eye-opening, regardless of whether visual experience is prevented or not (Demas et al. 2003). In these species, the patterns of retinal waves are transmitted and replicated into the dLGN, SC, and V1 (Ackman et al. 2012). Previously to retinal innervation, intrinsic spontaneous activity is already present in dLGN and SC (Moreno-Juan et al. 2017), and is maintained in the absence of adequate retinal drive (Burbridge et al. 2014). However, once RGC axons arrive, retinal input starts to drive post-synaptic activity.

1.3.3.4 Stages of retinal waves

In mammals, retinal waves have been divided into three stages along perinatal development with unique cellular and pharmacological signatures that are remarkably similar across species (Sernagor et al. 2001; Wong 1999) (Figure 1.5).

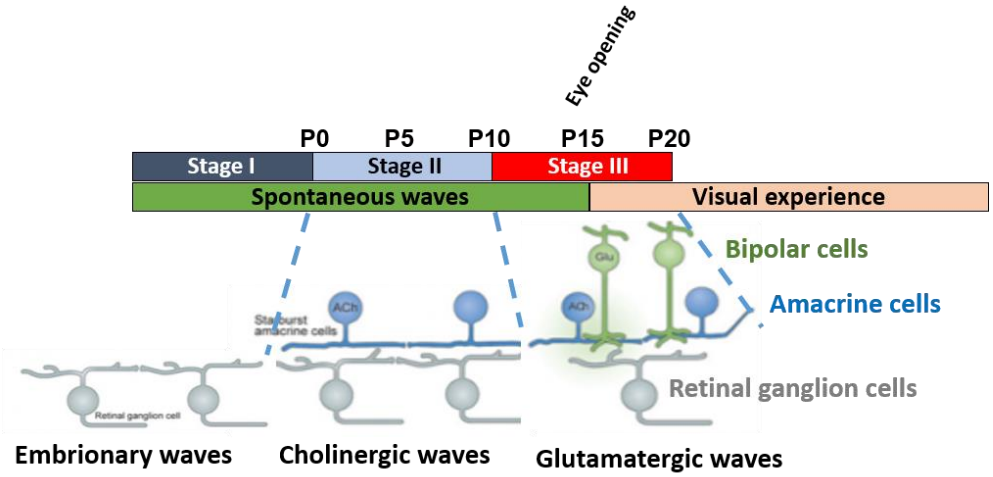

Figure 1.5: Three successive circuits mediate retinal waves. Adapted from Ford and Feller 2011.

- **Stage I or embryonic** waves emerge before birth and depend on gap junction contacts between RGCs since amacrine cells are not yet differentiated (Bansal et al. 2000; Syed et al. 2004). They are relatively infrequent and confined to domains (Bansal et al. 2000).
- **Stage II** waves emerge around the time of birth in mice and ferrets (Bansal et al. 2000; Syed et al. 2004) and take place during the first 1–2 postnatal weeks, coincident with retinotopic and eye-specific refinement. Stage II waves are driven by acetylcholine released from starburst amacrine cells (Feller et al. 1996; Syed et al. 2004; Zheng, Lee, and Zhou 2004), and are called cholinergic waves. They occur relatively infrequently, with wide ranges in size, duration and propagation, varying with species (Bansal et al. 2000; Feller et al. 1996; Hennig et al. 2009, 2011).
- **Stage III or glutamatergic** waves begin at approximately P10–P12 in mice and ferrets and are mediated by glutamate released from retinal bipolar cells (Bansal et al. 2000; Wong et al. 2000; Zhou and Zhao 2000). Stage III waves persist until around the time of eye-opening at P14 (Bansal et al. 2000; Demas et al. 2003; Syed et al. 2004; Wong et al. 1993), when they become inhibited by GABA signaling (Maccione et al. 2014). At this stage, waves are much faster and frequent but their propagation is restricted to small domains. They are initiated in discrete hotspots

changing position over time (Maccione et al. 2014). Gap junctions between ON bipolar cells are also involved in lateral transmission (Akrouh and Kerschensteiner 2013). Within a glutamatergic wave, cells fire repetitive non-overlapping bursts in a fixed order: ON before OFF (Chen and Regehr 2000). Alpha, beta, and gamma RGCs, also exhibit differences in their spontaneous firing patterns during stage III waves (Liets et al. 2003). Cellular recruitment within waves increases dramatically with development (Maccione et al. 2014).

1.3.3.5 Gap junctions

During the stage of embryonic waves, immature RGCs establish contacts called gap junctions even before the appearance of amacrine cells. In later stages, such connections are established also with amacrine and bipolar cells, being necessary for correlated spontaneous activity to occur. Knock-out mice lacking the connexins *Cx36/Cx45*, which are the proteins integrating gap junctions in the retina, still exhibit waves but have severe defects in eye specific segregation (Blankenship et al. 2011; Torborg, Hansen, and Feller 2005). In these mice, the spontaneous firing rate occurring between bursts is increased (Hansen et al. 2005), decreasing nearest-neighbor correlation.

1.3.3.6 GABAergic and adenosine signaling

Around P4-5, GABAergic signaling starts to modulate waves performing a depolarizing effect (Hennig et al. 2011; Zhang et al. 2006), as it usually does in the rest of the central nervous system (Ben-Ari et al. 2007). Cholinergic waves rapidly increase in size and speed, but a switch in GABA signaling to become hyperpolarizing between P7 and P9 correlates with a decrease in frequency and propagation (Barkis, Ford, and Feller 2010; Zhang et al. 2006). The neuromodulator adenosine is secreted from starburst

amacrine cells (Blazynski 1989) and is essential for the generation of retinal waves (Stellwagen, Shatz, and Feller 1999; Syed et al. 2004). Adenosine signaling also performs a similar switch from excitatory to inhibitory (Zhou 2001a) in order to regulate wave frequency (Singer et al. 2001).

1.3.3.7 Permissive or instructive role

For quite some time, there was intense controversy about whether retinal waves play an instructive or permissive role in the development of the visual map. While the influence of neural activity in the modulation of brain development had been already established (Spitzer 2006), it was still thought by a part of the scientific community that this activity worked as a way of passively activating subsequent signaling routes that would be the real responsible for mediating these processes (Chalupa 2009; Huberman et al. 2003; Sun et al. 2008). The firing patterns exhibited by this type of activity had not yet been analyzed in depth but it is currently known that their complexity far exceeded that required to exercise a passive role. Experiments that maintain the activity level but alters the firing pattern or wave dynamics have confirmed an instructive role for retinal waves (Xu et al. 2011). Guidance mechanisms direct the axons to the right place, but the spatial information provided by the correlated firing of neighboring RGCs is essential for fine-tuning axonal refinement and achieve the resolution of the final retinotopic maps (Butts, Kanold, and Shatz 2007).

Beyond the refinement of retinal projections, retinal waves also play an important role sculpting the circuits of the retinorecipient targets. The disturbance of retinal waves produces larger receptive fields in dLGN and SC cells (Chandrasekaran et al. 2005; Grubb et al. 2003; Mrsic-Flogel et al. 2005), an anticipation of corticothalamic innervation (Seabrook et al. 2013) as well as defects in migration and connectivity in inhibitory interneurons of the dLGN (Golding et al. 2014). In addition, the visual cortex maintains a high dependence on retinal activity during development before the opening of the eye, it has

been described that the alteration of the retinal waves produces a modulation of the initial selectivity of neurons in the cortex (Bonetti and Surace 2010). Recent computational models have implicated slow features of retinal waves in the establishment of the visual cortex network, both in the initial biases of orientation maps (Hagihara et al. 2015) and in the training of complex cell-like functions (Dähne, Wilbert, and Wiskott 2014).

1.3.3.8 Intra-eye and inter-eye activity correlation

Both the refinement of retinal axons from the same eye (intra-eye refinement) and refinement of axons from the different eyes reaching the same side (inter-eye refinement) have been proposed to depend on retinal activity. Inter-eye refinement leads to eye specific segregation, and takes place in the binocularly innervated region of the target. It occurs early, during the cholinergic stage of retinal waves, when spontaneous activity displays low frequency but high propagation. Contralateral and ipsilateral axons coming from equivalent regions of their respective eye are guided to the same area of the target by a similar Ephs expression levels and begin to arborize in an overlapping manner. Inter-eye activity correlation is very low and therefore axons coming from each eye segregate. Intra-eye refinement takes place during a longer period, taking advantage of the higher frequency and restricted wave domains occurring during the glutamatergic stage (Maccione et al. 2014). This feature provides the additional spatial information necessary to achieve the resolution of the retinotopic map displayed at the time of eye opening (Figure 1.6-A,B).

Regarding inter-eye correlation, a forced synchronization of the two eyes results in a severe disruption of eye specific segregation (Zhang et al. 2011). Pharmacological studies altering inter-retinal correlation also result in severe segregation defects (Huberman, Stellwagen, and Chapman 2002; Penn et al. 1998; Rossi et al. 2001). In both scenarios, the discordance in terms of activity correlation required

to discriminate between both inputs does not occur, so that their projections directed to the binocular region are established overlapping in the disputed territory. On the other hand, the corresponding territory for each retina is determined by the relative, rather than absolute, levels of spontaneous activity.

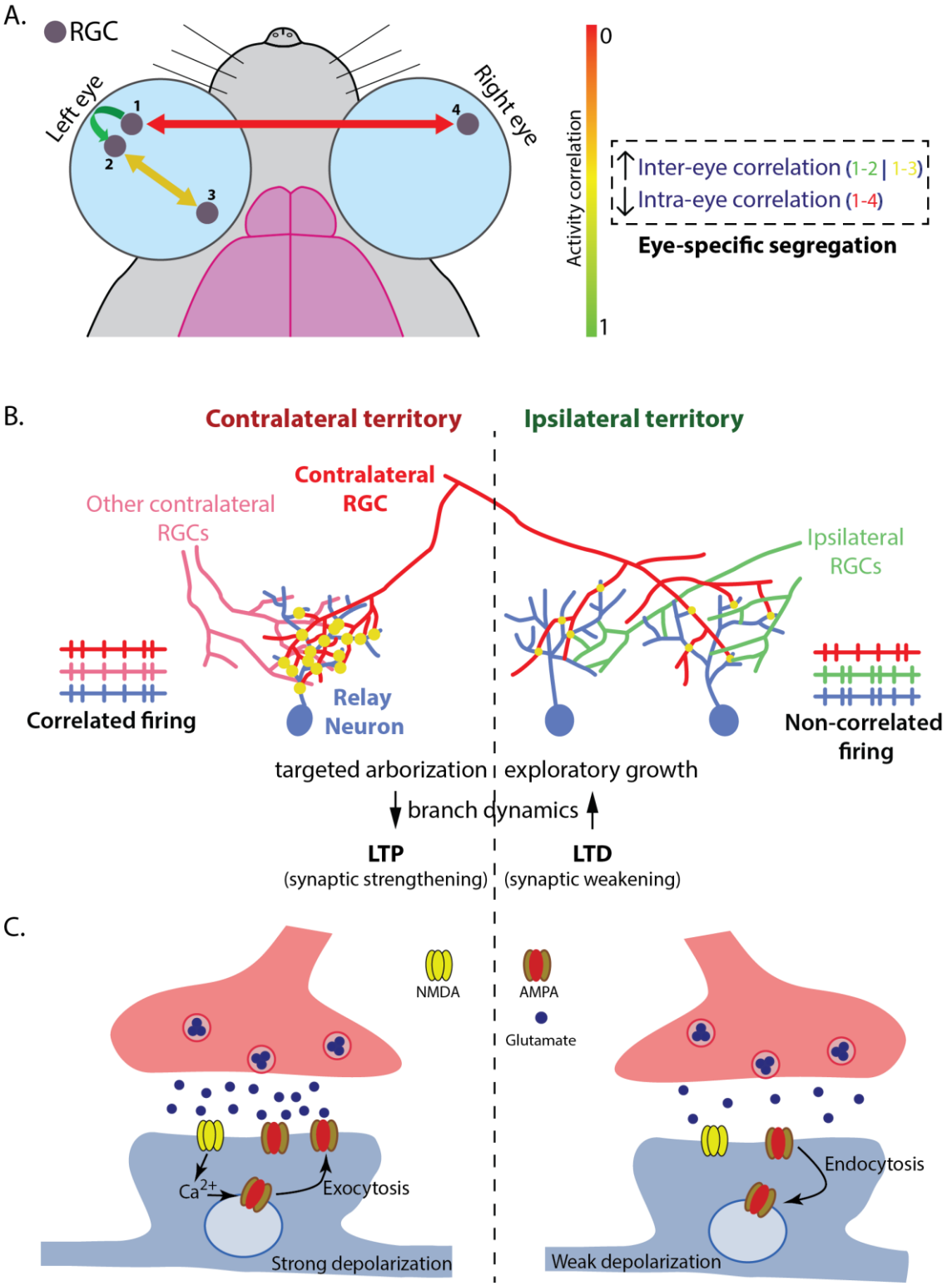

Figure 1.6: Spontaneous activity-dependent refinement. **(A)** Activity correlation mediates both intra- and inte-eye segregation. **(B)** According to Hebbian rules, simultaneous firing induce synapse stabilization while asynchronous firing promote synape weakening and exploratory axonal growth. **(C)** Hebbian mechanisms for LTP and LTD. Adapted from Kutsarova et al., 2017 (B).

Monocular injections of forskolin or cpt-cAMP increase wave frequency in the treated eye, which has a greater facility to perform LTP and thus to stabilize its synaptic buttons (Figure 1.6-C), resulting in an increase of its territory at the expense of that corresponding to the opposite retina (Stellwagen and Shatz 2002). When wave frequency is increased binocularly the projection pattern is unaffected (Stellwagen and Shatz 2002). This procedure does not impair segregation since activity correlation is maintained. Such approaches aimed to alter the activity levels do not allow to study the importance of the specific patterns of retinal waves.

$\beta2^{-/-}$ mice exhibit a modified pattern of activity consisting on infrequent and large waves, so depolarization induced by RGCs are not enough to induce postsynaptic SC neurons (Burbridge et al. 2014). In these mice, global intra-retinal correlation and a stronger inter-retinal correlation disturb eye-specific segregation. In addition, they produce larger receptive fields. On the other hand, in transgenic mice in which the expression of the β2 acetylcholine subunit is restricted to RGCs (β2(TG) mice), single RGCs display activity indistinguishable from that of WT mice, but the cholinergic silencing of starburst amacrine cells (SACs) decreases the propagation of the waves so that activity correlation is restricted to small groups of neighbouring cells. In this case, intra-retina correlation is restricted but maintained, so the larger receptive fields observed in $\beta2^{-/-}$ mice were rescued. Inter-retinal correlation is still disrupted, and therefore eye specific segregation does not take place. Restoration of activity frequency and wave size in β2(TG) mice through binocular application of CPT-cAMP rescued eye specific segregation (Xu et al. 2011). In summary, eye-specific segregation require both low inter- and high intra-eye correlation. Rather than just levels of activity, the patterns that characterize retinal waves are essential for the process.

1.3.3.9 Retino-retinal projections

As previously mentioned, inter-eye asynchronicity is key for eye-specific segregation. The emergence of these patterns in neonatal retina from the very beginning of synaptic activity suggested the existence of direct communication between both eyes. It has been observed that bilaterally correlated activity often begins in one retina and then propagates with a small temporal lag to the contralateral retina (Burbridge et al. 2014). Retino-retinal projections were first described decades ago. However, it was thought that they were defects in development or even labelling artefacts, with no apparent relevance (Ackman et al. 2012; Bunt and Lund 1981). Retino-retinal projections disappear in mouse few days after their establishment, but precisely this time window coincides with the emergence of the retinal waves (Murcia-Belmonte et al. 2019a). Our laboratory has demonstrated that RGC axons from one eye transverse the optic chiasm and establish physical contacts with both amacrine and RGCs in the contralateral retina. Predictive models established a requirement for such connections in the arrangement of bilateral coordination during axonal refinement (Murcia-Belmonte et al. 2019a) (Figure 1.7). In the near future technical advances should allow the specific elimination of this direct communication between retinas to finally clarify its role in the coordination of inter-eye spontaneous activity.

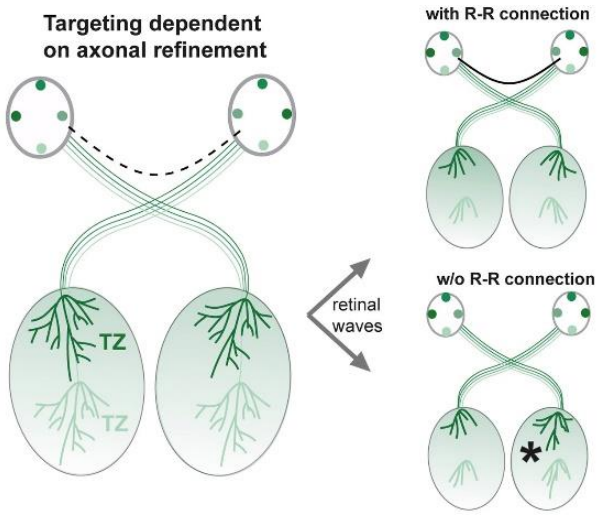

Figure 1.7: Retino-retinal projections likely coordinate inter-eye spontaneous activity since the onset of retinal waves, driving symmetrical refinement in both hemispheres. Adapted from Murcia-Belmonte et al., 2019.

1.3.3.10 Hebbian and non-Hebbian mechanisms

Spontaneous activity dependent refinement relays on both Hebbian and non-Hebbian mechanisms. Hebbian synaptic plasticity is driven by the input in order to strengthen (via LTP-like mechanisms) or weaken (via LTD-like mechanisms) the transmission efficacy of individual synapses, as it happens in retinogeniculate and retinocollicular nascent connections (Butts et al. 2007; Shah and Crair 2008; Ziburkus et al. 2009). However, Hebbian plasticity leads to a positive feedback loop that could result in either saturated or silenced synapses. In contrast, homeostatic plasticity seeks to maintain a stable firing rate and increase the signal to noise ratio. Both types of plasticity work by adjusting the same biological parameters: synaptic strength, neuronal excitability, neuronal connectivity, presynaptic transmitter release or the balance between excitation and inhibition (Tien and Kerschensteiner 2018). Local homeostatic plasticity can work at the level of sub-compartments or even single synapses (Branco et al. 2008; Chen, Lau, and Sarti 2014; Hou et al. 2008) modulating Hebbian plasticity (Yee, Hsu, and Chen 2017), so it has become considered as a mechanism of metaplasticity. Regulation of synaptic strength, also known as synaptic scaling, is a major converging point between Hebbian and homeostatic plasticity. It involves the regulation of AMPAR trafficking and accumulation (Pérez-Otaño and Ehlers 2005; Pozo and Goda 2010; Turrigiano 2008) (Figure 1.6-C). In response to activity deprivation or overexcitation, AMPAR presence at the postsynaptic boutons is scaled up or down (Gonzalez-Islas and Wenner 2006; Krahe and Guido 2011).

Synapses in immature SC and dLGN neurons are predominantly mediated by NMDA receptors. As neurons mature, their dendritic arbors become more complex and synaptic transmission are strengthened through the addition of AMPA receptors (Chen and Regehr 2000; Hamos et al. 1987; Wu, Malinow, and Cline 1996). Increased α-CaMKII activity both increases glutamatergic synaptic strength and stabilizes dendritic arbor structure by reducing rates of branch additions and retractions. During the

development of the retinotectal circuit in *Xenopus*, the intrinsic excitability modulates the strength and pattern of local recurrent activity, generated by local tectal-tectal connections (Dong and Aizenman 2012; Pratt and Aizenman 2007). A transient phase of increased intrinsic excitability occurs between stages 42-46. This facilitates the induction of synaptic plasticity, coinciding with an increase in axonal branching of RGCs and tectal neurons and a peak in tectal BDNF expression (Cohen-Cory, Escandón, and Fraser 1996). The increase of synaptic contacts leads to a higher RGC input strength. As synaptic input increases, intrinsic excitability decreases (between stages 46-49). This homeostatic mechanism maintains a constant input–output function within a useful dynamic range during development, a permissive environment for activity-dependent refinement (Pratt and Aizenman 2007). A similar process has been described in the SC and dLGN of mice (Chen and Regehr 2000; Hamos et al. 1987; Wu et al. 1996). In $\beta2^{-/-}$ mice, retinocollicular synapses at P6-P7 turn out to be weaker but also more numerous (Chandrasekaran, Shah, and Crair 2007). Such dysfunctional retinal input is not able to overcome homeostatic pressures in the collicular circuit and triggers the mentioned switch in the intrinsic excitability, whereas the previous local spontaneous activity is preserved (Burbridge et al. 2014).

The synaptic remodeling that takes place during spontaneous activity dependent refinement drives the strengthening, consolidation, as well as the elimination of synapses, but this process also involves molecular signals and physical recruitment of non-neural cells (Chung et al. 2013; Noutel et al. 2011; Stephan, Barres, and Stevens 2012). For example, it seems that microglia participates in the elimination of weakened synaptic inputs by the complement pathway (Schafer et al. 2012) while astrocytes phagocyte synapses but through independent complement pathway that includes MEGF10 and MERTK signaling (Chung et al. 2013). Disrupting this collaboration severely impedes axonal refinement.

1.3.4 Relationship between guidance cues and spontaneous activity

Guidance cues and retinal spontaneous activity are both involved in retinotopic map formation. The disruption of both forces simultaneously results in a nearly complete loss of topography in the SC (Cang et al. 2008; Pfeiffenberger, Yamada, and Feldheim 2006). Altering the levels of Eph or ephrins disrupts the topographic organization but not the bilateral segregation (Pfeiffenberger et al. 2005). When retinal wave patterns are disrupted, axons target correctly their corresponding area but fine-tune refinement is impaired. Receptive fields are enlarged only in the bilateral region of the nucleus because activity competition is required (Xu et al. 2011). Originally, it was proposed that refinement occurs in a step-wise manner, in which guidance cues give rise to an inaccurate map displaying broad axonal arbors and later activity-dependent mechanisms perform a more precise refinement to define the definitive map organization (Bevins, Lemke, and Reber 2011; Reber, Burrola, and Lemke 2004). Multiple proteins defined as axon guidance molecules seem to be not only involved in the establishment of a rough topographic map but also in the refinement step. In fact, it has been proposed that some proteins initially identified as guidance molecules can be modulated by altering patterns of spontaneous neural activity (Hanson and Landmesser 2004; Ming et al. 2001) and that they could impact neural activity patterns as well (Bouzioukh et al. 2006; Sahay et al. 2005). The neurotrophic factor BDNF govern retinotopic mapping regulating axon dynamics through its interaction with ephrinA/EphA signaling (Lim et al. 2008), and BDNF levels in visual targets during development are controlled by neural activity (Schwartz, Schohl, and Ruthazer 2011). Because temporal windows framing sequential steps during the formation of the retinotopic maps are difficult to define, a stochastic model has proposed that guidance cues and retinal waves interact simultaneously and stochastically rather than sequentially (Koulakov and Tsigankov 2004; Tsigankov and Koulakov 2006, 2010). Mutant $Isl2^{EphA3}$ KI mice express ectopic levels of EphA3 in a subset of RGCs positive for the transcription factor Isl2, increasing EphA signaling only in that population. In homozygous mice, the difference between RGCs that express EphA3 ($Isl2^{+}$) or not ($Isl2^{-}$) is so large that

the projections of these two populations segregate in the SC, resulting in a double map. However, heterozygous mice exhibit single, double or mixed collicular maps, including different phenotypes even between hemispheres of the same individual (Owens et al. 2015). In this case, guidance and activity components are not able to act in concert and the mapping occurs stochastically. Such heterogeneity is not possible when retinal waves are abolished as observed in $Isl2^{EphA3/+}$::$\beta2^{-/-}$ mice (Owens et al. 2015). EphA/ephrinA signaling is able to define the termination zone of a particular RGC axon along the anterior-posterior axis of the SC even in the absence of neural activity(Benjumeda et al. 2013), but according to the stochastic model it seems that EphA/ephrins and neural activity would act in concert working as balanced forces during the formation of the circuit to finally refine the map.

Eye-specific segregation is ruled by spontaneous activity, but this refinement results insufficient if ipsilateral and contralateral axons have not been previously sorted in their corresponding targeting areas. In carnivores like ferrets, the dLGN exhibits physically separated eye-specific layers (Guillery 1971; Hutchins and Casagrande 1990) and the existence of domain specific guidance cues in dLGN discriminating ipsilateral and contralateral axons has been long time postulated in mouse and rat. However, no molecules specifying eye-specific territories in these species had been found until recently. The extracellular glycoprotein Nell2 is expressed in the dorsomedial region of the dLGN, mediating contralateral repulsion. In Nell2 null mutant mice, contralateral axons invade the ipsilateral territory, and ipsilateral axons are segregated but form a patchy distribution (Nakamoto et al. 2019). This discovery opened the door to new molecules defining eye specific domain in other nuclei, more related to guidance than to fine refinement.

1.4 NON-IMAGE FORMING VISUAL NUCLEI

Non-imaging circuits work unconsciously to indirectly support vision: olivary pretectal nucleus (OPN) and nucleus of the optic tract (NOT) mediate the pupillary reflex (Young and Lund 1994) and saccadic

movements (Kato et al. 1986) respectively, in order to help image stabilization. This kind of circuits also regulates core physiological functions independent of sight: suprachiasmatic nucleus (SCN) regulates entrainment of the circadian clock, regulation of hormone rhythms and sleep cycles (Dhande et al. 2013; Hattar et al. 2003; Noseda and Burstein 2011; Yonehara et al. 2009).

Non-image forming nuclei receive input from intrinsically photosensible retinal ganglion cells (ipRGCs), which respond directly to light due to their expression of melanopsin photopigment (OPN4) and function as autonomous photoreceptors (Berson, Dunn, and Takao 2002; Do and Yau 2010; Hattar et al. 2002; Schmidt et al. 2011). Autonomous activation of ipRGCs as early as P0 in mice (Sekaran et al. 2005; Tu et al. 2005), long before rods and cones arousal, plays a role in the patterning of early retinal activity (Kirkby and Feller 2013) influencing RGC axonal refinements within the brain (Akerman, Smyth, and Thompson 2002; Renna, Weng, and Berson 2011; White, Coppola, and Fitzpatrick 2001). ipRGCs can be activated by the retinal waves , so that they carry out modulatory effects even in absence of light (Renna et al. 2011). Eye specific segregation in vLGN and OPN has been shown to be independent of light, and only dLGN seems to require visual experience (Tiriac, Smith, and Feller 2018).

In mouse and rats, there are at least five subtypes of ipRGCs (M1-M5) that project specifically to more than a dozen of central targets (Ecker et al. 2010) (Figure 1.8). Each subtype is characterized by its morphology, dendritic arborization pattern and melanopsin expression level, which translates into a different intrinsic photosensitivity (Sand, Schmidt, and Kofuji 2012). M1 subtype was the first ipRGC population described, it exhibits the highest melanopsin expression and intrinsic photosensitivity, while M4 and M5 cells have hardly detectable melanopsin levels (Ecker et al. 2010; Sand et al. 2012). M1 ipRGCs can be subdivided in two groups based on Brn3b expression. The selective ablation of M1 $Brn3b^+$ ipRGCs suppresses the pupillary reflex while leaving the circadian entrainment intact. $Brn3b^+$ M1 ipRGCs target the outer shell of the OPN while $Brn3b^-$ M1 cells target the SCN (Chen, Badea, and Hattar 2011).

Like other RGCs, a single ipRGC can project to multiple nuclei. For example, a cell innervating the SCN can send collateral projections to intergeniculate leaflet (IGL), ventral medial hypothalamus (VMH), peri-habenular region (pHb), ventro lateral geniculate nucleus (vLGN), pretectal nucleus (PN) and/or SC (up to five nuclei). There are no interneurons that exclusively receive input from ipRGCs, and even in SCN and OPN, where ipRGCs are virtually the only retinal input, they only account for less than 20% of the total input (Kim et al. 2019).

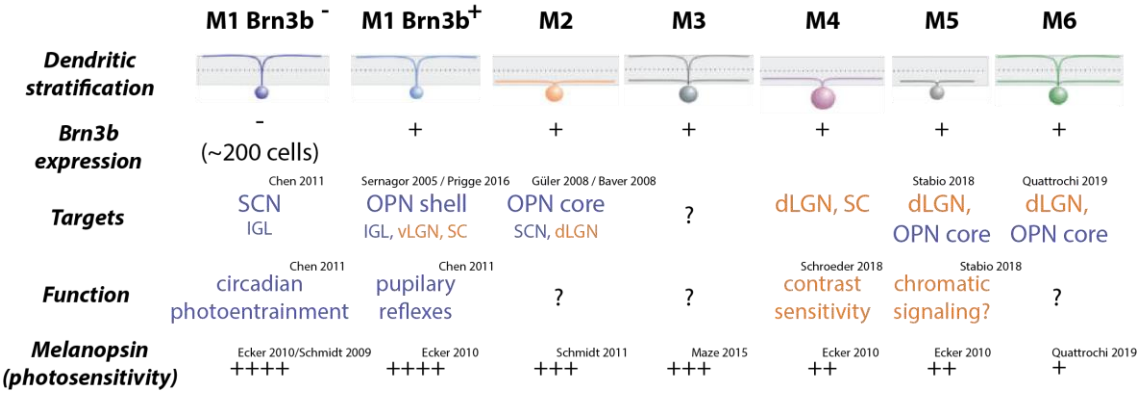

Figure 1.8: ipRGC subtypes: dendritic stratification, connectivity and function. Adapted from Dhande and Huberman 2014.

1.4.1 Suprachiasmatic nucleus

The SCN is located against the third ventricle on top of the optic chiasm. This nucleus is divided in shell and core according to their afferent and efferent connectivity along with their specific expression of various neuropeptides (Figure 1.9-A). Vasoactive intestinal peptide (VIP) and gastrin-releasing peptide (GRP) are expressed in the core while the shell contains arginine vasopressin (AVP) expressing cells (Abrahamson and Moore 2001; Colwell 2011). VIP neurons send projections to the entire SCN, affecting clock cells even in the shell (Kalamatianos et al. 2004). SCN neurons are known to receive synaptic input from at least 5 different types of neurons: ipRGCs in the retina, serotonergic neurons in the raphe nucleus, indirect retinal input from the IGL, the paraventricular thalamus, and local input from other SCN neurons (Welsh, Takahashi, and Kay 2010) (Figure 1.9-B).

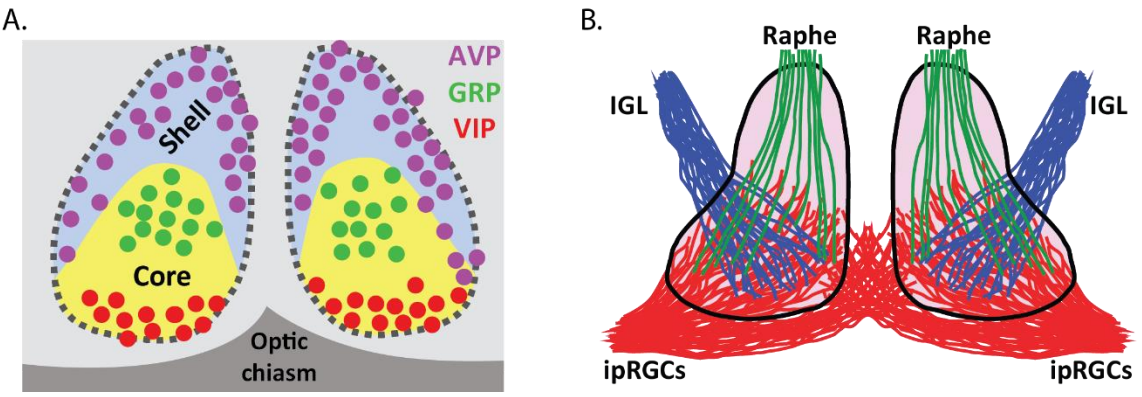

Figure 1.9: Anatomy of the Suprachiasmatic nucleus. (A) Cell-type distribution. (B) Afferents to the SCN. Adapted from Fernández et al., 2016 (A); Bedont et al., 2015 (B).

1.4.1.1 Afferent projections

ipRGCs begin to project to the ventrolateral SCN and establish synaptic contacts in the SCN at P0, evoking photic induction of the neural activity marker c-fos (Sekaran et al. 2005; Sernagor 2005). C-fos expression reaches significant levels at P4, mainly in VIP neurons from this first innervated region (Leard et al. 1994; Muñoz Llamosas et al. 2000; Weaver and Reppert 1995). Then, light response is decreased due to a developmental phase of RGC death (Young 1984) and SCN cells death (P5-P9) (Ahern et al. 2013). Synaptogenesis is increased from P2 to P6 , coinciding with the onset of AVP expression (Moore and Bernstein 1989). Adult levels of synapse density are achieved around P10 (Moore and Bernstein 1989). Although a ventral preference exists in mammals, all SCN regions receive some direct retinal input (Hattar et al. 2006; Ibata et al. 1989; Juárez et al. 2013; Morin 2007; Muscat et al. 2003; Tanaka et al. 1993).

Although there are SCN afferents from many different regions, including the olfactory and limbic systems (Krout et al. 2002) the majority of projections innervating these nuclei comes from the raphe and the IGL. Projections coming from the raphe nuclei arrive to the dorsal region shortly after birth (P0) and axons from the IGL innervate the SCN one week later (P7), often converging with raphe axons (Guy et al. 1987). Around P12, the innervation of these nuclei resembles the adult state (Bedont and Blackshaw

2015; Migliarini et al. 2013). Both IGL and raphe projections show preference for VIP neurons in ventrolateral SCN (Abrahamson and Moore 2001; Bosler and Beaudet 1985; Hisano et al. 1987; Kiss, Léránth, and Halász 1984). Each SCN subdomain receives input from multiple origins, with some types being particularly present in certain areas (Abrahamson and Moore 2001). Intra-SCN interconnectivity is also extremely intricate and diverse (Abrahamson and Moore 2001; Castel and Morris 2000; LeSauter et al. 2002).

1.4.1.2 Circadian cycle

The SCN contains an intrinsic genetic program that determines the period length of circadian oscillations, which emerges without the need for visual experience (Brzezinski et al. 2005; Güler et al. 2008). SCN cells isolated *in vivo* or *ex vivo* exhibit spontaneous firing reproducing circadian cycles (Weaver 1998). Luminance information does not mediate circadian cycles; it is instead responsible for adapting its duration to environmental conditions (Colwell 2011; LeGates, Fernandez, and Hattar 2014) (Figure 1.10-A). The SCN receives indirect light input through the IGL. Both environmental and physiological information need to be integrated and processed in order to perform an effective regulation of the circadian pacemaker system.

The SCN network needs to synchronize the body clock and environmental cues. Glia can perform an homeostatic drive of circadian rhythmicity in order to prevent misalignments between SCN neurons (Freeman et al. 2013), but this process has been described in flies (Suh and Jackson 2007) and currently there are only indirect evidences of its existence in mammals (Prosser et al. 1994; Shinohara et al. 1995). This synchronized firing rate is quicker during the day (6-10 Hz) than in the night (1 Hz) (Atkinson et al. 2011; Colwell 2011). Although it is a synchronized network, the SCN oscillators are not in the same phase. Activity waves follow a dorsal to ventral course, differing by 2-3h. Changes in gene expression occur subsequently according to the same spatiotemporal pattern (Evans et al. 2011;

Yamaguchi et al. 2003). It is called the transcription-translation feedback loop (TTFL), and seems to be a necessary feature for pacemaker function (Figure 1.10-B).

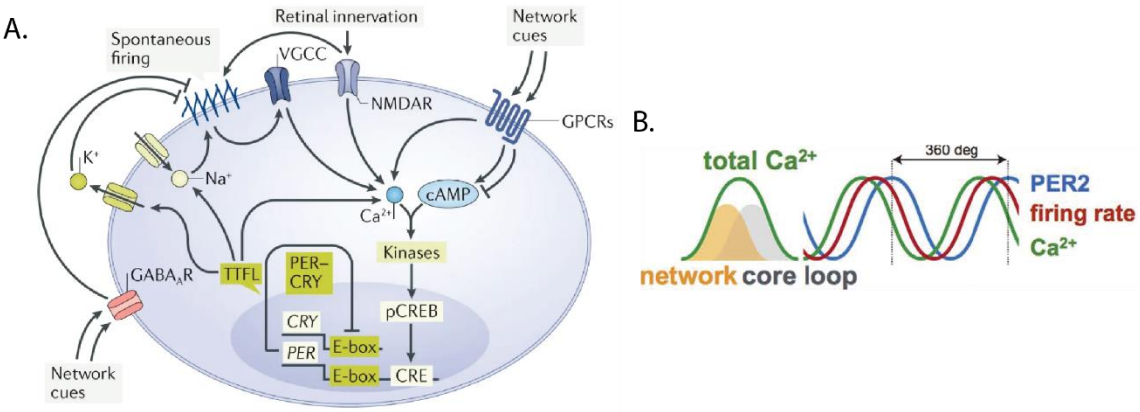

Figure 1.10: Circadian cycle is mediated by SCN oscilations. (A) Retinal input modulate SCN spontaneous firing. **(B)** Activity oscilations are followed by calcium waves and activity-dependent transcription. Hastings et al., 2018 (A); Enoki et al., 2017 (B).

1.4.1.3 Neonatal SCN

Circadian synchrony is established embryonically, the SCN already exhibits strong cell-autonomous rhythms at E15.5, then activity is coordinated at circuit level around P2 when synaptogenesis is shortly started (Carmona-Alcocer et al. 2018). The TTFL depends on CRY1 and CRY2 circadian clock components expression in the adult SCN, but not at neonatal stages (Maywood et al. 2011; Ono, Honma, and Honma 2013). In Cry1,2$^{-/-}$ neonatal SCN, VIP signaling is involved in the integration of cell clusters, while AVP signaling seems to be involved in both building and integration of clusters (Ono, Honma, and Honma 2016). Embryonic circadian synchrony at E15 is not impaired by GABA or VIP antagonist, and the later coupling is not completely prevented in mice that lack connexins, VIP or the VIP receptor (Herzog et al. 2017). Indeed, VIP is not yet expressed at those early stages (Carmona-Alcocer et al. 2018).

1.4.1.4 Retinal input to the SCN

The retinal input to SCN regulates circadian rhythms, with ipRGCs sending information about light irradiance (luminance intensity) preferentially to VIP neurons in the core (Hastings, Maywood, and

Brancaccio 2018). According to its role regulating the circadian cycle, spatial information should not be important in this nucleus. However, a raw retinotopic map formed by widespread RGC axonal arborization has been described (Fernandez et al. 2016). The arborization pattern in the SCN is very intricate, covering a significant portion of the target. Collateral projections from those same cells to the IGL are less elaborated and those directed to the SC are even simpler (Fernandez et al. 2016).

Regarding eye-specific segregation, such extended arborization leads to an overlapping of contralateral and ipsilateral projections. Indeed, both types of projections tend to follow the same paths through the nucleus targeting cells receiving bilateral input. This innervation pattern is more convenient to provide a unitary regulation of circadian rhythms that integrate all the photoentrainment information. Eye specific segregation would be detrimental for this purpose. The ipsilateral/contralateral ratio is around 1:9 (Rice, Williams, and Goldowitz 1995; Thompson and Morgan 1993) in most visual nuclei. However, in the case of the SCN it is close to 2:3. By definition, contralateral axons cross the midline whereas the ipsilateral axons avoid it. However, in the SCN, a large fraction of contralateral ipRGCs axons project bilaterally (Fernandez et al. 2016). This is possible because the innervation of the nucleus occurs at postnatal stages (McNeill et al. 2011), once that midline repellent molecules such as ephrin-B2 have disappeared (Williams et al. 2003).The mechanisms controlling the bilateral arborization of ipRGCs into the SCN have not been elucidated so far.

Although retinal afferents to the SCN occupy the whole nucleus, they target preferably VIP neurons in the ventral SCN. These cells project their dendrites through the entire nucleus, even interacting with clock cells in the shell (Kalamatianos et al. 2004). This population establish a network of dendro-dendritic chemical synapses (DDCSs) that are preferentially targeted by ipRGCs (Kim et al. 2019). Although ipRGC collaterals to the SCN give rise to much less branched arbors, they can still innervate multiple cells. Moreover, targeting distal dendrites produces a decrease of the synaptic potential towards the soma (Häusser, Spruston, and Stuart 2000; Magee 2000; Williams and Stuart 2002), so simultaneous

input signals are aggregated working as coincidence detectors (Williams and Stuart 2002). Therefore, the network is only activated when a large portion of the retina is illuminated (Fernandez et al. 2016). We have to take into consideration that the retinal input to the SCN accounts for less than 15%, and it must be processed and integrated with the rest of the information in a process known as dendritic computation (London and Häusser 2005; Magee 2000). Thus, this network has built an effective system to coordinate and synchronize the whole nucleus according to the light input without interfering with the circadian pacemaker (Figure 1.11).

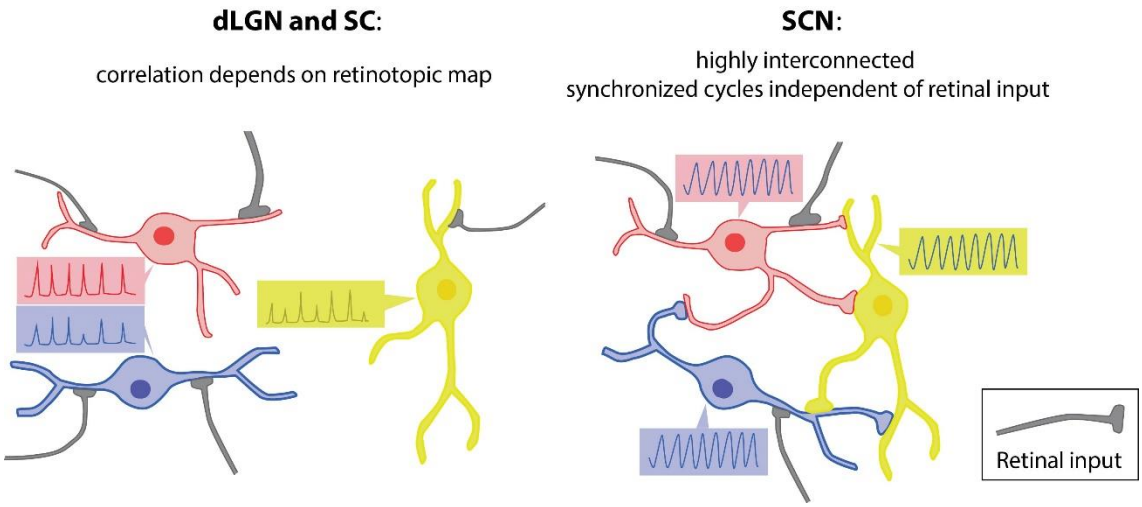

Figure 1.11: Relay interconnectivity in different retinorecipient targets. (A) Relay cells in dLGN and SC interact between them mainly through homeostatic regulation mechanisms, and their activity correlation depends on the retinotopic map. **(B)** Pacemaker neurons in the SCN compose a synchronized network, and retinal input just modulates the length of the light/dark cycles.

1.4.2. Olivary pretectal nucleus

Retinal input to the OPN mediate the pupillary reflex (Güler et al. 2008; Young and Lund 1994) and there is no evidence about topographical arrangement of retinal projections to this target (Kubota et al. 1987). Indeed, the OPN has never been involved in functions requiring spatial information.

OPN can be divided into core and shell. A few days after birth, the core is occupied by M5 or M6 ipRGC projections, possibly both (Quattrochi et al. 2019), and M2 ipRGCs (Osterhout et al. 2014). Later, the shell is innervated by M1 ipRGCs (Baver et al. 2008; Hattar et al. 2002, 2006). The pupillary

reflex is mainly mediated by the M1 cells in the shell (Güler et al. 2008), but its total abolition is only achieved when all ipRGCs are ablated (Hatori et al. 2008; Hattar et al. 2003; Mao et al. 2014; Panda et al. 2003; Sweeney, Tierney, and Feldheim 2014), involving to a certain extent projections to the core.

Innervation of the OPN begins shortly after birth. In this case, refinement does not occur simultaneously for the input of both eyes as it happens in the rest of the visual nuclei analyzed, but takes place sequentially. Contralateral projections refine in the following days and the process is almost completed by P4-5. However, axons from the ipsilateral eye are barely present until P4, when they begin to expand to occupy the entire nucleus between P6 and P8, largely overlapping with the contralateral projections. Later, ipsilateral axons retract to the dorsal region and eye-specific segregation is completed by P10 (Marques and Clarke 1990). The sequential nature of OPN innervation and refinement may lead to differences in the influence of spontaneous activity in this nucleus.

1.5 CROSSTALK BETWEEN THE IMAGE AND NON-IMAGE FORMING VISUAL NETWORKS

Recent evidences have demonstrated a functional crosstalk between the image-forming and non-image forming pathways (Estevez et al. 2012; Hicks 2011; Renna et al. 2011; Schmidt et al. 2014; Zhang et al. 2008).

1.5.1 ipRGCs in vision

When the embryo is still in the uterus, light stimulation of ipRGCs regulates eye vascularization (Rao et al. 2013). Shortly after birth, these early light exposure is involved in photoentrainment of circadian rhythms (Duncan, Banister, and Reppert 1986), light avoidance (Delwig et al. 2012; Johnson et al. 2010) and the maturation of intra-retina synapses (Dunn et al. 2013). In developing ferrets, visual stimuli through the closed eyelids drive responses in dLGN and V1, coding visual scene in immature receptive fields (Akerman, Grubb, and Thompson 2004; Akerman et al. 2002).

The ipRGCs are characterized by their performance as photoreceptors and for transmitting irradiance information. However, the analysis of their activity has yielded more complex patterns that encode for other features depending on the ipRGC subtype. M1 ipRGCs are able to send color information coming from cones to the SCN and OPN, which is required for circadian clock as well as for pupillary light reflex (Hayter and Brown 2018; Walmsley et al. 2015). M2-M5 subtypes project to the dLGN, where they transmit coarse pattern vision independently of rods and cones (Brown et al. 2010). M4 ipRGCs are similar to alpha ON cells, but thanks to its melanopsin phototransduction they can carry out responses in luminous intensities that were thought to be reserved to rods (Estevez et al. 2012; Schmidt et al. 2014). On the other side, M5 cells also receive color information from cones, but exhibiting a strong chromatic opponency that is sent to the dLGN (Stabio et al. 2018). This role is beyond unconscious reflexes and probes the capability of ipRGCs to influence cortical vision.

The difference between M1 and M4-M5 ipRGCs seems to be related to their birth time. As for the rest of the RGCs, the temporal window in which the ipRGCs are differentiated is very wide, extending from E11 to E18 (McNeill et al. 2011). M1 are generated in the later stages, when other types of RGCs have already emerged, and they exhibit features that largely diverge from conventional RGCs. They have the highest melanopsin expression, project to virtually exclusive non-visual pathway regions in the targets, and experience a late innervation. On the other hand, M4-M5 ipRGCs differentiate along with other RGCs and share some functions with them (Ecker et al. 2010).

1.5.2 Interaction of ipRGCs and retinal waves:

Multiple studies have suggested a significant influence of ipRGCs on spontaneous activity dependent refinement in retinorecipient targets. Mice lacking melanopsin raised in permanent light exhibit a decreased eye-specific segregation than controls (Renna et al. 2011), but segregation is not affected when light/dark timing is normal (Chew et al. 2017). At P7, ipRGC phototransduction prolong wave bursts

duration and increase wave and non-wave firing frequency in control, but not in Opn4$^{-/-}$ mice (Chew et al. 2017; Renna et al. 2011). At this stage, rod and cone pathways are not established yet, and ipRGCs are the only photosensitive cells. Therefore, it seems that light acts through melanopsin to alter the spiking properties of retinal waves in the entire RGC population.

Ablation of Brn3b+ ipRGCs (M2-M5), which includes the subtypes that innervate the dLGN, has no effect on eye specific segregation. As mentioned before, Brn3b- M1 ipRGCs does not target the dLGN, but segregation is reduced when this population is selectively removed (Chew et al. 2017). At P7, they have established intra-retinal axonal collaterals that synapse onto dopaminergic amacrine cells (Prigge et al. 2016) as well as an extensive network of gap junctions with other retinal neurons (Sekaran et al. 2003), including other ipRGCs. Dopamine amacrine cells are first detected at P6 in mice, coinciding with the photic modulation of retinal waves by ipRGCs. These connections produce a bidirectional signaling. M1 ipRGCs produce the mentioned regulation in wave dynamics (Chew et al. 2017; Renna et al. 2011) through an excitatory drive to dopaminergic amacrine neurons (Zhang et al. 2008), while these can in turn perform a feed inhibition into M1 ipRGCs (Arroyo, Kirkby, and Feller 2016; Vuong et al. 2015). Somatotropin release–inhibiting factor (SRIF) amacrine cells would complete this pathway providing inhibitory modulation to both cell types in order to stabilize light responses (Vuong et al. 2015) (Figure 1.12).

Dopamine also modulates synchronous spiking in conventional RGCs through changes in membrane conductance and coupling strength (Baldridge, Vaney, and Weiler 1998). Light and dopamine modulation of coupling has been extensively described for horizontal cells (Bloomfield, Xin, and Persky 1995), AII amacrine cells (Kothmann, Massey, and O'Brien 2009; Mills and Massey 1995), and alpha-ganglion cells (Hu et al. 2010; Mills et al. 2007). In the absence of cholinergic waves (β2$^{-/-}$ mice), the described light modulated network starts to be mediated by dopamine and gap junctions. In this scenario, ipRGCs establish more and stronger gap junctions, increasing the number of light-

responding cells. These "recovered waves" mediated by gap junctions are suppressed by cholinergic signaling (Kirkby and Feller 2013; Stacy et al. 2005; Stafford et al. 2009; Sun et al. 2008) (Figure 1.12).

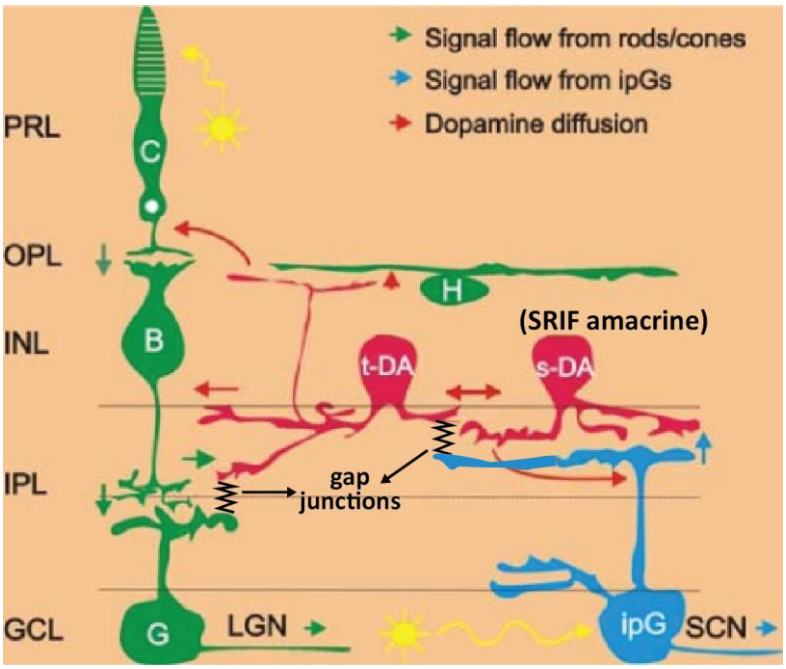

Figure 1.12: Cross-talk between RGCs, ipRGCs and dopamine amacrine cells. Adapted from Zhang et al., 2008.

SACs initiate and control the firing frequency of cholinergic waves, spaced by a characteristic refractory period (Ford, Félix, and Feller 2012; Zheng, Lee, and Zhou 2006). Glutamatergic waves were thought to be initiated stochastically by bipolar cells (Kerschensteiner 2016), but recent studies suggest that photoreceptor signaling is involved. The earliest rod/cone phototransduction coincides with the emergence of glutamatergic waves (Chen et al. 2009; Rosa et al. 2016; Tian and Copenhagen 2003), triggering a subset of retinal waves based on changes in light intensity. Dopamine released during glutamatergic retinal waves is modulated by rod phototransduction through ipRGC-independent pathways (Brooks, Patel, and Canal 2014; Munteanu et al. 2018). This light dependent regulation works in conjunction with light independent tuning of excitability performed by ipRGCs. The interaction between these regulatory pathways modulates the overall light response of the developing retina, which is essential to complete retinogeniculate eye-specific segregation (Tiriac et al. 2018).

1. 6. PECULIARITIES OF THE DIFFERENT RGCs SUBTYPES AND RETINORECIPIENT TARGETS

Synaptic contacts by retinal afferents exhibit differences on each target. All ipRGCs are glutamatergic, but within the glutamatergic synaptic buttons two main categories can be distinguished based on their size and synaptic properties: large class 1 boutons and small class 2 boutons (Petrof and Sherman 2013). Class 1 boutons are seen as drivers, while class 2 boutons use to carry out a modulatory role. Conventional RGCs display class 1 boutons in the dLGN and SC (Hammer et al. 2015), also boutons in ipRGC dorsogeniculated projections and most of the projections going to the OPN are considered class 1. This kind of boutons are adapted to transmit strong signals that elicit fast direct responses. In contrast, ipRGC boutons in the SCN belong to class 2. These boutons are smaller and have a modulatory function (Petrof and Sherman 2013), being appropriate for photoentrainment of the SCN clocks. Such divergence is a consequence of the cross talk of spontaneous activity with this specific trophic factors and electrophysiological dynamics in each target.

RGC axons reach the SC after passing over the LGN and start to innervate both nuclei around E16 (Godement, Salaün, and Imbert 1984). Generally, early arrival correlates with an earlier maturation while axons arriving later to the target mature later (Sretavan and Shatz 1987). However, retinocollicular projections refine and mature during the first postnatal week while retinogeniculate projections mature one week later. Even collaterals from the same RGC show different maturation times for each target (Dhande et al. 2011). Furthermore, critical periods for different activity-dependent refinement exist for each target. In the SC this critical period coincides with cholinergic retinal waves while in dLGN mainly correlates with the glutamatergic stage.

Serotonin signaling has been implicated in activity-dependent mechanisms that refine visual circuits. The transcription factor Zic2, that is expressed specifically in ipsilateral RGCs and specifies ipsilaterally projecting RGCs (Herrera et al. 2003), induces a transient expression of the serotonin transporter Slc6a4/Sert in this population (García-Frigola and Herrera 2010). Therefore, ipsilateral axons

exhibit a high affinity uptake of serotonin (Upton et al. 2002). It is known that the neurotransmitter serotonin interacts with microglial cells that mediate synapse maturation and elimination in the dLGN (Kolodziejczak et al. 2015). This discovery opens a window to the existence of a whole cohort of molecules that would act differentially in contralateral and ipsilateral activity-dependent refinement in specific targets.

vGLUT2 is the only vesicular glutamate transporter expressed by RGCs (Fujiyama et al. 2003; Johnson et al. 2003; Sherry et al. 2003; Stella et al. 2008). In mice lacking vGLUT2 specifically in ipsilaterally projecting neurons (Slc6a4-Cre::vGluT2^{fl}) glutamatergic waves are disrupted in this population and as a consequence, contralateral axons invade the ipsilateral territory decreasing eye specific segregation (Koch et al. 2011). No refinement defects were reported in the SC of these mutant mice indicating once again that glutamatergic waves play a different function in the retino-geniculated than in the retino-collicular projections and, confirming that the visual pathway has different critical periods in each target depending on the local environment. On the other hand, although the ipsilateral territory is enlarged in the dLGN of $\beta2^{-/-}$ mice (Xu et al. 2011), which exhibit altered cholinergic waves, this area is maintained in the Slc6a4-Cre::vGluT2^{fl} mice (Koch et al. 2011), pointing at different maturation and synaptic stabilization times for the contralateral and ipsilateral RGC populations.

In summary, spontaneous activity takes place in the neonatal retina and presents a correlation pattern that encodes spatial information, which is necessary for the precise refinement of retinotopic maps and for eye-specific segregation in the different visual targets. However, because the different visual targets play different functions, the refinement process in each of them may suit particular requirements. Two types of retinal projections are distinguished in the visual system of mammals to encode binocular vision, ipsilateral and contralateral projections. They respond differently to guidance molecules and present different timeframes in differentiation, targeting and refinement. Given the specific

characteristics of the different retinal projections and visual nuclei, it is possible that the importance of retinal waves and the consequences of impaired activity are different in each particular population. This thesis work aims to perform an in-depth characterization of the peculiarities on the refinement of ipsi- and contralateral axon terminals at the different visual nuclei and the influence of spontaneous retinal activity in this fine-tuning process.

2- OBJECTIVES

The main aim of this thesis project was to investigate whether retinal waves are necessary for the refinement of retinal afferents in non-image forming nuclei in which topography and eye-specific segregation are not as important features as in image-forming nuclei.

In order to address this issue we set two main objectives:

1. To establish and characterize two conditional mouse lines with altered spontaneous activity in ipsilateral and contralaterally projecting RGCs.

2. To analyze the refinement of RGC axon terminals at the different visual nuclei in these two mouse lines.

3- MATERIALS AND METHODS

3.1 ANIMALS

Mice were housed in a timed-pregnancy breeding colony at the Instituto de Neurociencias de Alicante, Spain. Females were checked for vaginal plugs at approximately noon each day. E0.5 corresponds to the day when the vaginal plug was detected, with the assumption that conception took place at approximately midnight. Conditions and procedures were approved by the IN Animal Care and Use Committee and met European (2013/63/UE) and Spanish regulations (RD 53/2013). Every mouse line used in this study is maintained in C57BL/6J genetic background.

Kir2.1eYFPF$^{fl\text{-}Stop}$ mouse was generated using human Kir2.1 cDNA obtained from Dr. Guillermina López-Bendito's lab in Instituto Neurociencias de Alicante, which was subcloned in pEYFP-N1 to add the reporter protein enhanced YFP in open reading frame at the C-terminal of Kir2.1. Subsequently, it was subcloned in A-102 with a CAG promoter and a flP-flanked STOP cassette upstream the transgene. The construct probed to induce Kir2.1 expression in electroporated HEK293 cells, producing inward potassium (Ik) currents that do not occur in control (Figure 3.1). The linearized and purified construct was injected in mice oocytes (CEBATEG, Barcelona). Brn3b-Cre line was obtained from Dr. George Vann Bennet's laboratory in Duke University Medical Center. Sert-Cre line (Tg(Slc6a4-cre)ET33Gsat) was obtained from GENSAT Project at Rockefeller University (Stock Number: MMRC. 031028-UCD). Its founder genetic background was FVB/N but mice were back-crossed to C57BL/6J. Rosa^{TdTm} mouse line (B6.Cg-Gt(ROSA)26Sortm14(CAG-tdTomato)Hze/J) was obtained from Jackson laboratories (007914). Zic2CreER line (Zic2CreER1463) was obtained from Rudiger Klein's laboratory in Max Planck Institut für Biochemie in Munich, Germany. CreER was inserted into the first codon of the Zic2 gene (in the ATG), so Zic2 is not overexpressed. It also contains a neo cassette flanked by fl sites.

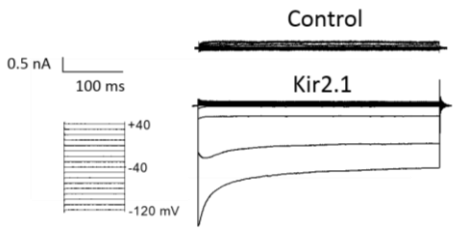

Figure 3.1: Kir2.1 overexpressing cells exhibit premature spontaneous action potentials. Whole cell recordings of Ik currents recorded in lipofected HEK 293 cells expressing Kir2.1 channel using the indicated protocol at a holding potential of -60 mV.

3.2 RETINAL CTB-ALX ANTEROGRADE LABELING

Mice younger than 5 days old were anaesthetized burying them in ice for 3 minutes. In the case of mice older than one week isoflurane were used instead. Whole-eye anterograde labelling was performed using a Nanoject II Auto-Nanoliter Injector (Drummond, 3-000-204) injecting twice on opposite points of the retina with 0.5µl of cholera toxin B subunit conjugated with Alexa Fluor 488/555/647 (Invitrogen, C34775/C22843/C34778).

3.3 TAMOXIFEN ADMINISTRATION

Tamoxifen (Sigma, F5392) was dissolved in warm corn oil (Sigma, F9665) at the desired concentration and stored at 4°C. It was administered by intraperitoneal injections into pregnant mice. The treated mothers have problems in childbirth, so cesarean section was performed on the final day of pregnancy and the offspring were raised using foster mothers.

3.4 SACRIFICE AND TISSUE COLLECTION

Mice were sacrificed one-two days after the anterograde tracer injection in order to allow its active transport across the optic nerve. They were administered an overdose of isoflurane and perfused transcardially with tempered 4% paraformaldehyde (PFA) in 0.1M PBS. Retinas and brains were incubated O/N in the same PFA solution at 4ºC and stored in PBS.

3.5 RETINAL ENUCLEATION

Early after birth, P0 pups were anaesthetized and binocularly injected with CTB-Alx at P0, as described in 3.2 section, to ensure that no retinal projections remain after enucleation. The next day, the animals were anaesthetized and monocularly enucleated, days in advance of the targets' innervation. The retina was replaced with a small piece of absorbent gauze with coagulation solution.

3.6 IMMUNOFLUORESCENCE

PFA fixed tissue was embedded in 3% agarose diluted in PBS, then sectioned in vibratome. Sections were incubated in blocking solution (0.2% gelatin, 5% FBS, 0.005-0.01% Tx) at RT for 1h. Incubation with primary antibodies diluted in blocking solution was applied O/N at 4ºC. The posterior incubation with secondary antibodies diluted 1:1000 in blocking solution was performed for 2h at RT. Before and after each incubation, sections were washed 3 times in PBS. The next primary antibodies were used at the specified concentrations: rabbit anti-Dsred Pab (Clontech, 632496) (1:500), rabbit polyclonal Kir2.1 (Abcam, ab65796) (1:500), chicken anti-GFP (Aves Lab, GFP-1020) (1:1000), rabbit anti-Zic2 (homemade) (1:2000), rabbit polyclonal anti-melanopsin (Advanced targeting systems, AB-N38) (1:2500). Antigen retrieval was performed before blocking for anti-Brn3a and anti-Zic2.

For whole-mount retinas, the protocol was the same used for sections but Triton concentration was increased to 1% and a methanol pre-treatment was added. It includes successive washes with 25%-50%-80%-100% methanol/H2O for 20'' at RT, a bleaching in 3% H2O2 in methanol for 1h at RT, two washes in methanol, rehydration in 80%-50%-25% methanol/PBS 20' each at RT and blocking in 5% BSA PBST (3% Tween) for 1 hour at RT.

3.7 BRAIN CLARIFICATION:

Clarification section from iDISCO protocol (Renier et al. 2014) (December 2016) was performed in mice injected intraocularly with CTB-546 and CTB-647. Briefly, samples are dehydrated in methanol/H2O series (20%-40%-60%-80%-100%-100%) 1h each at RT. Then samples were incubated 3h, with shaking, in 66% Dichloromethane /methanol at RT, and then washed in 100% dichloromethane (Sigma, 270997) to wash the methanol. Finally, brains were incubated and stored in a glass tube totally filled with DiBenzylEther (Sigma, 108014) at RT. Nuclei with contralateral projections labelled with CTB-546 and ipsilateral with CTB-647 were selected.

3.8 IMAGE ACQUISITION

Images from tissue sections were captured using Olympus FV1000 confocal IX81 microscope and FV10-ASW software (Olympus). Acquisitions from clarified brains were made using a Light Sheet microscope (LaVision Ultramicroscope II) and LaVision BioTec Inspector Pro (LaVision). 3D rendering and processing were carried out in Imaris 9.1.2 (Bitplane).

3.9 IMAGE ANALYSIS AND STATISTICS

Images were processed in the ImageJ distribution Fiji (Schindelin et al. 2012) in order to denoise, enhance, threshold, co-localize or measure areas and distances, depending on the type of quantification. In all cases, background fluorescence was subtracted from sections using a rolling ball filter and gray scale was renormalized so that the range of gray-scale values was from 0 to 256. Data obtained from the image analysis were loaded into R 3.6.0 (R Core Team 2019) to perform mathematical calculations and generate some of the graphs. Statistical analysis and the rest of graphs were carried out using GrapPhad Prism version 6.00 (GraphPad Software). Figures and graphs were edited with Adobe Illustrator CS6 (Adobe Systems Inc.). Error bars indicate ± SEM. (**$p < 0.01$, ***$p < 0.001$, Student's unpaired t test). Envelope functions of cumulative distributions and Ripley's function were computed using SEM.

3.9.1 R-distribution:

Eye-specific segregation in dLGN was quantified using methods described in detail in Torborg, et al. (Torborg and Feller 2004). Three consecutive 70-micron coronal sections from the central part of the nucleus were selected per sample, and all analyses were performed on the side with ipsilateral projections labeled by Alexa Fluor 546 and contralateral projections by Alexa Fluor 488. dLGN nuclei were delineated in order to exclude label from the optic tract and IGL. The intensity threshold was set at 5 and empty pixels in both channels were discarded. For each pixel we computed the logarithm of the intensity ratio ($\mathrm{R} = \log_{10}(F_I/F_C)$), where F_I is the fluorescence intensity in the ipsilateral channel and F_C is the fluorescence intensity in the contralateral channel. To allow the calculation of the logarithm, the remaining zero-value pixels were replaced by 0.01. Pseudo-color images were generated from the distribution to facilitate visualization. Range [-0.5,+0.5] was considered non-segregated area and [+1.75,+2.5] as ipsidominant area. The ipsilateral territory was obtained by comparing the pixels with ipsilateral signal to the total number of pixels of the dLGN.

3.9.2 Analysis in the superior colliculus:

5-6 consecutive 100-micron sagittal sections from the medial part of the superior colliculus were included per sample, selecting the side with Alexa Fluor 546-labeled contralateral and Alexa Fluor 488-labeled ipsilateral projections. After preprocessing, intensity threshold was applied using “moments” algorithm. The misplacement of ipsilateral projections in the stratum *griseum superficiale* was normalized by the total ipsilateral signal. The distance of each pixel with ipsilateral signal to the surface of the superior colliculus was calculated using an Exact Euclidean Distance Transform. To study ipsilateral scattering, Ripley's function was computed, when the distribution takes higher values than the one corresponding to the control, it is a more clustered configuration and vice versa. For both analysis, data from the different

sections were aggregated and the resulting vector was rescaled so that each replica contains the same number of points.

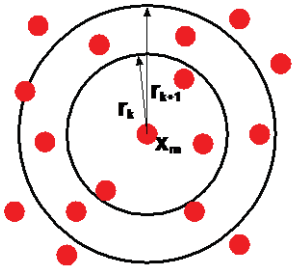

$$\widehat{K}(r) = \frac{a}{n(n-1)} \sum_i \sum_j I(d_{ij} \leq r) e_{ij}$$

3.9.3 CTB-Alx colocalization:

The intersection between the ipsilateral and the contralateral channel was computed using their corresponding binary masks, generated using the "IsoData" algorithm to the Z-stacks. Binocular overlap was always normalized using the total area of the nucleus. For dLGN, the same sections selected for the R-distribution were analyzed here. Ollivary pretectal nuclei with contralateral projections labelled with Alx-488 and ipsilateral with Alx-546 were selected. Two consecutive 70-micron coronal sections were averaged per sample

3.9.4 Suprachiasmatic nucleus density maps and ipsilateral-contralateral proximity analysis:

All 60-micron coronal sections of the nucleus were analyzed, being aggregated by sample and averaged by group. In co-localization of Alx with TdTomato, pixels with signal for both Alx-488 and Alx-647 were discarded because of the inability to assign them to a specific input. Proximity analyses of ipsilateral projections to contralaterals were conducted in Sert-Cre::Rosa^{TdTm} mice. Regions with high CTB-Alx accumulation were selected as an approximation to synaptic buttons, considering as ipsilateral projections the area positive for the corresponding CTB-Alx and TdTomato. Contralateral projections were determined by a stringent exclusion of TdTomato+ areas since Sert-Cre line labels the ipsilateral

population of RGCs completely. In the computation of the density maps, the sum of the two sides of the nucleus was considered as the total signal. In addition, both channels were averaged and signal intensity was normalized prior to grouping the samples.

3.9.5 Quantification of apoptotic retinal cells:

Immunostaining against caspase-3 was performed as described in methods section for immunofluorescence. The three 60-micron coronal retinal sections with the maximum diameter where selected for each animal. 3-4 subjects per condition were analyzed, comparing control Brn3b-Cre mice and Kir2.1eYFP$^{fl\text{-}Stop}$::Brn3b-Cre mice at three ages, P2, P6 and P9 . Only positively stained cells located in the ganglionar cell layer were considered, and the recount was normalized dividing by the total area of the layer.

3.10 ELECTROPHYSIOLOGY

Retinas were extracted from P4 or P9 mice and placed in artificial cerebrospinal fluid solution (ACSF) at 4 ºC, containing (in mM): 126 mM NaCl, 26 mM $NaHCO_3$, 10 mM Glucose, 5 mM $MgCl_2$, 3 mM KCl, 1.25 mM NaH_2PO_4, 1 mM $CaCl_2$. pH of the ACSF solution was tampered using carbogen (5% CO2 and 95% oxygen) and the resulting osmolarity was ~310 mOsmol/Kg. Further, retinas were subjected to enzymatic digestion with collagenase/dispase diluted in ACSF (1:3) for 15-20 min at 35ºC with carbogen. Collagenase/dispase mix was prepared as follow: 155 mM NaCL, 1.5 K_2PO_4, 10 mM HEPES, 5 mM glucose), collagenase type XI (Sigma, D9542) 900 uni/ml, dispase (BDBiosciences, 10103578.001) 5.5 uni/ml.

Recordings were performed using a Leica DMI 3000B inverted microscope and constant perfusion with ACSF solution at ~37 ºC. Temperature was controlled by a feedback Peltier device CL-

100 (Warner Instruments, Hamdem, CT, USA). The images were acquired using an Orca ER CCD camera (Hamamatsu Photonics K.K., Hamamatsu, Japan). Whole-cell patch clamp experiments were performed in current configuration using a Multiclamp 700B amplifier, pCLAMP 10 software and a Digidata 1322A (Molecular Devices, Sunnyvale, USA). Borosilicate electrodes were pulled using a puller P-1000 (Sutter instrument) with resistance ranging between 4 to 8 MΩ and filled with an intracellular solution containing: 115 mM K-gluconate, 25 mM KCl, 9 mM NaCl, 10 mM HEPES, 0.2 mM EGTA, 1 mM $MgCl_2$, 3 mM K_2-ATP and 1 mM Na-GTP adjusted to pH 7.2 with KOH (280–290 mOsmol/kg). Td-tomato$^+$ cells were selected and held at -60 mV. Data were sampled at a frequency of 20 KHz and low-passed filtered at 10 KHz. Series of depolarizing steps of 20 pA were using to induce action potentials (AP), and cells were stimulated supra threshold using 100 pA over rheobase to identify burst or tonic responses. Data analyzed were: size, rheobase, resting membrane potential and threshold. Further, we recorded responses at resting membrane potential for 5 min. Firing frequency was measured and the firing patterns were classified as tonic/train, bursts, oscillations/events or no responses (NR). The data were analyzed with the Clampex 10.1 software (Molecular Devices Corp., Sunnyvale, CA, USA). Statistical analyses were performed with Origin Pro8 software (OriginLab Corporation) and the data are reported as the mean ± SEM: Significance was set as *$P < 0.05$, ** $p<0.01$ and *** $p<0.001$ as assessed by Student's t-test.

3.10 MATERIALS

NAME	Producer	Catalog nº	Packaging
Agarose D1 Low EEO	Conda Pronadisa	Cat nº 8010	1 kg
Tween 20	Sigma	P1379	100 ml
Triton X-100	Sigma	T8787	100 ml
Phosphate Buffered Saline Tablets	VWR	97062-732	200
Dichloromethane	Sigma	270997	1 L
Benzyl ether	Sigma	108014	1 kg
Methanol	J.T.Baker	8402	2.5 L
Ethanol absolute pure	Panreac	50019100	1 L
Isoflurane	Zoetis	C34775	250 ml
Cholera Toxin Subunit B (Recombinant), Alexa Fluor™ 488 Conjugate	ThermoFisher	C22843	500 µg
Cholera Toxin Subunit B (Recombinant), Alexa Fluor™ 555 Conjugate	ThermoFisher	C34778	500 µg
Cholera Toxin Subunit B (Recombinant), Alexa Fluor™ 647 Conjugate	ThermoFisher	14175053	100 µg
HBSS, no calcium, no magnesium, no Phenol red	ThermoFisher	25200-056	500 ml
Trypsin	Gibco	18047-019	100 ml
Deoxuribonuclease I	Invitrogen	112372	20K U
Ethyl cinnamate	Sigma	T5648	100 g

Tamoxifen	Sigma	F5392	5 g
FGF2	SIgma	354235	1 µg
Dispase	BDBiosciences	10103578.001	100 ml
Collagenase	Sigma	D9542	100 mg
DAPI	Sigma	G6144	1 mg
Gelatin from porcine skin	Sigma	11773	500 g
Mowiol 20-98	Sigma	C8267	250 g
Corn oil	Sigma	F9665	500 ml
Fetal Bovine Serum	Sigma		500 ml

Primary antibodies

	Specie	Company	Catalog	Dilution
Antiliving colors Dsred Pab	Rabbit	Clontech	632496	1:500
Anti-Calbindin D-28k	Rabbit	Swant	CB-38a	1:1000
Polyclonal Kir2.1	Rabbit	abcam	ab65796	1:500
GFP	Chicken	AVES LABS	GFP-1020	1:1000
ChAT	Goat	Chemicon	AB144P	1:500
Brn3a	Mouse	Chemicon	MAB1585	1:300
Tuj1	Mouse	Covance	MMS-435P	1:1000
Zic2	Rabbit	Housemade	-	1:2000
Islet1-2	Mouse	Hybridoma Bank	39.4D5	1:500
Syntaxin-1	Mouse	Synaptic Systems	110011	1:100
Ap2a	Mouse	Santa Cruz	sc-12726	1:500

Chx10	Mouse	Santa Cruz Biothecnologies	sc-365519	1:100
Melanopsin Polyclonal	Rabbit	Advanced targeting systems	AB-N38	1:2500

Secondary antibodies

	Specie	Company	Catalog	Dilution
Anti-rabbit IgG Alexa 546	Donkey	Invitrogen	A10040	1:2000
Anti-rabbit IgG Alexa 488	Donkey	Invitrogen	A21206	1:2000
Anti-chicken IgY Alexa 488	Donkey	Jackson Inmunoresearch	703-545-155	1:2000
Anti-goat Alexa 647	Donkey	Invitrogen	A21447	1:2000
Anti-mouse IgG Alexa 488	Goat	Invitrogen	A11001	1:2000
Anti-mouse IgG Alexa 546	Donkey	Invitrogen	A10036	1:2000
Anti-mouse IgG Alexa 546	Donkey	Invitrogen	A10036	1:2000
Anti-Mouse Alexa 633	Goat	Invitrogen	A21052	1:2000

Instruments

Device	Name	Company
Micro injector	Nanoject II Auto-Nanoliter Injector	Drummond
Vibratome	Leica VT1000 S	Leica
Stereomicroscope	Leica MZ16 F, Fluorescence Stereomicroscope	Leica
Power supply unit	ebq100	Leica
Camera	Leica DFC350FX	Leica

OLYMPUS CONFOCAL	Olympus FV1000 confocal IX81 microscope	Olympus
Power supply unit (fluorescence)	X-Cite Series 120Q	Lumen Dynamics
Objectives	Olympus IX2-VCB	Olympus
Controller	Proscan III	Prior
Argon Laser	Argon Laser GLS3135	Showa Optronics
Wavelength Conversion Yellow Laser	Opti λ 559 589	Acal BFi
Software	FV10-ASW	Olympus
LIGHT SHEET	LaVision Ultramicroscope II	LaVision
Microscope	Olympus MVX-10 microscope	Olympus
Objectives	Olympus MVPLAPO 2x	Olympus
Camera	Andor Neo sCMOS camera	Andor
Laser	SuperK EXTREME EXW-12, white light laser	NKT Photonics
Software	LaVision BioTec ImSpector Software	LaVision

4- RESULTS

4.1 CONDITIONAL EXPRESSION OF KIR2.1 IN RETINAL GANGLION CELLS

In order to investigate the influence of spontaneous retinal waves in different visual nuclei in the ipsilateral and contralateral RGC populations, we generated a transgenic mouse line in which the potassium inward rectifier channel Kir2.1 is conditionally expressed when the premature stop codon is removed by the action of the cre-recombinase (Kir2.1eYFP$^{fl\text{-}Stop}$) (Figure 4.1A, see methods for further details). We then combined this line with two cre-lines specific for each populations of RGCs (Figure 4.1A):

i/ A previously reported knock-in line in which the cre-recombinase is inserted into the *POU4F2/Brn3b* locus (Brn3b-Cre line) (Fuerst et al. 2012; Simmons et al. 2016) to express Kir2.1 mostly in contralaterally projecting RGCs.

ii/ A previously reported transgenic line in which the cre-recombinase is inserted into the *Slc6a4/Sert* locus (Sert-Cre line) (Koch et al. 2011) to express Kir2.1 in ipsilaterally projecting RGCs.

To validate and characterize these conditional lines we first analyzed the expression of Kir2.1 in the retinas of P11 Brn3b-Cre::Kir2.1eYFP$^{fl\text{-}Stop}$ and Sert-Cre::Kir2.1eYFP$^{fl\text{-}Stop}$ mice. We did not find Kir2.1 expression in the retinas of control Kir2.1eYFP$^{fl\text{-}Stop}$ mice but both Kir2.1 and eYFP were clearly detected in Brn3b-Cre::Kir2.1eYFP$^{fl\text{-}Stop}$ and Sert-Cre::Kir2.1eYFP $^{fl\text{-}Stop}$ retinas (Figure 4.1B). To track recombination in the cre lines, we also crossed them with a TdTomato reporter line (Rosa^{TdTm}) (Figure 4.1C). We then confirmed that in the Brn3b-line, the majority of the RGCs positive for the marker of contralateral RGC Brn3a expressed TdTomato (Figure 4.1D; left). On the other hand, in the Sert-line those cells that express the marker for ipsilateral RGC Zic2 were positive for TdTomato (Figure 4.1D; right). We also performed intraocular injections of the anterograde tracer Cholera Toxin subunit B fused to different Alexa fluorophores (CTB-Alx) into the eyes of both mouse lines (Figure 4.4A). The contralateral eye was injected

with CTB-Alx647 and the ipsilateral with CTB-Alx488; the dLGN of these mice were analyzed. Projections

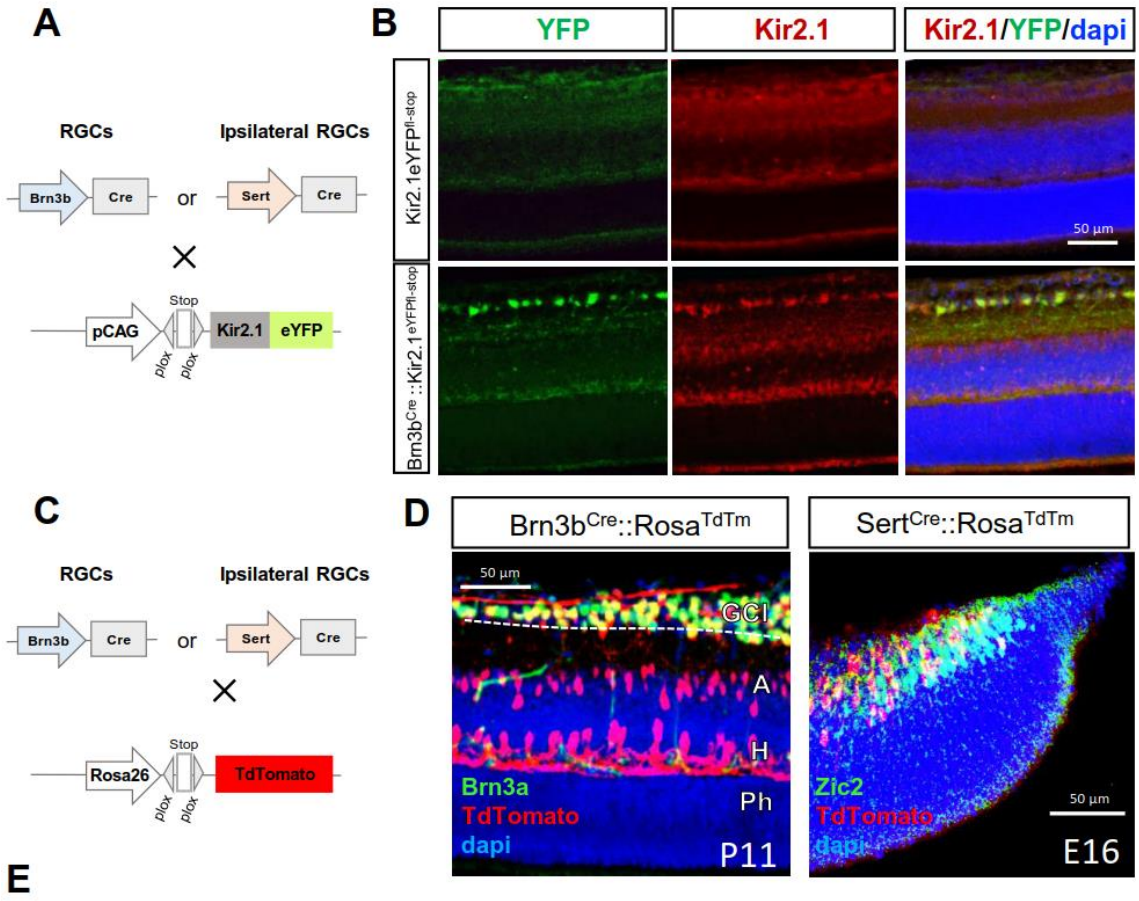

Figure. 4.1: Kir2.1eYFP$^{fl\text{-}Stop}$ mouse specifically express Kir2.1 upon Cre recombination. (A) Schemes illustrating the gene constructs for (i-ii) Kir2.1eYFP$^{fl\text{-}Stop}$, (i) Brn3b-Cre and (ii) Sert-Cre lines. **(B)** Radial retina sections from wildtype and Brn3b-Cre::Kir2.1eYFP$^{fl\text{-}Stop}$ mice stained with **α**Kir2.1 (red) and **α**YFP (green) antibodies revealed that Kir2.1 expression is specifically drived by cre recombination. **(C: two columns on the left)** Radial retina sections at the indicated stages from Brn3b-Cre::Rosa^{TdTm} (upper row) and Sert-Cre::Rosa^{TdTm} (bottom row) mice stained with the stated antibodies showed that Kir2.1 expression colocalizes with markers for RGCs. **(E)** Coronal dLGN sections displaying retinal projections labeled with CTB fused to Alexa fluorophores (ipsilaterals: CTB-Alx488, contralaterals: CTB-Alx647) stained with **α**TdTomato antibody (red) show that retinal input from recombined RGCs occupy the whole mucleus in Brn3b-Cre::Rosa^{TdTm}, and the ipsilateral territory in Sert-Cre::Rosa^{TdTm} mice.

from recombined RGCs visualized in coronal sections through the dLGN of these reporter lines demonstrated the specificity of these cre-lines (Figure 4.1E).

4.2 ECTOPIC EXPRESSION OF KIR2.1 IN RGCs GENERATES UNCORRELATED PATTERNS OF SPONTANEOUS ACTIVITY

To evaluate the impact of Kir2.1 ectopic expression in the physiology of RGCs, we performed whole cell patch-clamp recordings in both Brn3b-Cre::Kir2.1eYFP$^{fl\text{-}Stop}$ and Sert-Cre:: Kir2.1eYFP$^{fl\text{-}Stop}$ mice, which were also crossed with the reporter Tomato line (Rosa^{TdTm}) in order to better visualize Kir2.1 overexpressing RGCs. In control mice, RGCs execute action potentials in response to calcium fluxes arising from the retinal waves, separated by a characteristic refractory period (Figure 4.2A, blue). Due to this behavior, neighboring cells are able to fire at the same time, producing a strong correlation that will lead these projections to refine together (Torborg and Feller 2005; Torborg et al. 2005). However, in RGCs overexpressing Kir2.1, regardless of the cre-line used, arbitrary firing pattern was independent of the refractory periods (Figure 4.2A, green). As expected, Kir2.1 overexpression leads a significant decrease in the resting potential of TdTomato positive cells recorded from both Brn3b-Cre::Kir2.1eYFP$^{fl\text{-}Stop}$::Rosa^{TdTm} or Sert-Cre::Kir2.1eYFP$^{fl\text{-}Stop}$::Rosa^{TdTm} retinas when compared to their respective controls (Figure 4.2B). It is known that the different subpopulations of RGCs differ in their electrophysiological properties. Accordingly, in control mice we observed a large majority of cells responding with events (depolarization that not evoke an action potential) and bursts of activity, a small number of cells with train responses, and some cells without response (Figure 4.2C; left). In contrast, in mice overexpressing Kir2.1, the amount of RGCs with train responses was doubled in the Brn3b-Cre line and three-folded in the Sert-Cre line and we did not find unresponsive cells (Figure 4.2C; rigth). These results indicated a net increase in neuronal activity and the quantification of the firing frequency in the registered cells showed that while the sum of events and burst remains constant, the number of action potentials is significantly

increased when Kir2.1 is overexpressed (Figure 4.2D). The hyperpolarization of the resting potential produced by Kir2.1 overexpression could lead to a sensitization, so that stimuli which would only evoke events in control cells would be enough to produce action potentials. This phenomenon was even more evident at earlier stages. Recordings in P4 mice showed that control cells still do not fire action potentials at this stage (Figure 4.2E; blue line), but in triple mutant mice Brn3b-Cre::Rosa^{TdTm}::Kir2.1eYFP$^{fl\text{-}Stop}$ a solid activity was observed (Figure 4.2E; green line). Immunostaining against Caspase 3 in the retinas of Kir2.1

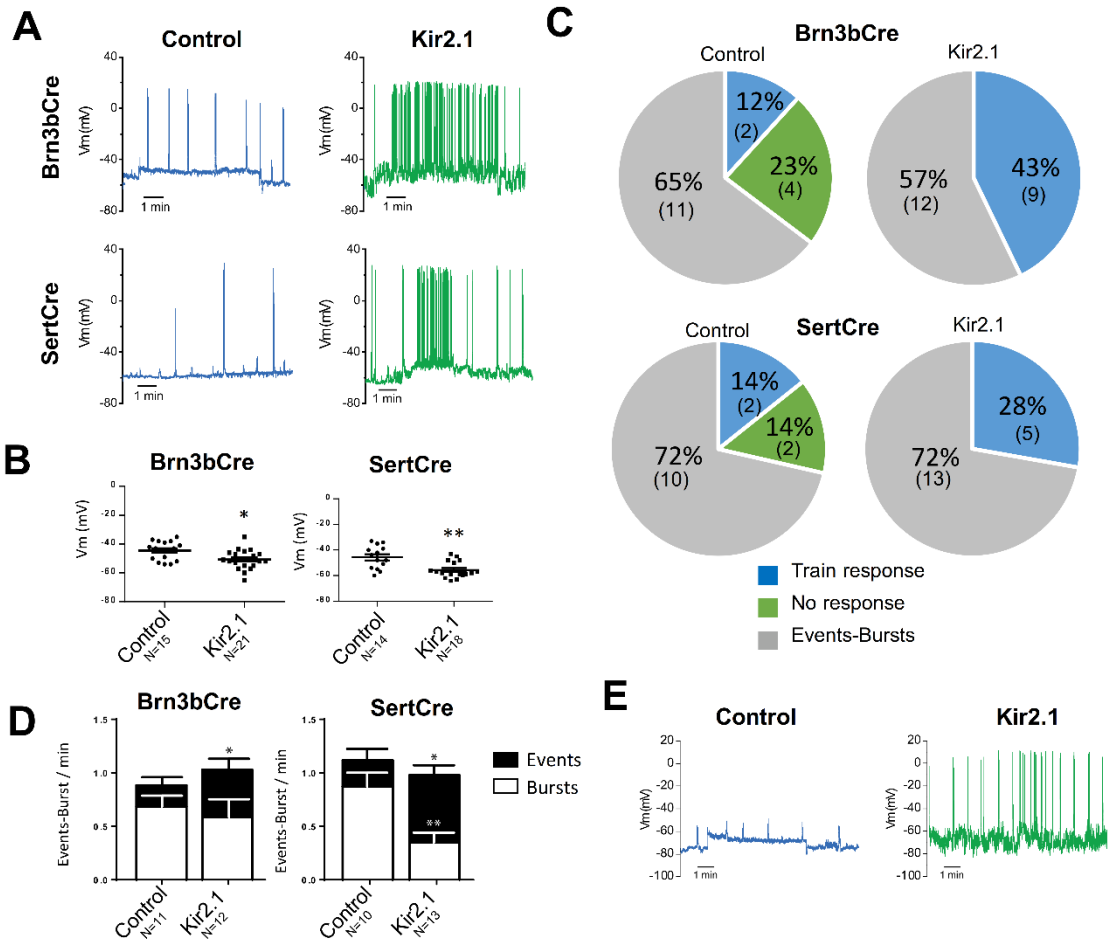

Figure 4.2: Kir2.1eYFP$^{fl\text{-}Stop}$ mouse exhibits a more active but disorganized electrophysiological behavior. (A) Patch-clamp recordings from control Brn3b-Cre or Sert-Cre neurons and Kir2.1eYFP$^{fl\text{-}Stop}$::Brn3b-Cre or Kir2.1eYFP$^{fl\text{-}Stop}$::Sert-Cre neurons in current clamp configuration at -60 mV. Control RGCs periodically fire action potentials spaced by refractory periods while Kir2.1 overexpressing cells exhibit unpatterned spontaneous activity. (B) Resting membrane potential. (C) Recorded cells organized according to their activity pattern. (D) Firing frequency distinguishing between events and bursts. (E) Patch-clamp recordings in neurons from Brn3b-Cre and Kir2.1eYFP$^{fl\text{-}Stop}$::Brn3b-Cre P4 mice in current clamp configuration at -60 mV. Error bars indicate ±SEM (***$p < 0.001$, Student's unpaired T-test).

overexpressing-mice discarded an increase in apoptosis due to the observed altered electrophysiological behavior (Figure 4.3), indicating that although Kir2.1-overexpressing cells show increased activity, they do not die. These results show that RGCs ectopically expressing Kir2.1 have an arbitrary increase in spiking frequency that likely generate uncorrelated patterns of retinal activity

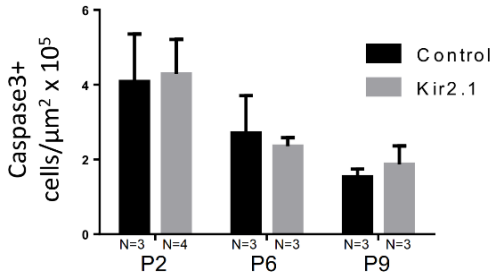

Figure 4.3: Kir2.1 overexpression do not induce apoptosis in RGCs. Quantification of apoptotic cells (caspase3+) comparing control Brn3b-Cre and Kir2.1eYFP$^{fl\text{-}Stop}$::Brn3b-Cre mice. Error bars indicate ±SEM (***p < 0.001, Student's unpaired T-test).

preventing the transmission of spatial information normally encoded by retinal waves.

4.3 GENETIC ALTERATION OF RETINAL WAVES IN RGCS PRODUCES EYE-SPECIFIC SEGREGATION DEFECTS IN THE VISUAL THALAMUS

A critical role for retinal waves in the refinement of retinal terminals at the visual nuclei has been widely stated in numerous studies (Ackman and Crair 2014). Kir2.1eYFP$^{fl\text{-}Stop}$ mice exhibit aberrant spontaneous activity in the retina and consequently, they should exhibit defects in visual axons refinement at the targets. To confirm that this is the case, we injected CTB fused to a far-red (Alx647) or green (Alx488) fluorophores respectively into each eye (Figure 4.4A) and analyzed the extent of labelling overlay in the dLGN. In neonatal stages, ipsi and contralateral axons project intermingled in the dLGN, so that sections of this nucleus from P4 mice with altered activity are indistinguishable from those of wild type mice. (Figure 4.4B, first column).

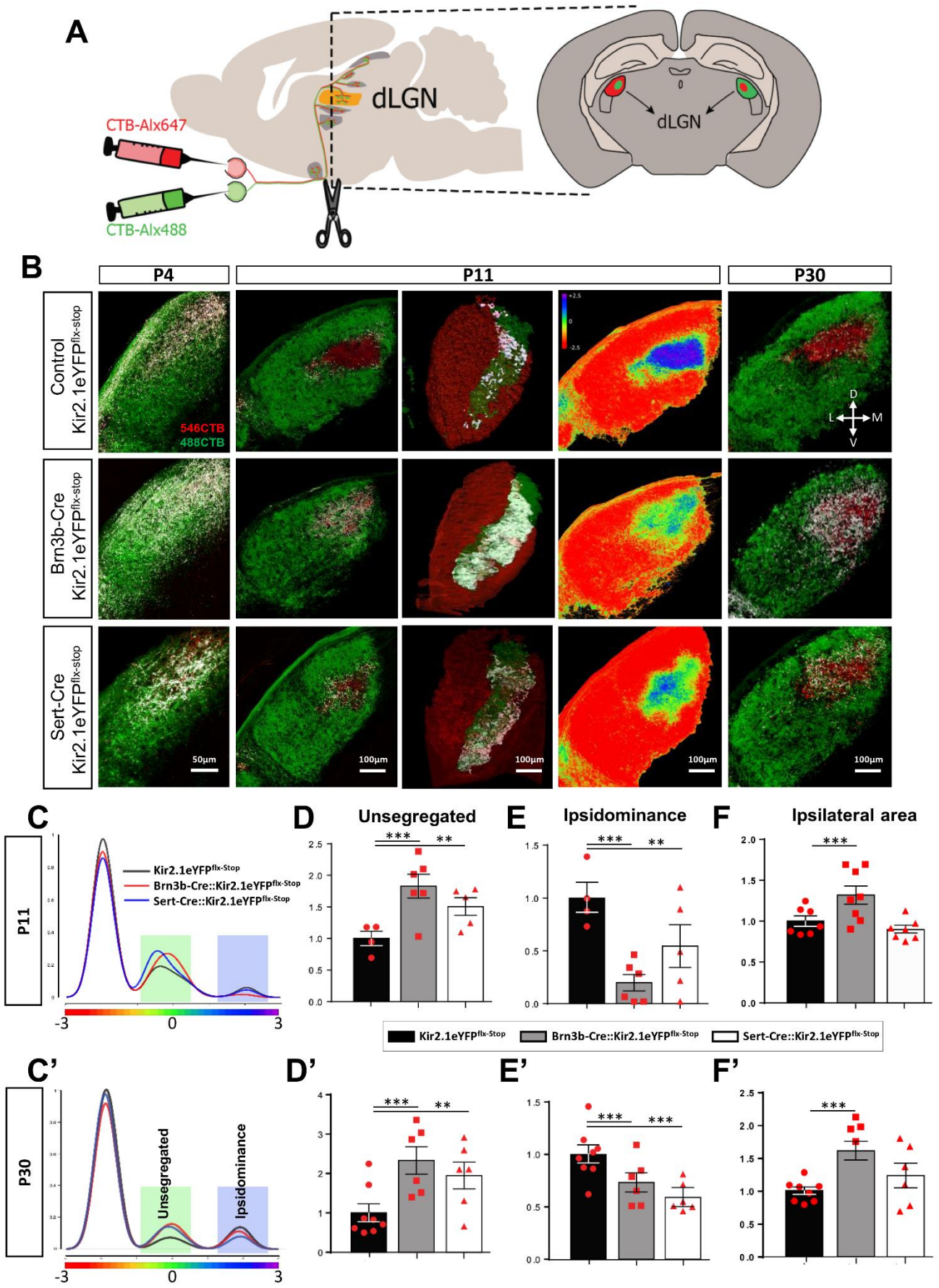
A
dLGN
CTB-Alx647
CTB-Alx488
dLGN
B
P4
P11
P30
Control Kir2.1eYFPflx-stop
Brn3b-Cre Kir2.1eYFPflx-stop
Sert-Cre Kir2.1eYFPflx-stop
546CTB
488CTB
D
L
M
V
50µm
100µm
C
P11
Kir2.1eYFPflx-Stop
Brn3b-Cre::Kir2.1eYFPflx-Stop
Sert-Cre::Kir2.1eYFPflx-Stop
-3
0
3
D
Unsegregated
E
Ipsidominance
F
Ipsilateral area
***
**
C'
P30
Unsegregated
Ipsidominance
D'
E'
F'

Figure 4.4: Kir2.1eYFP$^{fl\text{-}Stop}$ mice exhibit eye specific segregation defects in dLGN. (A) Scheme illustrating the experimental paradigm consisting in intraocular injections of cholera toxin subunit B fused to different Alexa fluorophores for each eye (ipsilateral: CTB-Alx488, contralateral: CTB-Alx647). dLGN nuclei were analyzed at P11 and P30. **(B, first, second and fifth columns)** Coronal dLGN sections from P4 (first column), P11 (second column) and P30 (fifth column) showing contralateral retinogeniculate projections in green, ipsilateral in red and overlapping areas in white. Eye-specific segregation is clearly altered in both Kir2.1eYFP$^{fl\text{-}Stop}$::Brn3b-Cre or Kir2.1eYFP$^{fl\text{-}Stop}$::Sert-Cre mice compared to control at P11 and P30. **(B, third column)** 3D reconstruction of P11 dLGN in a coronal perspective. **(B, fourth column)** R distribution (log[ipsilateral/contralateral]) from P11 coronal dLGN sections (second column) representing contralateral dominant area in red, unsegregated in green and ipsilateral dominant in blue. **(C-C')** Histogram representing an average of the R-distribution for each group. **(D-D')** Unsegregated area [-0.5,0,5] and **(E-E')** ipsilateral dominant area (>1.75) were obtained from the R distribution. **(F-F')** Portion of dLGN occupied by ipsilateral projections. **(D-F)** Measures are showed in fold-change values normalized with their corresponding Kir2.1eYFP$^{fl\text{-}Stop}$ control. Error bars indicate ±SEM (***p < 0.001, Student's unpaired T-test).

At P11, when segregation between ipsilateral and contralateral terminals is finished (Godement et al. 1984; Pham et al. 2001; Upton et al. 1999), we observed a well-defined ipsilateral territory with no presence of contralateral innervation in control mice (Figure 4.4B, second and third column, overlapping in white). dLGN sections were then converted to R-distribution (Figure 4.4B, fourth column; $\log[F_{ipsilateral}/F_{contralateral}]$), which can be averaged and represented as histograms (Figure 4.4C) to determine the relative contribution of both retinal inputs in each image. In this analysis we observed that control mice exhibit an ipsi-dominant area (Figure 4.4B, third column; blue/purple). In contrast, Brn3b-Cre::Kir2.1eYFP$^{fl\text{-}Stop}$ mice showed unsegregated retinal inputs from both eyes at the dLGN (white) (Figure 4.4B, second and third columns; Figure 4.4D). In addition, these mice had no clear ipsi-dominant area (Figure 4.4B, fourth column, green; Figure 4.4E) and an expanded area receiving ipsilateral axons (Figure 4.4F) compared to the controls.

In the Sert-Cre::Kir2.1eYFP$^{fl\text{-}Stop}$ mice in which only ipsilateral projections are affected, there was also a significant lack of segregation but the phenotype was milder than in the Brn3b-Cre::Kir2.1eYFP$^{fl\text{-}Stop}$ mice (Figure 4.4B-D). In this case, there was a decrease in the dominance of ipsilateral terminals (Figure 4.4E), but the area occupied by ipsilateral axons was similar to the controls (Figure 4.4F).

The disruption in the segregation of ipsi and contralateral terminals at the dLGN was not corrected after the onset of visual stimulus, as observed in P30 animals (Figure 4.4B fifth column; Figure 4.4D'). In contrast to what we observed at P11, where the defects in ipsi-dominance at the dLGN vary in the two mouse lines, ipsi-dominance defects are similar in both genotypes at P30, although they were still significantly different from the control mice (Figure 4.4E'). The fact that both lines show similar defects at longer times could be explained by the decrease in the density of projections that usually occurs along the visual stimuli dependent refinement period.

During refinement, Hebbian mechanisms strengthen correlated synapses while eliminating the uncorrelated ones, decreasing synaptic density and increasing synaptic strength. Since Kir2.1eYFP$^{fl\text{-}stop}$ displays an unpatterned spontaneous activity in the presynaptic terminals, we wondered whether the

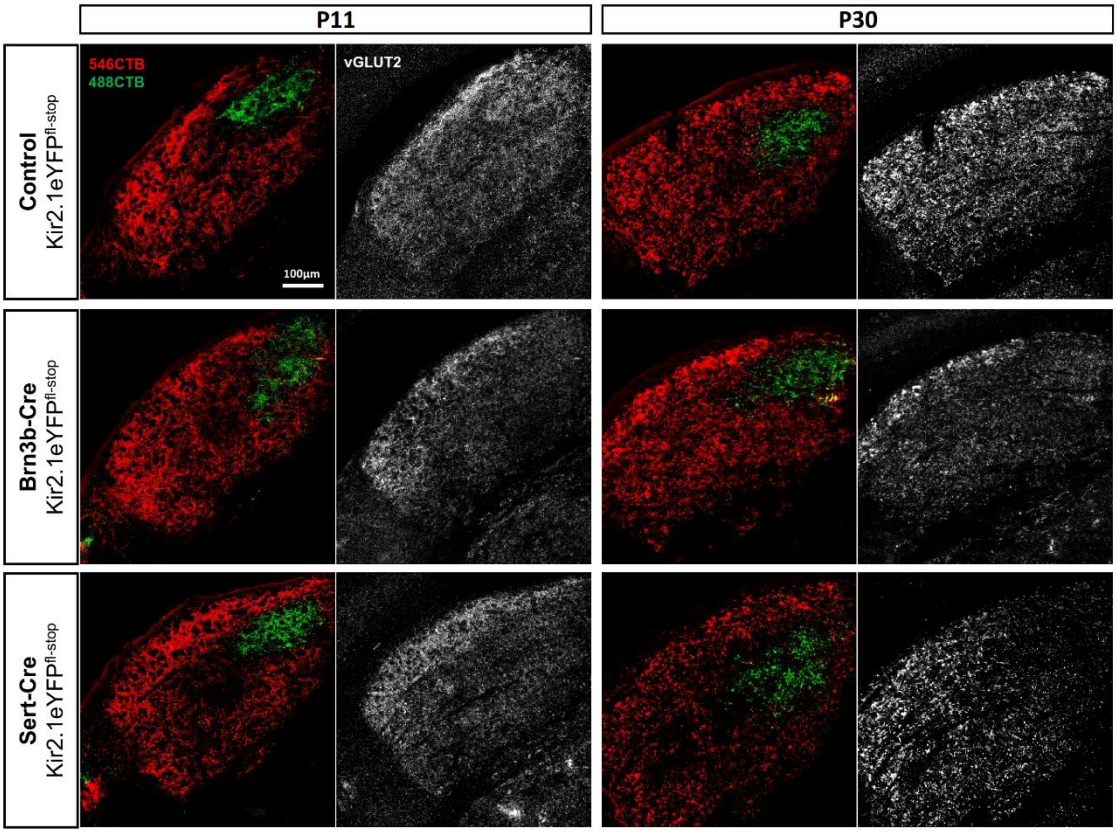

Figure 4.5: Kir2.1 overexpressing RGCs exhibit a glutamatergic maturation deffect in retinogeniculate terminals. Coronal P11 dLGN sections from control Kir2.1eYFP$^{fl\text{-}Stop}$, Brn3b-Cre::Kir2.1eYFP$^{fl\text{-}Stop}$ and Sert-Cre::Kir2.1eYFP$^{fl\text{-}Stop}$ mice at the indicated stages. Contralateral retinogeniculate projections are labeled in red (CTB-Alx 546) and ipsilaterals in green (CTB-Alx 546). Sections were stained with αvGlut2 (white).

observed segregation defects are due to problems in bouton clustering and synaptic maturation. To analyze this process, we performed immunofluorescence in coronal dLGN sections for vGLUT2, a presynaptic glutamatergic marker specific for retinal afferents in this target (Figure 4.5, left). Control mice exhibit a clear punctate vGLUT2 labeling over the whole nucleus, as a result of a correct synaptic maturation. However, in the Brn3b-Cre::Kir2.1eYFP$^{fl\text{-}stop}$ mice, the fluorescence is faint and scattered through the tract of the retinal projections in contralateral and ipsilateral territories, suggesting a severe impairment in the refinement and maturation of both retinal inputs. In the case of Sert-Cre::Kir2.1eYFP$^{fl\text{-}stop}$ mice, the defective distribution of vGLUT2 seems to be more diffused for the ipsilateral projections, precisely those whose spontaneous activity has been altered. This impairment in synaptic maturation persist at P30 (Figure 4.5, right), revealing that visually evoked activity is not able to rescue this phenotype.

4.4 GENETIC ALTERATION OF RETINAL WAVES IN RGCS PRODUCES AXON REFINEMENT DEFECTS IN THE SUPERIOR COLLICULUS

This image-forming nucleus consists on a series of layers that expand during the first postnatal week. RGC projections coming from both eyes initially grow along the SC surface. As the nucleus grows and the layers are defined, ipsilateral terminals retract. At P11, most ipsilateral projections have refined and are located in in the deeper layer of the SC, the SO, concentrated in dense areas or patches (Figure 4.6B'). Contralateral afferents remain in the SGS layer which is more superficial (Figure 4.6B).

In order to track retinal projections at the SC, we injected CTB fused to a different fluorophore into each eye and selected the medial sagittal sections of the SC to analyze all the cases (Figure 4.6A). In contrast to control animals that showed no invasion of ipsilateral axons into the SGS (Figure 4.6B', 4,6E), a significant amount of ipsilateral projections were aberrantly located into the SGS of Brn3b-

Cre::Kir2.1eYFP$^{fl\text{-}Stop}$ mice (Figure 4.6C', 4.6E) and distributed closer to the SC surface at P11 (Figure

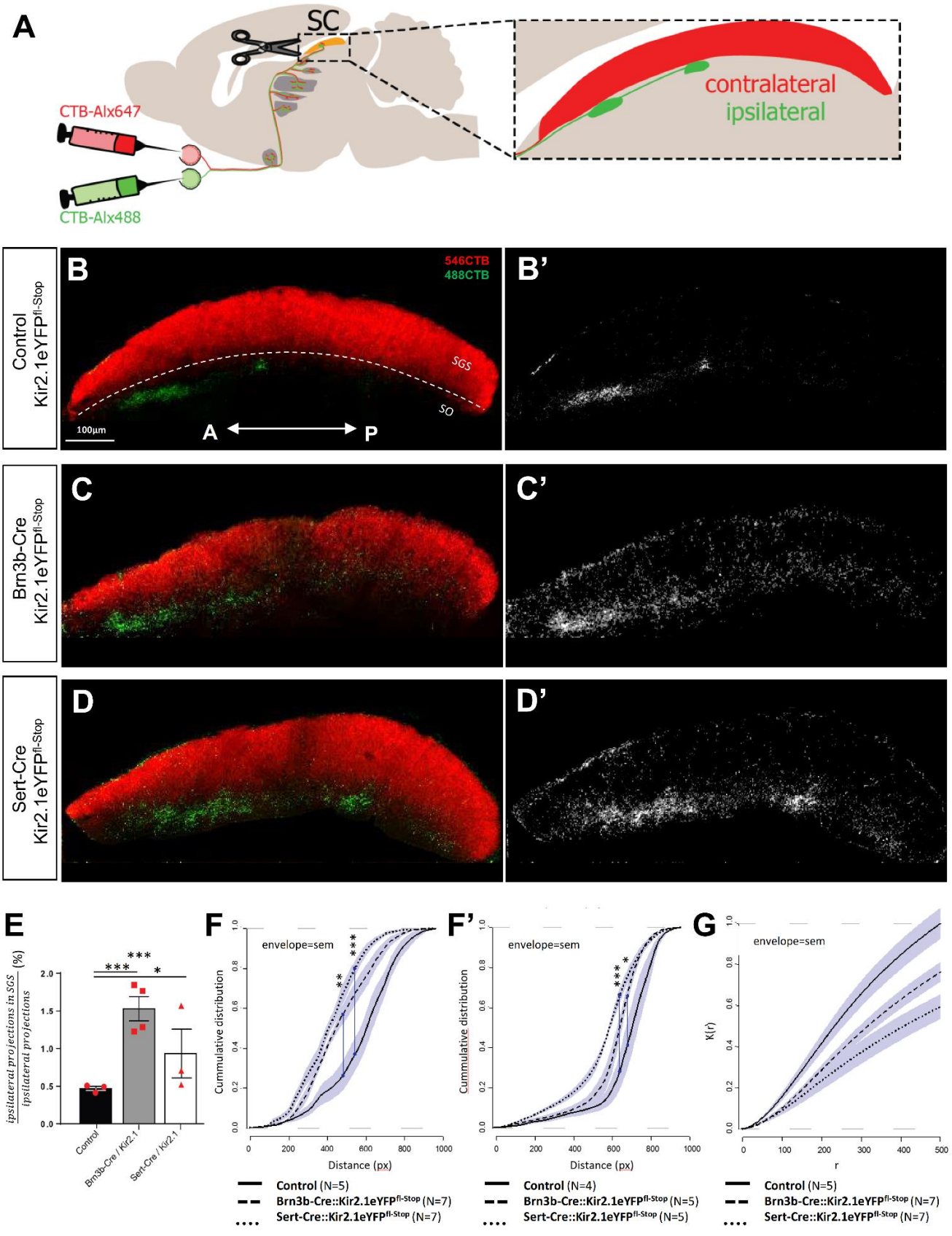

Figure 4.6: Refinement of the ipsilateral retinal input to the SC is disrupted in Kir2.1eYFP$^{fl\text{-}Stop}$ mice. (A) Scheme illustrating the experimental approach consisting in intraocular injections of CTB fused to different Alexa fluorophores for each eye (ipsilateral: CTB-Alx488, contralateral: CTB-Alx647). SC nuclei from P11 and P30 subjects were analyzed. **(B-D)** SC sagital sections at P11 showing CTB labelling of retinocollicular projections. **(E)** Portion of psilateral projections invading the SGS. **(F-F')** Cummulative distribution of the distance of ipsilateral projections to the SC surface in P11 **(F)** and P30 **(F')** mice. **(G)** Ripley's function corresponding to retinocollicular ipsilateral projections in P11 mice, showing a more scattered distribution in Brn3b-Cre::Kir2.1eYFP$^{fl\text{-}Stop}$ and Sert-Cre::Kir2.1eYFP$^{fl\text{-}Stop}$ mice than in Kir2.1eYFP$^{fl\text{-}Stop}$ control mice. Error bars indicate ±SEM (***p < 0.001, Student's

4.6F). In Sert-Cre::Kir2.1eYFP$^{fl\text{-}Stop}$ mice, this defect was less evident (Figure 4.6D-F). This process takes place just after birth and by P4, eye-specific layering is almost completely defined. As in the dLGN, refinement defects were not rescued by experience-driven activity in adult mice (Figure 4.6F').

In the SO, ipsilateral axons do not gather as dense patches as they normally do in wildtype mice, indicating that intra-eye refinement is also affected in the absence of correlated retinal activity (Figure 4.6B', 4.4C', 4.6D'). By dispersion analysis we found that ipsilateral terminals were significantly more scattered in Brn3b-Cre::Kir2.1eYFP$^{fl\text{-}Stop}$ mice compared to the controls while exhibited an intermediate phenotype in Sert-Cre::Kir2.1eYFP$^{fl\text{-}Stop}$ mice (Figure 4.6G). We should take into account that Brn3b-Cre line drives recombination in collicular cells (Figure 4.7). On the other hand, Sert-Cre line induces recombination in a residual population of contralateral RGCs (Figure 4.8). These issues and their repercussions have been addressed in the discussion.

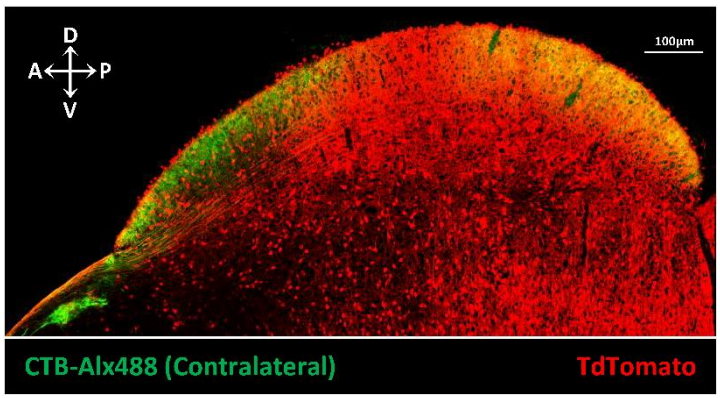

Figure 4.7: Recombination in SC relay cells by Brn3b-Cre line. Sagital SC sections from Brn3b-Cre::Rosa^{TdTm} mice stained with αTdTomato antibody (red). Contralateral projections are labeled with CTB-Alx488 (green). A significant SC neuron population overexpress Kir2.1 in Brn3b-Cre::Kir2.1$^{fl\text{-}Stop}$ mice.

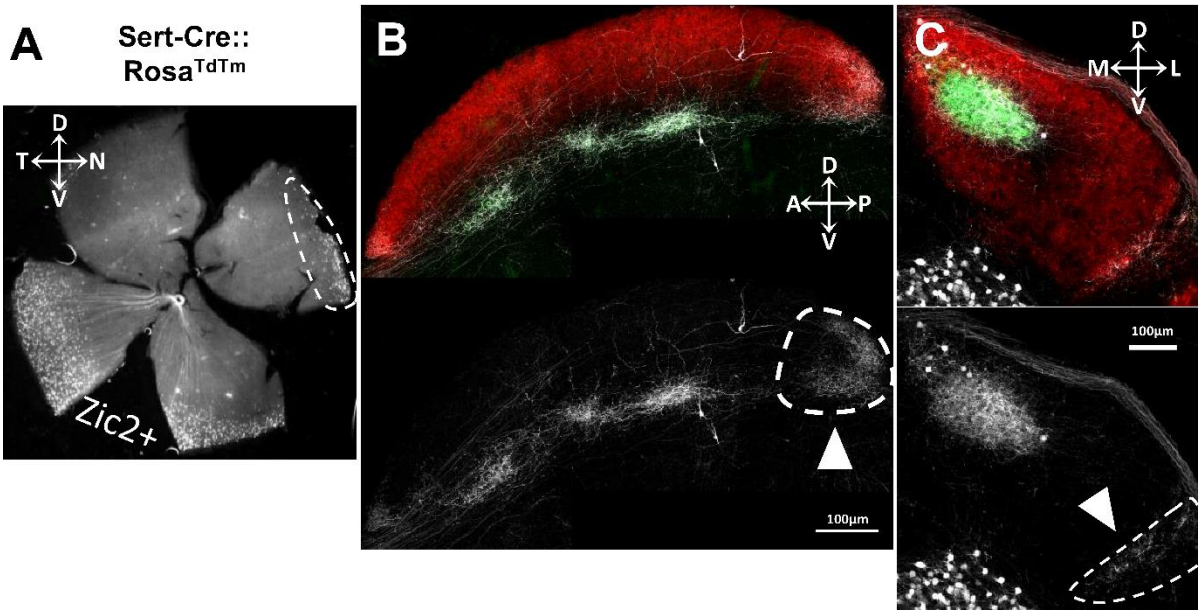

Figure 4.8: Leaky expression in contralateral RGCs driven by the Sert-Cre line. (A) Wholemount retina stained with αTdTomato antibody (white) showing nasal peripheral labeling far from the established ventro-temporal Zic2+ region. **(B)** Sagital SC section stained with αTdTomato antibody (white), showing retinocollicular contralateral projections in red (CTB-Alx647) and ipsilaterals in green (CTB-Alx488). TdTomato^{+} contralateral projections can be found in the posterior part of the nucleus. **(C)** Coronal dLGN section stained with αTdTomato antibody (white) and retinocollicular projections as described in (B). TdTomato^{+} contralateral projections are located in the opposite region of the nucleus to the ipsilateral territory. White dashed lines and white arrows indicate the TdTomato^{+} contralateral labeling.

These results indicate that impairment in the correlation of spontaneous activity in ipsilateral RGCs is sufficient to produce defects in both eye-specific segregation and intra-eye refinement and these effects are magnified when contralateral projections are also affected.

4.5 SPONTANEOUS ACTIVITY IN NON-IMAGE FORMING NUCLEI

Both Brn3b-Cre:: and Sert-Cre::Kir2.1eYFP$^{fl\text{-}Stop}$ mice exhibit defective refinement that affects eye specific segregation and fine-tune retinotopic mapping in image-forming nuclei. However, not all the retinal targets have a function in the processing of spatial information. As mentioned before, intrinsically photosensitive RGCs innervate the suprachiasmatic (SCN) as well as nuclei in the pretectal area (PTN) providing irradiance information. The functions of these nuclei are not related to spatial information and therefore, we wondered whether the refinement of visual terminals in these non-image forming nuclei is

affected by the alteration of retinal waves as much as in the image-forming nuclei. To address this issue, we analyzed the refinement of retinal axons in the SCN and PTN of Brn3b-Cre::Kir2.1eYFP$^{fl\text{-}Stop}$ and Sert-Cre::Kir2.1eYFP$^{fl\text{-}Stop}$ mice.

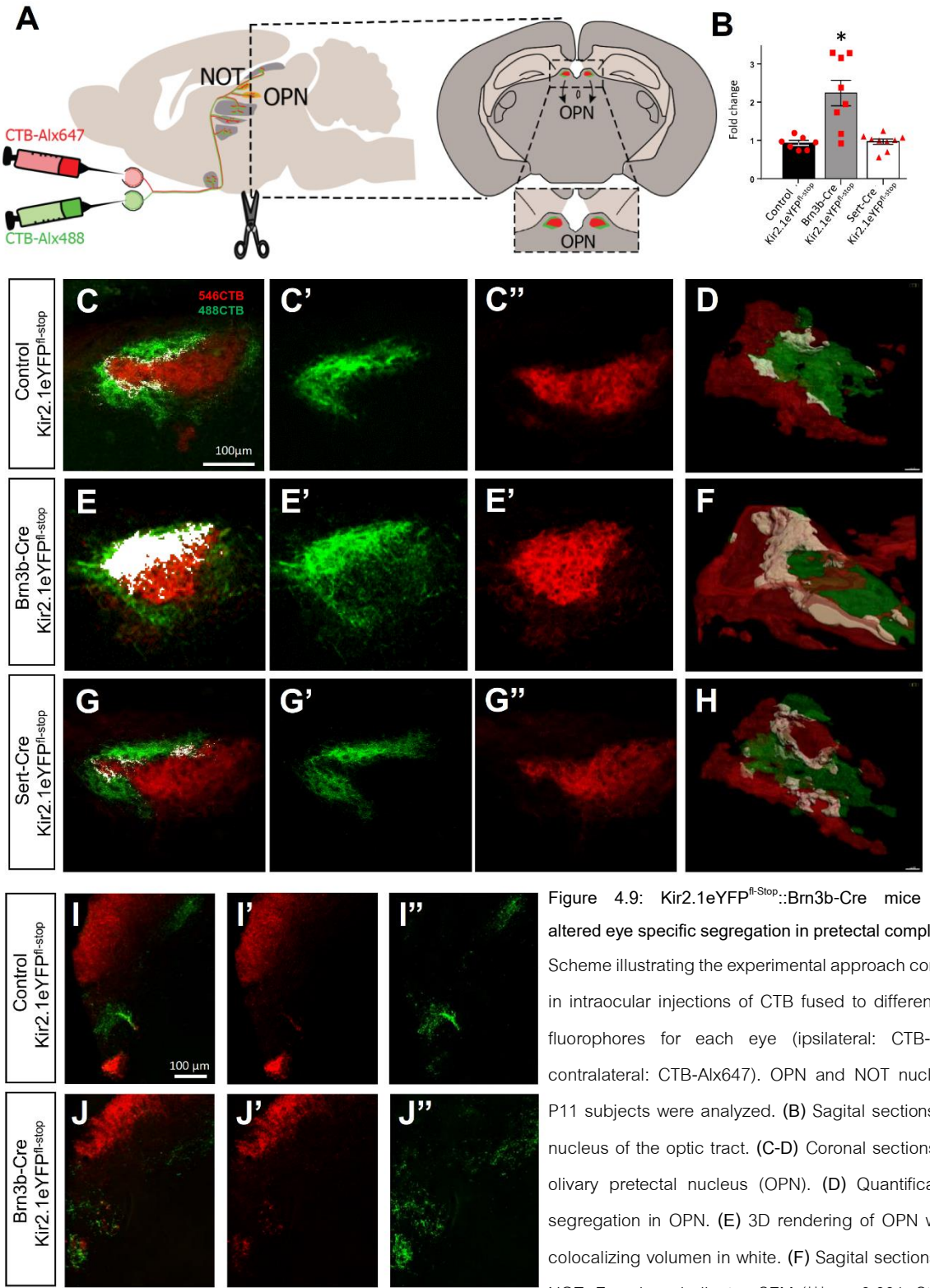

Figure 4.9: Kir2.1eYFP$^{fl\text{-}Stop}$::Brn3b-Cre mice exhibit altered eye specific segregation in pretectal complex. **(A)** Scheme illustrating the experimental approach consisting in intraocular injections of CTB fused to different Alexa fluorophores for each eye (ipsilateral: CTB-Alx488, contralateral: CTB-Alx647). OPN and NOT nuclei from P11 subjects were analyzed. **(B)** Sagital sections of the nucleus of the optic tract. **(C-D)** Coronal sections of the olivary pretectal nucleus (OPN). **(D)** Quantification of segregation in OPN. **(E)** 3D rendering of OPN with the colocalizing volumen in white. **(F)** Sagital sections of the NOT. Error bars indicate ±SEM (***p < 0.001, Student's unpaired T-test).

4.5.1. The olivary pretectal nucleus

The PTN is located in an region anterior to the SC and comprises seven different nuclei including the olivary pretectal nucleus (OPN) and the nucleus of the optic tract (NOT) (Gamlin 2006). Coronal and sagittal sections from mice that were intravitreally injected with CTB fused to different fluorophores into each eye were analyzed (Figure 4.9A). In the NOT, Brn3b-Cre::Kir2.1eYFP$^{fl\text{-}Stop}$ mice exhibited clear eye-specific segregation defects (Figure 4.9I-J). However, the diffuse distribution, tiny size and heterogeneity between subjects displayed by this nucleus did not allow us to perform a systematic quantification of the NOT in the Sert-Cre mice. In the OPN, ipsi and contralateral retinal inputs project into adjacent areas with almost no overlay in control animals (Figure 4.9B, 4.9C-D). In this nucleus, segregation defects were clearly detected in Brn3b-Cre::Kir2.1eYFP$^{fl\text{-}Stop}$ mice (Figures 4.9B, 4.9E-F) but Sert-Cre::Kir2.1eYFP$^{fl\text{-}Stop}$ mice displayed no alterations (Figures 4.9B, 4.9G-H). Unlike in the dLGN, innervation occurs sequentially in the OPN (Baver et al. 2008; Hattar et al. 2002, 2006; Osterhout et al. 2014; Quattrochi et al. 2019). At P1, contralateral axons reach the core and their refinement is completed by P5. In contrast, ipsilateral projections arrive at P4 and do not retract to the shell until P10 (Marques and Clarke 1990). The sequential axon arrival to this nucleus could explain the absence of defects observed in Sert-Cre:: Kir2.1eYFP$^{fl\text{-}Stop}$ mice.

4.5.2. The suprachiasmatic nucleus

The SCN is located in the diencephalon just behind the optic chiasm. Although it is located close to the retina if compared to other visual nuclei, the SCN is innervated at the same time than the SC and the dLGN, meaning that collateral branches innervate this nucleus days after RGC axons decided to cross or not the midline at the optic chiasm region (Sekaran et al. 2005; Sernagor 2005). Melanopsin (OPN4)-expressing cells (ipRGCs) are the only RGCs innervating this target and are distributed over the whole retina forming a network (Figure 4.10-A) (Prigge et al. 2016; Sekaran et al. 2003). ipRGCs constitute 2%

of the total RGC population (Berson et al. 2002; Do and Yau 2010; Hattar et al. 2002; McNeill et al. 2011; Schmidt et al. 2011) but it is unclear whether this percentage is maintained among the population of ipsilaterally-projecting RGCs. To address this issue, we incubated retinas from Sert-Cre:: Rosa^{TdTm} mice with OPN4 antibodies. Interestingly, we found a two-fold increase in the number of OPN4 RGCs among the ipsilateral population (4.32%) compared to the total population of RGCs (Figure 4.10-A'; 4.10-B, top). Ipsilateral RGC constitute only ~3% of the total RGCs, but our measurements indicated that 1/10 of the ipRGCs project ipsilaterally (Wang et al. 2016) (Figure 4.10-B, bottom). This enrichment is likely reflecting the necessity of ipsilaterally projecting RGCs to include the different ipRGCs subtypes (M1-M6) that innervate the diversity of visual targets.

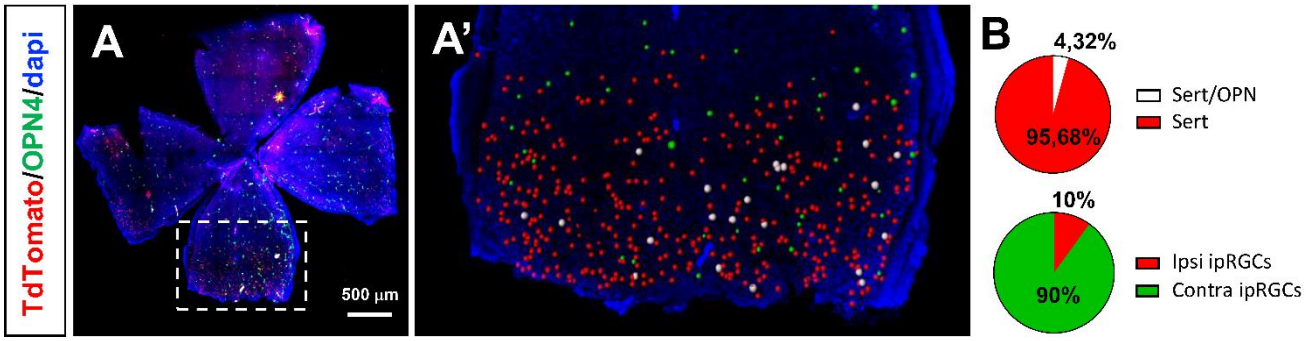

Figure 4.10: Ipsilateral RGC population is enriched in ipRGCs. (A) Whole-mount retina from Sert-Cre::Rosa^{TdTm} mice at P9 stained with αOPN4 (green) and αTdTomato (red) antibodies. **(B)** Quantification of ipRGCs (OPN4^{+} cells) showing an enrichment in ipsilateral RGC population compared with the contralateral.

It has been shown that in the SCN, unlike in the rest of the visual nuclei, contralateral RGCs send collaterals to both sides (Fernandez et al. 2016) (Figure 4.11). Supporting these observation we have seen by analysis of the SCN in Brn3b-Cre:: Rosa^{TdTm} mice monocularly injected with CTB-Alx488 and CTB-Alx647 (Figure 4.12A-B), that about half of the axons projecting contralaterally in this nucleus also project to the ipsilateral SCN (Figure 4.12D). To determine whether ipsilaterally-projecting RGCs, as contralateral RGCs, send collaterals to innervate the opposite side of the SCN, we analyzed the SCN of Sert-Cre:: Rosa^{TdTm} mice (Figure 4.12C). In this case, because Sert^{+}-neurons from the raphe nucleus also innervate the SCN (Welsh et al. 2010), we had to inject CTB-Alx647 monocularly and analyze

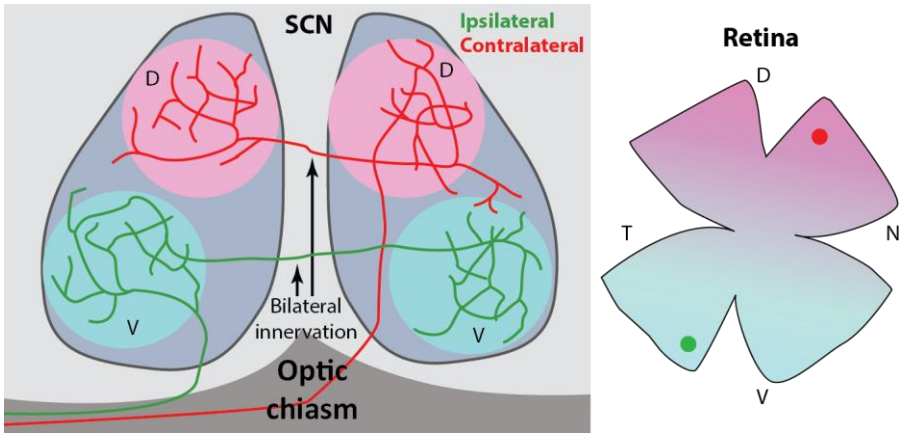

Figure 4.11: Bilateral innervation of retinal afferents to the SCN. Both contralateral and ipsilateral axons can cross the midline to elaborate arbors in both sides of the nucleus. Each ipRGC project to the SCN according to its location in the retina. In this way, all ipsilateral ipRGCs project to the ventral SCN since they are dristributed in the ventrotemporal retina.

TdTomato/CTB-Alx647 arbors in order to specifically label ipsilateral RGCs terminals. Moreover, we enucleated Sert::Rosa^{TdTm} mice to assure specific analysis of ipsilateral projections. In enucleated animals, the contralateral SCN was still ostensibly targeted by Sert+ projections. This result suggests that ipsilateral terminals target both sides of the nucleus (Figure 4.12C'). Strikingly, we noticed that almost 40% of the ipsilateral area corresponds to bilateral branches elaborated by ipsilateral ipRGCs (Figure 4.12D).

These data suggested that OPN4/Sert RGC also project bilaterally in the SCN as the rest of the OPN4 ipRGCs. To further confirm this issue, we analyzed a tamoxifen-inducible conditional mouse line that specifically labels ipsilateral RGCs (Zic2-CreER::Rosa^{TdTm} mice). The transcription factor Zic2 specifies ipsilateral RGCs (Herrera et al. 2003) but it is also expressed in some neurons at the chiasm region. To avoid TdTomato expression in chiasm cells, we injected tamoxifen at E15.5-16.5 obtaining very few cells labeled at the chiasm and allowing the visualization of only those axons from ipsilaterally projecting RGCs coming from the ventrotemporal retina. Because these mice were not previously characterized, we injected CTB-tracers in each eye and analyzed their dLGN to confirm that TdTomato specifically labels ipsilaterally projecting neurons (Figure 4.12E). TdTomato/CTB-Alx647 axons crossing

from one side of the SCN to the opposite side were observed (Figure 4.12F-F''), definitively confirming that ipRGCs from the ventrotemporal retina that express markers specific for ipsilateral RGCs such as

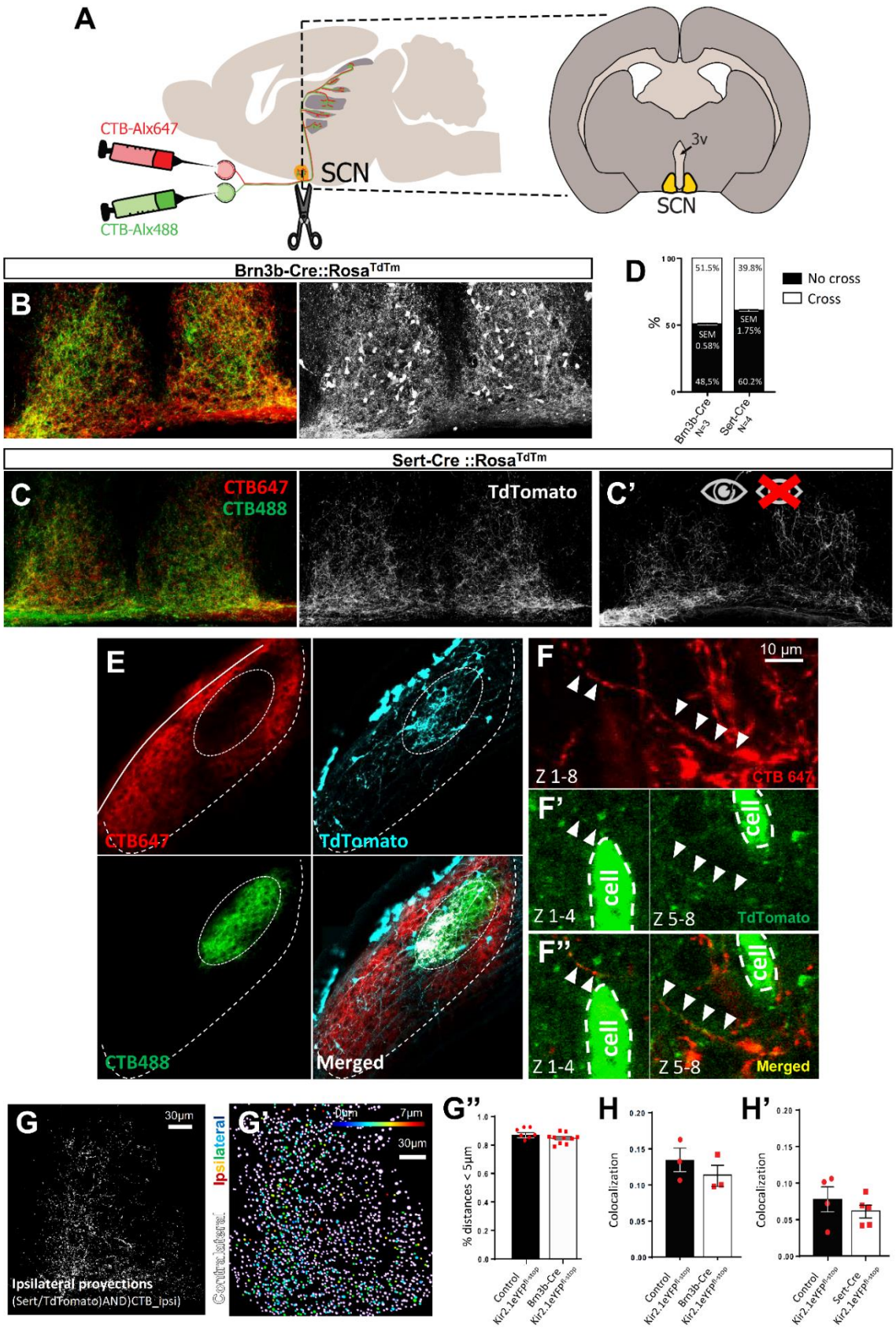

Figure 4.12. Retinal input to the SCN innervate bilaterally and do not perform eye-specific segregation. **(A)** Scheme illustrating the experimental approach consisting in intraocular injections of CTB fused to different Alexa fluorophores for each eye (ipsilateral: CTB-Alx488, contralateral: CTB-Alx647). SCN nuclei from P11 subjects were analyzed. **(B,C,C')** Coronal SCN sections from **(D)** Brn3b-Cre::Rosa^{TdTm}::Kir2.1$^{fl\text{-}Stop}$, **(C)** Sert-Cre::Rosa^{TdTm}::Kir2.1$^{fl\text{-}Stop}$ and **(C')** monocularly enucleated Sert-Cre::Rosa^{TdTm}::Kir2.1$^{fl\text{-}Stop}$ mice stained with αTdTomato antibody. **(D)** Ratio of unilateral/bilateral inervation of TdTomato+ retinal projections to the SCN in Brn3b-Cre::Rosa^{TdTm} and Sert-Cre::Rosa^{TdTm} mice. **(E-F'')** Coronal dLGN **(G)** and SCN **(H)** sections from Zic2-CreER::Rosa^{TdTm} mice stained with αTdTomato antibody and retinal projections labeled with CTB-Alx647 and CTB-Alx488. **(E)** Zic2-CreER::Rosa^{TdTm} mice injected with tamoxifen at E15.5 and E16.5 exhibit recombination in a subset of ipsilateral RGCs. **(F)** We can observe that ipsilateral axons (CTB647^{+}/TdTomato^{+}) are able to cross the midline to project bilaterally. White arrows indicate the path of the axon. **(F'-F'')** The stacked planes for each image are indicated as Z. **(G)** Binary mask of a coronal section of SCN from Sert-Cre::Rosa^{TdTm} mouse showing ipsilateral retinal projections (TdTomato^{+}/CTB-Alx488). **(G')** Ipsilateral (TdTomato^{+}/CTB-Alx488) and contralateral (TdTomato^{-}/CTB-Alx647) terminals were converted into spots. Contralaterals spots are showed in white and ipsilateral spots are colored in a gradient according to how close they are from their nearest contralateral spot. **(G'')** Percentage of ipsilateral spots closer than 5 µm to a contralateral spot. Both retinal inputs project together instead of segregating. **(H-H')** Ipsilateral/contralateral colocalization ratio within the TdTomato^{+} area in coronal SCN sections from **(H)** Brn3b-Cre::Rosa^{TdTm}::Kir2.1$^{fl\text{-}Stop}$ and **(H')** Sert-Cre::Rosa^{TdTm}::Kir2.1$^{fl\text{-}Stop}$ mice compared to their corresponding controls. Error bars indicate ±SEM (***$p < 0.001$, Student's unpaired T-test).

Zic2 or Sert innervate the SCN bilaterally.

To then determine whether axon terminals from ipsilateral and contralateral ipRGCs segregate in the SCN we analyzed Sert-Cre::Rosa^{TdTm} mice injected with CTB (Alx488 and Alx647 in each eye). Almost 90% of the terminals from ipsilateral RGCs were located only within 2µm apart from contralateral axons (Figure 4.12G- G''), meaning that ipsi and contralateral arbors do not segregate in this nucleus and revealing that eye-specific segregation is not a feature of this visual target. We also observed that ipsilateral terminals were restricted to the ventrolateral region of the SCN in the ipsilateral side (Figure 4.13B) and the terminals from ipsilateral RGCs projecting to the other side elaborated arbors in the ventral region in a mirroring manner (Figure 4.13B') delineating a very rudimentary topographic map.

All these results together demonstrate that both ipsi and contralateral ipRGCs project bilaterally into the SCN following a rough topographic map in which terminals from the ipsi and contralateral RGCs do not segregate. Our results agreed with the idea that topography and eye-specific segregation are not

as significant features in the SCN as in image-forming nuclei. We next wondered whether retinal waves are important for the refinement of retinal afferents to this non-image forming nucleus. To address this issue, we analyzed density maps in the SCN of Sert-Cre::Rosa$^{TdTm:}$::Kir2.1$^{fl\text{-}Stop}$ mice and noticed that axons from ipsilateral RGCs were distributed over a larger extension than similar terminals in control mice (Figure 4.13B-B' and 4.13C-C') without increasing the occupied area (Figure 4.13D), suggesting that spontaneous activity plays a role in the refinement of axons innervating the SCN, even when eye-specific segregation and topography do not seem to be as important in this nucleus.

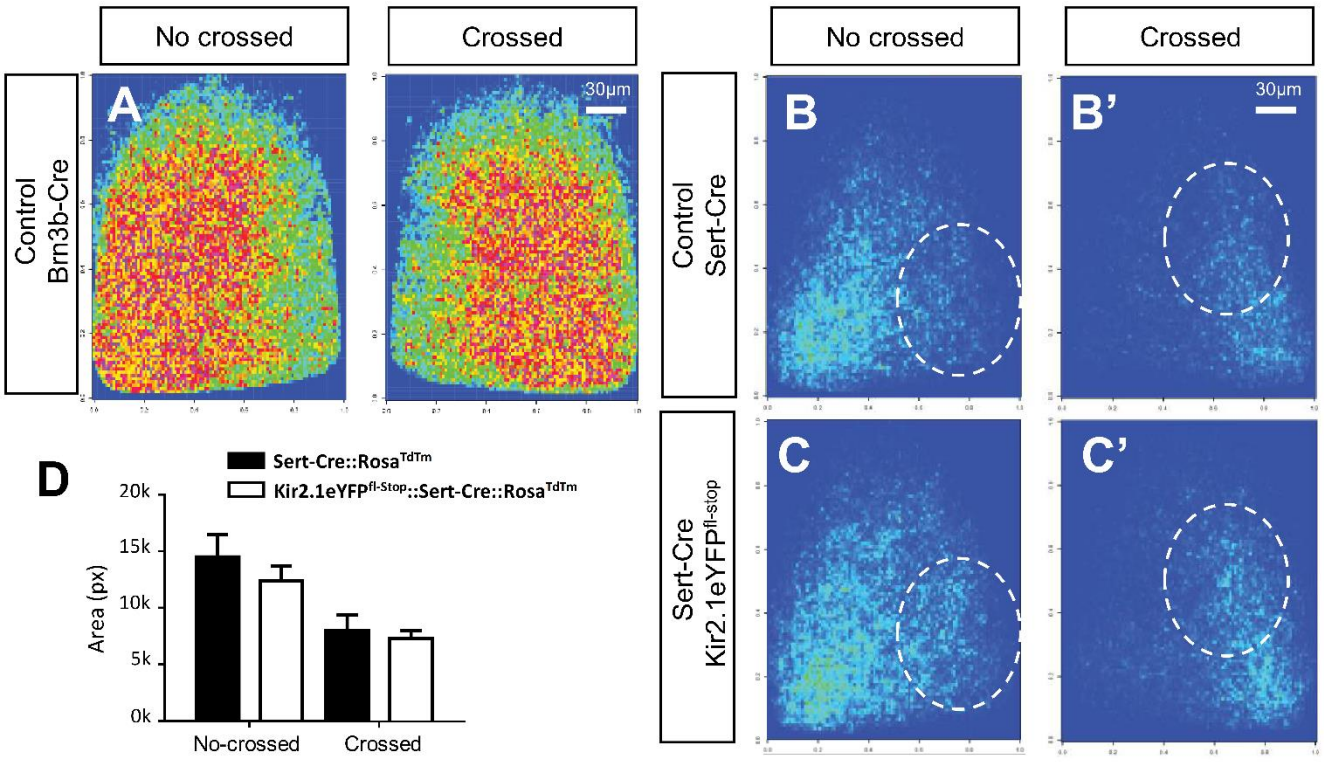

Figure 4.13. Altered eye specific segregation in pretectal complex in Kir2.1eYFP$^{fl\text{-}Stop}$::Brn3b-Cre mice. **(A-C)** Aggregated density maps of coronal SCN sections and averaged by group from **(A)** Brn3b-Cre::Rosa^{TdTm}::Kir2.1$^{fl\text{-}Stop}$ (N=3), **(B)** Sert-Cre::Rosa^{TdTm}::Kir2.1$^{fl\text{-}Stop}$ (N=3) and **(C)** Sert-Cre::Rosa^{TdTm}::Kir2.1$^{fl\text{-}Stop}$ (N=4) mice in both sides of the nucleus. TdTomato^{+}/CTB-Alx647 or TdTomato^{+}/CTB-Alx488 labeled projections from the contralateral **(A)** or the ipsilateral eye **(B-C)** were analyzed. **(D)** Quantification of the area occupied by ipsilateral projections in the density maps showed in (C-C'). Although the total area do not change, the distribution of the ipsilateral terminals in Sert-Cre::Rosa^{TdTm}::Kir2.1$^{fl\text{-}Stop}$ seems to be more scattered than the one displayed by Sert-Cre::Rosa^{TdTm} mice. The dashed white ovals indicate the expanded area in (C-C') compared to (B-B'). Error bars indicate ±SEM (***$p < 0.001$, Student's unpaired T-test).

5- DISCUSSION

5.1 NEURAL SPONTANEOUS ACTIVITY HAS A UBIQUITOUS PRESENCE IN THE DEVELOPING NERVOUS SYSTEM

Neural activity has been shown to be essential in a multitude of processes through the developing nervous system. Spontaneous calcium transients have been already detected in neocortex and thalamus at E16 (Antón-Bolaños et al. 2019; Corlew et al. 2004), modulating neurogenesis (Bonetti and Surace 2010) and neurotransmitter identity (Borodinsky et al. 2004). Programmed cell death is also affected by spontaneous activity levels (Heck et al. 2008; Ikonomidou et al. 1999), as well as neuronal migration. At later stages, dendro- and axonogenesis (Chen and Ghosh 2005; Yamamoto and López-Bendito 2012), axon guidance (Nicol et al. 2007) and myelination (Barrera et al. 2013; Demerens et al. 1996) seem to be also influenced. In the early postnatal period, neuronal activity regulates vessel development and patterning (Lacoste et al. 2014; Whiteus, Freitas, and Grutzendler 2014), CNS (Luhmann et al. 2016), motor (Jiang, Zaaimi, and Martin 2016) and the different sensory systems (Kerschensteiner 2016; Martini et al. 2018; Moreno-Juan et al. 2017; Wang and Bergles 2015). The developing visual system is the circuit in which spontaneous activity has been more deeply studied and discoveries that were initially found in this model, have later been described in other circuits.

Certain diseases or developmental disorders produce alterations in the normal patterns of spontaneous activity and this could lead to serious irreversible consequences. For example, Shoykhet et al described how correlated spontaneous activity becomes altered in several neuron populations after hypoxic-ischemic injury during developmental stages (Shoykhet and Middleton 2016). Rescuing that abnormal activity may be an interesting therapeutic approach to help preserve neurological functions. It

is therefore of great interest, even from a therapeutic point of view, to study in depth the mechanisms mediated by spontaneous activity in the different circuits.

5.2 RETINAL WAVES IN DIFFERENT RGC POPULATIONS AND VISUAL PATHWAYS

Amniotes are deprived of visual experience during the perinatal period and retinal waves provide activity input during this time recreating basic features of the visual scenery and mediating the refinement of visual maps in retinorecipient targets. This prepares the network to receive environmental stimuli when eyes open. Some time ago, spontaneous activity was considered a permissive agent. Now that the complexity of the information codified by retinal waves and their exquisite level of regulation have been explored, our concept about this kind of activity has passed from a merely permissive role to endowing it with a crucial importance. In this study, we performed a comparative analysis of the spontaneous activity dependent refinement in nuclei from both image-forming and non-image-forming pathways prior visual experience, discriminating between the contralateral and ipsilateral components and found differences related to the specific requirements of each nucleus according to their corresponding functions.

5.3 ECTOPIC EXPRESSION OF KIR2.1 AFFECTS SPONTANEOUS ACTIVITY IN RGC NEURONS

Overexpression of rectifying potassium channels is a common approach to electrically silence neurons in both *in vitro* and *in vivo* experiments, because K^+ current increases producing a hyperpolarization of the resting potential that hampers to reach the spike threshold (Burrone, Byrne, and Murthy 2002). Kir2.1 is a known suppressor of intrinsic excitability, which has a crucial role in establishing connectivity in various circuits. However, intrinsic excitability can play a different role on each neuron population during development. For example, Kir2.1 overexpression in CA1 pyramidal neurons results in altered spine development and synaptic transmission but does not affect normal development in CA3 pyramidal neurons. In dentate granule cells, a compensatory enhancement of neurotransmitter release ameliorate

the ectopic expression of Kir2.1 producing only a decrease in spine density (Johnson-Venkatesh et al. 2015). Neuronal maturation appears to be an important factor in order to respond to increases in Kir2.1 expression. Using hippocampal cultures *Burrone et al.* showed that immature neurons are successfully silenced through Kir2.1 electroporation. However, once they develop mature synapses these cells are later rescued by cell-autonomous homeostatic mechanisms (Burrone et al. 2002). Therefore, depending on the cell population and stage of development it seems that neurons respond in a different manner to artificial increase of Kir2.1 levels.

It has been shown that experiments in which ectopic expression of Kir2.1 is achieved by electroporation lead to a higher expression of Kir2.1 in targeted cells producing electrical silencing of the neuron (Béïque et al. 2011; Benjumeda et al. 2013). Ectopic expression of Kir2.1 by a transgenic mouse has been also reported to block neural activity in the olfactory system (Yu et al. 2004). In the Sert-Cre::Kir2.1eYFP$^{fl\text{-}stop}$ or Brn3b-Cre::Kir2.1eYFP$^{fl\text{-}stop}$ mice, recombined RGCs exhibit a more negative resting potential and decreased input resistance compared to controls but instead of being silenced, RGCs expressing Kir2.1 show a higher firing frequency, suggesting a higher sensitization that likely results from homeostatic responses. Although our mice lines do not achieve the intended silencing of spontaneous activity in RGCs, they do not fire in a coordinated manner and the absence of coordinated pattern is enough to alter the refinement of retinal projections.

Spontaneous activity in RGCs and target cells control axonal and dendritic arbors dynamics through hebbian mechanisms. When a synchronous firing occurs, it produces LTP that increases the AMPA/NMDA ratio, strengthening and stabilizing that synapse. As a result, new synapses are generated in that region (synaptotropism). Asynchronous spikes between pre- and postsynaptic neurons would lead to the opposite effect. As a result, the refined network contains a much smaller number of synapses than in early stages, but those that remain are strong and clustered. In Kir2.1eYFP$^{fl\text{-}stop}$ mice, some RGCs fire

much more frequently than in the controls. Such unpatterned activity disturbs the spatial information needed to refine. In this scenario, LTP and LTD are produced more weakly and in a stochastic way, so that incorrect synaptic contacts are not eliminated and branch dynamic is not restricted to the corresponding region. The resulting projections of both RGCs and target cells cover a much larger area overlapping those of adjacent cells. Therefore, eye-specific segregation does not take place properly, and ipsilateral and contralateral projections remain unsegregated even in adult mice.

5.4 INTER- AND INTRA-RETINA COMPENSATIONS

It has been recently demonstrated that monocular enucleation alters retinal waves in the surviving eye, increasing frequency and reducing pairwise correlation (Failor, Ng, and Cheng 2018). As a result, the intra-eye competition increases and produces an expansion of the projections coming from the remaining eye. This change in the pattern of spontaneous activity is presumably due to the lack of the modulatory activity from the retino-retinal connections (Murcia-Belmonte et al. 2019b). In this scenario of higher frequency of shorter bursts, the balance between guiding molecules and neuronal activity proposed by the stochastic model (Koulakov and Tsigankov 2004; Tsigankov and Koulakov 2006, 2010) would be shifted towards the second element. For example, it has been shown that ipsilateral projections from the remaining retina largely expand their territory and occupy a huge portion of the dLGN, so they would be overwhelming the guiding cues gradients (Failor et al. 2018). This modification of the retinotopic map is not likely to be a developmental error resulting from a lesion, but rather a plasticity mechanism in response to the sensory experience received aimed to optimize resources. For example, in blind people the visual areas in both the thalamus and the cortex are partially occupied by the somatosensory circuit (Bronchti et al. 1992; Karlen and Krubitzer 2009).

Former single-eye studies must be reinterpreted in light of this finding. Similarly, transgenic lines in which the spontaneous activity of contralateral or ipsilateral RGCs are specifically affected should note

that the retinal waves of the opposing eye are susceptible to being affected. However, this effect will be negligible in the case of targeting the ipsilateral axons (Kir2.1eYFP$^{fl\text{-}stop}$::Sert-Cre mice), since this population only accounts for 4% of the total RGCs.

5.5 RGC AXONS REFINEMENT IS SEVERELY IMPAIRED IN IMAGE-FORMING NUCLEI WHEN RETINAL SPONTANEOUS ACTIVITY IS GENETICALLY DISTURBED

Retinal axon refinement in the thalamus is most extended takes longer than in the rest of the visual nuclei likely due to the great complexity of the thalamic network. Thalamic neurons receive inputs from both eyes but also from nodes formed by a great variety of subtypes of RGCs (Liang et al. 2018; Morgan et al. 2016; Rompani et al. 2017). RGCs of the same type have different axonal elaboration depending on their location in the nucleus (Hong et al. 2019), thus the different target regions have a huge influence in the shape of those arborizations. Additionally, the dLGN suffers a corticothalamic amplification of the retinal waves that ends just prior eye-opening, when these projections switch to release feedforward inhibition (Murata and Colonnese 2016). Therefore, the dLGN is a very peculiar visual nucleus. Ipsilateral and contralateral axon terminals initially invade this nucleus occupying overlaying territories and they need later to be pruned from the territory that corresponds to the other eye competing with the contrary retinal input in terms of activity correlation. Interestingly, our results show an expansion of the territory occupied by the contralateral axons in Brn3b-Cre::Kir2.1eYFP$^{fl\text{-}stop}$ mice. However, the altered ipsilateral activity in Sert-Cre::Kir2.1eYFP$^{fl\text{-}stop}$ mice do not lead to an expansion in the ipsilateral-occupied territory. There are several explanations for this *a priori* conflicting result:

1. The recombination driven by Brn3b-Cre in a portion of ipsilateral RGCs could alter their activity pattern. However, Brn3b is expressed in less than 20% of the ipsilateral RGCs (Pak et al. 2004) and cre-recombination is not total in the Brn3b-Cre::Kir2.1eYFP$^{fl\text{-}stop}$ mice, so such alteration of spontaneous activity in the ipsilateral population is likely insignificant.

2. The alteration of spontaneous activity in contralateral RGCs could affect ipsilateral electrophysiological behavior through a homeostatic modulation, impeding ipsilateral RGCs to interact correctly with postsynaptic neurons in the target for Hebbian-refinement. Supporting this hypothesis we found a more dispersed and weaker labelling for vGLUT2 in the ipsilateral region of Brn3b-Cre::Kir2.1eYFP$^{fl\text{-}stop}$ mice compared to the controls (Figure 4.5), suggesting a decrease in the maturation and clustering of glutamatergic synaptic buttons. Such homeostatic regulation would not occur in the opposite direction in Sert-Cre::Kir2.1eYFP$^{fl\text{-}stop}$ animals, as the ipsilateral population accounts for a very small portion.

3. The refinement of contralateral and ipsilateral projections may have a different requirement in relation to spontaneous activity. Since defects in contralateral refinement are observed for both lines, these terminals would need patterned spontaneous activity from both inputs. In contrast, the lack of alteration of the ipsilateral territory in Sert-Cre::Kir2.1eYFP$^{fl\text{-}stop}$ mice indicates that ipsilateral activity could be merely permissive, and a correlated contralateral activity would be sufficient for the refinement of ipsilateral projections.

Contra- and ipsilaterally projecting RGCs differ in their genesis period, with ipsilateral cells being differentiated later (Marcucci, Soares, and Mason 2019). However, mice in which glutamatergic activity has been abolished specifically in ipsilateral RGCs show an increase in the contralateral but not in the ipsilateral territory (Koch et al. 2011). This result suggests a stabilization of the ipsilateral territory prior to the glutamatergic stage, and therefore an earlier maturation of ipsilateral projections during the cholinergic stage even though their delayed differentiation. Our mouse overexpressing Kir2.1 in ipsilateral RGCs (Sert-Cre::Kir2.1eYFP$^{fl\text{-}stop}$) exhibits impaired spontaneous activity also during the cholinergic phase, and still no alterations occur in the ipsilateral territory. It is also possible that progressive accumulation of Kir2.1 in the recombined neurons produces an escalating effect. According

to this, ipsilateral axons would be able to determine their corresponding territory before Kir2.1 is expressed enough to disrupt their refinement, whereas the hypothetically less mature contralateral RGCs would result particularly affected. The high affinity uptake of serotonin in ipsilateral RGCs (Upton et al. 2002) would be a serious candidate for this phenomenon.

5.6 SUPERIOR COLLICULUS:

While analyzing the SC of the Brn3b-Cre::Kir2.1eYFP$^{fl\text{-}stop}$ mice we noticed abundant recombination in collicular cells (Figure 4.7) indicating that cells in this target likely have spontaneous activity altered regardless of retinal input, making it impossible to draw clear conclusions about the effect of retinal activity in the refinement of RGC axons. This was not the case for the Sert-Cre::Kir2.1eYFP$^{fl\text{-}stop}$ line, where ectopic Kir2.1 expression is restricted to a residual amount of contralateral RGCs projecting to the most caudal zone of the SGS (Figure 4.8). Therefore we can conclude that refinement defects in the ipsilateral population are due exclusively to an unpatterned ipsilateral spontaneous activity.

vGluT2^{fl}::Sert-Cre mice were previously used to block glutamatergic activity in ipsilateral RGCs (Koch et al. 2011), but because retinocolicular refinement has been described to take place only during the cholinergic stage (Dhande et al. 2011) the SC was not analyzed in those mice(Koch et al. 2011). Our work in Sert-Cre::Kir2.1eYFP$^{fl\text{-}stop}$ animals is therefore the first one analyzing the role of spontaneous activity in the refinement of ipsilateral retinocolicular projections. Spontaneous activity in contralateral RGCs likely contribute to exclude ipsilateral projections from the SGS and therefore, impairment of this activity produces an additive effect to the phenotype. Nevertheless, our results demonstrate that patterned activity in ipsilateral RGCs is essential to restrict both ipsilateral projections to the deep layer of the SC and to mediate their remodeling into their characteristic dense patches.

During the first postnatal week, contralateral and ipsilateral retinocollicular projections exhibit a differential axonal dynamic. Ipsilateral axons elaborate sparser arbors extended along the rostro-caudal axis while the contralaterals are more spatially restricted (Dhande et al. 2011). Regarding the dLGN, both retinal inputs elaborate arbors that are very similar in complexity, density and area especially during the second postnatal week (Dhande et al. 2011).

5.7 THE EFFECT OF RETINAL ACTIVITY IMPAIRMENT IN NON-IMAGE NUCLEI

Because all RGCs that project to the dLGN also send collaterals to the SC (Ellis et al. 2016; Huberman, Manu, et al. 2008), the differences in timing and axonal dynamics may be due to specific target derived factors. Therefore, spontaneous activity dependent refinement appears to be modulated in a target dependent manner according to the requirement of each nucleus. Since non-forming image nuclei perform a very different set of functions mediated by an specific subset of RGCs (ipRGCs), we expect to find striking peculiarities not occurring in visual forming pathways

5.71 The Olivary pretectal nucleus: Sequential innervation by retinal afferents

In Brn3b-Cre::Kir2.1eYFP$^{fl\text{-}stop}$ mice, ipsilateral projections invade the core of the OPN decreasing segregation. In contrast, Sert-Cre::Kir2.1eYFP$^{fl\text{-}stop}$ mice do not exhibit apparent defects in the axonal refinement of this nucleus (Figure 4.9B). Because axonal innervation to the OPN is sequential, first contralateral and then ipsilateral axons (Marques and Clarke 1990), there is no bilateral activity competition like in other nuclei. Contralateral projections are already established in their corresponding territory when ipsilateral axons arrive to the target. In the Sert-Cre::Kir2.1eYFP$^{fl\text{-}stop}$ animals, patterned activity in the contralateral RGCs is able to restrain the ipsilateral territory as they does in the dLGN.

In contrast to the dLGN, where an expansion of the contralateral territory is observed, in the OPN there is not expansion of the region occupied by contralateral terminals. This may occurs because the projections of these terminals are regulated by mechanisms that do not depend on bilateral competition. Sequential innervation of ipsi and contralateral axons (Marques and Clarke 1990) and the different anatomical regions of the OPN to which axons are preferably directed (Fleming, Benca, and Behan 2006), made us think that there is a different composition of ipRGC subtypes for each eye input. At the same time that contralateral projections occupy the nucleus core, ipRGCs M2, M5 and M6 arrive to this region (Osterhout et al. 2014; Quattrochi et al. 2019). A few days later, the subsequent arrival of ipsilateral axons to the peripheral region of the target coincides with the appearance of M1 subtype projections in the OPN shell (Güler et al. 2008). Contralateral and ipsilateral projections to the OPN preferably come from different retinal regions, ventro-nasal and ventro-temporal respectively (Young and Lund 1998). Additionally, each ipRGC subtype exhibits a different distribution in the retina. Furthermore, each visual component (ipsi- and contralateral) would have a distinct composition of ipRGC subtypes, more adequate for the function that each of them plays in the OPN. Thus, eye-specific segregation in the OPN is likely determined by the order of arrival and patterned spontaneous activity results necessary only to expel ipsilateral axons from the contralateral territory.

There is no previous information about the existence of a retinotopic map in this nucleus but this possibility cannot be completely ruled out. As mentioned, each retinal input comes from different retina regions (Young and Lund 1998), so it is possible that an unknown guidance cue is providing topographic information about the naso-temporal axis determining the medio-lateral distribution in the target.

5.7.2 The Suprachiasmatic nucleus: A bilateral innervated nucleus without eye-specific segregation

5.7.2.1 A role for the SCN in vision? Image-forming tasks in a non-image forming target

For a long time, the SCN was thought to be just a regulator of the circadian clock. In this way, retinal activity would be just mediating the synchronization with light/dark cycles. However, firing rates in the SCN code a more complex visual information than necessary to perform this function, suggesting a potential role in spatial vision. Several pieces of evidence have pointed to this direction. For instance, it has been demonstrated that retinal input to the SCN regulates the contagious itch behavior (Yu et al. 2017). Moreover, 75% of light sensitive cells has been seen to tune slightly their firing rate correlating with simple spatial patterns without altering irradiance response (Mouland et al. 2017). Cells in the ventral region receive the majority of the retinal afferents though the mentioned DDCSs (Kim et al. 2019), and thanks to GABAergic inhibition they are receptive to the whole visual field with a higher irradiance response (Stinchcombe et al. 2017). Additionally, this inhibitory signal also give rise to center-surround receptive fields, pointless for an irradiance detector but well suited for spatial processing (Stinchcombe et al. 2017). Probably single neurons can perform both tasks since they are able to process that GABAergic signal discriminating tonic and phasic activity (Belle et al. 2009; DeWoskin et al. 2015; Paul et al. 2016). The co-existence of both types of messages, coding irradiance and spatial information, is possible thanks to this capability of the SCN for multiplexing both fast visual stimuli and slow photoentrainment information (Stinchcombe et al. 2017).

5.7.2.2 Does a retinotopic map exist in the SCN?

By analyzing the terminals of single ipRGCs, a previous study described a raw topographic map of contralateral ipRGCs in this nucleus (Fernandez et al. 2016). However, the authors only analyzed the terminals of two ipsilateral RGCs and therefore they were unable to determine whether the ipsilateral population also project bilaterally in this nucleus. By analyzing the behavior of ipsilateral ipRGCs in the SCN we have demonstrated that they innervate the ventrolateral region of the SCN (Figure 4.13). Guidance mechanisms in the SCN have been poorly studied. The molecules responsible for the entry of

axon terminals to this target and the formation of a topographic map remain unknown. Only a subset of M1-M2 ipRGCs target the SCN, so these axons should contain or lack a yet unknown molecule promoting their entry. Brn3b negative M1 ipRGCs target the SCN while the Brn3b positive avoid it (Chen et al. 2011), so this transcription factor has been proposed to be regulating a guidance program that mediates this selective entry. However, a 20% of the SCN retinal input is provided by M2 ipRGCs (Baver et al. 2008; Güler et al. 2008), which do not express Brn3b and therefore, it is unikely that this TF plays a role in this function.

Regarding the topography, the order in which the axons reach the nucleus could be an influence, but it is unlikely because they are stalled at the chiasm until the innervation begins early after birth. Some guidance cues such as F-spondin, Slit1 or ALCAM are expressed in the developing SCN (Carrillo et al. 2018). Lack of F-spondin affect the migration of VIP neurons (Carrillo et al. 2018), the main suprachiasmatic cell type targeted by retinal afferents (Leard et al. 1994; Muñoz Llamosas et al. 2000; Weaver and Reppert 1995). This receptor exhibit homology with Reelin, another extracellular matrix protein, which is involved in M1 ipRGC targeting to the vLGN and IGN (Su et al. 2011) along with its LRP8 and VLDLR receptors (Su et al. 2013). EVA1C, a novel Slit receptor, is expressed in the SCN from E17.5 to P10, that coincides with the arrival and refining of retinal afferents in the nucleus (James et al. 2013). At the present time, many aspects of the axonal arborization of ipRGCs in the SCN are still unknown.

5.7.2.3 Eye-specific segregation does not occur in the SCN

It has been also previously demonstrated that contralateral ipRGCs send collaterals at the level of the SCN that cross the midline and target the opposite side of the nucleus and therefore project bilaterally (Fernandez et al. 2016). It was suggested by single cell analysis that ipsilateral ipRGCs do not exhibit a bilateral projection pattern but this conclusion was based on the analysis of just two neurons (Fernandez

et al. 2016). Using Zic2CreER::Rosa^{TdTm} mice, we specifically labeled a large population of ipsilateral RGCs and were able to observe that, at the level of the SCN, ipsilateral axons also cross the midline and project to the other side (Figure 4.12F-F''). In fact, in the Sert-Cre::Rosa^{TdTm} mice, we noticed that one third of the projections from ipsilateral ipRGCs come from bilateral axons (Figure 4.12D).

Ipsi and contralateral ipRGCs send terminals to both sides of the SCN but their terminals do not segregate in this nucleus. The bilateral innervation of this nucleus and the abundance of postsynaptic cells targeted by both ipsi- and contralateral afferents (Fernandez et al. 2016) in fact point to a different purpose directed to the equalization of the irradiance signal coming from both eyes. We observe that alteration of spontaneous activity has an effect on the refinement of ipsilateral terminals because in the Sert-Cre::Kir2.1eYFP$^{fl\text{-}stop}$ mice ipsilateral projections are not so confined to the ventrolateral region of the nucleus as in control mice (Figure 4.13B-C). Because segregation does not take place in this nucleus, such fine-tune refinement rather than relying in inter-retina competition would likely depend on wave correlation. Such defect will hardly affect significantly photoentrainment, but it could affect the recently discovered role of the SCN in vision. Future behavioral experiments in mice with altered retinal activity should analyze these features in order to better define the putative role of retinal activity in the refinement of the SCN.

5.7.2.4 Spontaneous activity in the SCN

Patterned retinal spontaneous activity is required for the correct fine-tuning refinement of visual afferents to the SCN (Figure 4.13). We did not expect that the defects observed in the refinement of ipRGCs to the SCN in Brn3b::Kir2.1eYFP$^{fl\text{-}stop}$ and Sert-Cre::Kir2.1eYFP$^{fl\text{-}stop}$ mice would produce defects in the functions related to the SCN because in these mice only a minimal portion of SCN projecting ipRGCs are targeted (around 20% in the Brn3b –M2 ipRGCs– and about 2% in the Sert-cre mice). Future experiments using

more convenient models that block or alter retinal waves in all the ipRGCs should better analyze this question. Nevertheless, we find defects in the refinement of the small population of Sert positive ipRGCs in the SCN, indicating that spontaneous activity is important for axonal refinement in this nucleus and suggesting that its effect could be affecting the refinement of a larger population of ipRGCs.

5.8 Axonal collaterals

For a long time it has been a mystery how the reduced number of ipRGCs is able to perform such a variety of functions. Initially, subtypes of ipRGCs with high expression of melanopsin were discovered to differ in a large extent from conventional RGCs. Subsequently, other subtypes of ipRGCs expressing low levels of melanopsin previously described as RGCs came to light (Schmidt et al. 2014; Stabio et al. 2018)[1]. To date, at least six types of ipRGCs have been described: M1-M6. This diversified specialization would not be sufficient without the capacity of each neuron to project collaterals to several nuclei (Fernandez et al. 2016). Each of these ramifications exhibits region-specific arborization patterns and synaptic features (Fernandez et al. 2016; Kim et al. 2019) (Figure 5.1).

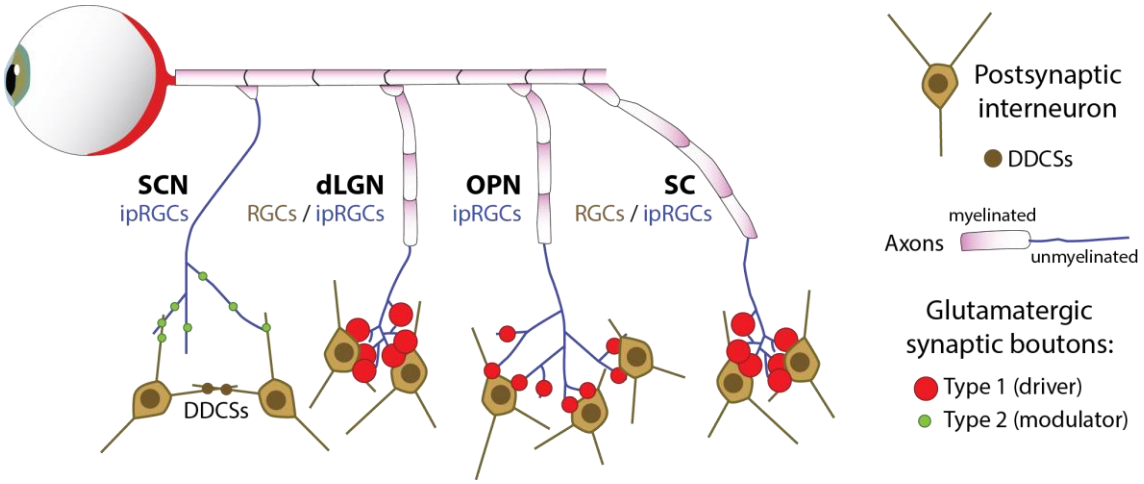

Figure 5.1: **Divergence between collaterals to different targets.** Adapted from Kim et al., 2019.

5.9 Future directions in the field

Nowadays, we are aware of the huge divergence of RGC subtypes, including conventional RGCs and ipRGCs, sending collaterals to multiple nuclei. Not to mention the interconnections among these targets. Next studies should focus on the hallmarks that distinguish each nucleus, the factors sensed by each collateral that induce such differential responses. As stated above, retinal terminals can vary greatly among targets, even for a single RGC. These variations include processes such as myelination, axonal dynamics or synaptic maturation (Figure 5.1). Furthermore, a deep understanding about the wiring of neural circuits cannot be fulfilled without tracking the different collaterals elaborated by single neurons.

The visual system, with its tremendous diversity of interactions between RGCs and the different retinal targets, is an excellent model to further explore the role of spontaneous activity in the development of the nervous system. To study the axonal dynamics of different collaterals from single RGCs, it would be necessary to scan large regions of the brain with high resolution and to label specifically the neurons. 3D serial block-face scanning electron microscopy (SBEM) (Denk and Horstmann 2004) combined with genetically encoded electron microscopy tags (Atasoy et al. 2014) could fulfill these requirements in a manner that region-specific branching and synaptic specialization can be studied properly (Kim et al. 2019). Regarding the electrophysiological behavior, simultaneous recording of the activity in the different collaterals of a single neuron would give us another crucial piece of this puzzle.

Neuronal activity can involve cellular changes at many levels that are of vital importance in both development and adulthood. Regulation of gene expression (Chen et al. 2016; Lee et al. 2017; Nakashima et al. 2019) and neural activity act in combination with selective transport and local translational machinery (Shen et al. 2014) in order to achieve a regulatory control over local activity-dependent synaptic plasticity (Shen et al. 2014; Shigeoka et al. 2016). Furthermore, to fully understand

the processes mediated by retinal waves, it would be necessary to perform single cell next generation sequencing experiments combined with local translation analysis in their corresponding collateral terminals. Unfortunately, the current state of the art does not allow such an ambitious project. Nevertheless, future technical advances may pave the way for experiments carried out under these conditions. On the other hand, a systematic analysis about the differential expression of trophic factors in relay cells located on each target would be very informative.

Since spontaneous activity is a widespread feature throughout the developmental nervous system, a greater understanding of retinal waves dependent refinement will help us to better address their role in other circuits. This topic is promising from a therapeutic point of view as well. Such knowledge would be potentially instrumental to rescue activity alterations produced by neurodevelopment disorders or other type of neurological diseases.

6. CONCLUSIONS

1. The newly generated Kir2.1eYFP$^{fl\text{-}stop}$ mouse line may be used to conditionally express the inward rectifyer potassium channel Kir2.1 in specific neural populations when combined with cre-lines.
2. RGCs that ectopically express Kir2.1 *in vivo* exhibit hyperpolarization of the resting membrane potential, decrease of the input resistance and increase in their firing frequency. This creates a randomized retinal activity pattern disabling them to encode spatial correlation information.
3. Mice with altered correlated retinal activity exhibit defects in eye-specific segregation in the image-forming nuclei (dLGN and SC) confirming that correlated patterns of retinal activity are essential for axon refinement in these nuclei.
4. Specific alteration of spontaneous activity in ipsilateral RGCs results in defects in eye-specific segregation at the dLGN as well as in the anterior-posterior refinement and layer specification of the SC. These results indicate that correlated activity among ipsilateral RGCs is essential to promote the expulsion of contralateral terminals from the ipsilateral territory in the dLGN and to stablish the proper patchy projection pattern of ipsilateral terminals in the SC.
5. Alteration of retinal activity in contralateral RGCs also affects eye-specific refinement in the olivary pretectal nucleus. However, alteration of patterned activity specifically in ipsilateral RGCs does not seem to alter axon refinement in this target.
6. Eye-specific segregation is not a feature of the suprachiasmatic nucleus. Instead, ipsilateral and contralateral projections project very closely and innervate the same SCN neurons.
7. The ratio of ipRGCs is higher in the ipsilateral than in the contralateral RGC population.
8. Ipsilateral ipRGCs innervate the suprachiasmatic nucleus bilaterally as contralateral ipRGCs do. Additionally, both RGC populations build a raw topographic map in this target.

9. Spontaneous retinal activity is important for the refinement of ipsilateral ipRGC projections in the non-image-forming suprachiasmatic nucleus.
10. Overall, the results presented here confirm previous data reporting an important function for patterned spontaneous retinal activity in the refinement of RGC terminals in the image-forming nuclei and reveal that this activity is also required for the proper fine-tune refinement of visual terminals in non-image forming nuclei.

6. CONCLUSIONES

1. La línea de ratón Kir2.1eYFP$^{fl\text{-}stop}$ generada puede utilizarse para expresar condicionalmente el canal rectificador entrante de potasio Kir2.1 en poblaciones neuronales específicas cuando se combina con líneas Cre.
2. Los CGRs que expresan ectópicamente Kir2.1 *in vivo* exhiben hiperpolarización del potencial de membrana en reposo, disminución de la resistencia de entrada y aumento de su frecuencia de disparo. Esto crea un patrón de actividad retinal aleatoria que les impide codificar información de correlación espacial.
3. Los ratones con actividad retinal correlacionada alterada presentan defectos en la segregación específica de ojo en los núcleos formadores de imágen (núcleo geniculado lateral y colículo superior), lo que confirma que los patrones correlacionados de actividad retiniana son esenciales para el refinamiento de los axones en estos núcleos.
4. La alteración específica de la actividad espontánea en las CGRs ipsilaterales da lugar a defectos en la segregación específica del ojo en el núcleo geniculado lateral así como en el refinamiento anterior-posterior y la especificación de la capa del colículo superior. Estos resultados indican que la actividad correlativa entre las CGR ipsilaterales es esencial para promover la expulsión de los terminales contralaterales del territorio ipsilateral en el núcleo geniculado lateral y para establecer el patrón de proyección corpuscular que les caracteriza en el colículo superior.
5. La alteración de la actividad retiniana en las CGRs contralaterales también afecta segregación específica de ojo en la oliva inferior. Sin embargo, la alteración del patrón de actividad específicamente en las CGRs ipsilaterales no parece alterar el refinamiento de los axones en este núcleo.

6. La segregación específica del ojo no es una característica presente en el núcleo supraquiasmático. En cambio, las proyecciones ipsilaterales y contralaterales proyectan muy próximas e inervan las mismas neuronas del núcleo supraquiasmático.
7. La proporción de ipCGRs es mayor en la población de CGRs ipsilateral que en la contralateral.
8. Los ipCGRs ipsilaterales inervan el núcleo supraquiasmático bilateralmente así como las ipCGRs contralaterales. Además, ambas poblaciones de CGRs elaboran un mapa topográfico poco refinado en este objetivo.
9. La actividad retiniana espontánea es importante para el refinamiento de las proyecciones ipCGR ipsilaterales en el núcleo supraquiasmático, a pesar de tratarse de un núcleo no formador de imágenes.
10. En general, los resultados presentados aquí confirman los datos anteriores que informan de una importante función para la actividad retiniana espontánea en el refinamiento de los terminales de las CGR en los núcleos formadores de imagen imagen y revelan que esta actividad también es necesaria para el adecuado refinamiento de los terminales visuales en los núcleos que no formadores de imágen.

REFERENCES

1. Abrahamson, E. E. and R. Y. Moore. 2001. “Suprachiasmatic Nucleus in the Mouse: Retinal Innervation, Intrinsic Organization and Efferent Projections.” *Brain Research* 916(1–2):172–91.
2. Ackman, James B., Timothy J. Burbridge, and Michael C. Crair. 2012. “Retinal Waves Coordinate Patterned Activity throughout the Developing Visual System.” *Nature* 490(7419):219–25.
3. Ackman, James B. and Michael C. Crair. 2014. “Role of Emergent Neural Activity in Visual Map Development.” *Current Opinion in Neurobiology* 24(1):166–75.
4. Ahern, Todd H., Stefanie Krug, Audrey V Carr, Elaine K. Murray, Emmett Fitzpatrick, Lynn Bengston, Jill McCutcheon, Geert J. De Vries, and Nancy G. Forger. 2013. “Cell Death Atlas of the Postnatal Mouse Ventral Forebrain and Hypothalamus: Effects of Age and Sex.” *The Journal of Comparative Neurology* 521(11):2551–69.
5. Akerman, Colin J., Matthew S. Grubb, and Ian D. Thompson. 2004. “Spatial and Temporal Properties of Visual Responses in the Thalamus of the Developing Ferret.” *The Journal of Neuroscience : The Official Journal of the Society for Neuroscience* 24(1):170–82.
6. Akerman, Colin J., Darragh Smyth, and Ian D. Thompson. 2002. “Visual Experience before Eye-Opening and the Development of the Retinogeniculate Pathway.” *Neuron* 36(5):869–79.
7. Akrouh, Alejandro and Daniel Kerschensteiner. 2013. “Intersecting Circuits Generate Precisely Patterned Retinal Waves.” *Neuron* 79(2):322–34.
8. Antón-Bolaños, Noelia, Alejandro Sempere-Ferràndez, Teresa Guillamón-Vivancos, Francisco J. Martini, Leticia Pérez-Saiz, Henrik Gezelius, Anton Filipchuk, Miguel Valdeolmillos, and Guillermina López-Bendito. 2019. “Prenatal Activity from Thalamic Neurons Governs the Emergence of Functional Cortical Maps in Mice.” *Science (New York, N.Y.)* 364(6444):987–90.
9. Arroyo, David A., Lowry A. Kirkby, and Marla B. Feller. 2016. “Retinal Waves Modulate an Intraretinal Circuit of Intrinsically Photosensitive Retinal Ganglion Cells.” *The Journal of Neuroscience : The Official Journal of the Society for Neuroscience* 36(26):6892–6905.
10. Atasoy, Deniz, J. Nicholas Betley, Wei-Ping Li, Helen H. Su, Sinem M. Sertel, Louis K. Scheffer, Julie H. Simpson, Richard D. Fetter, and Scott M. Sternson. 2014. “A Genetically Specified Connectomics Approach Applied to Long-Range Feeding Regulatory Circuits.” *Nature Neuroscience* 17(12):1830–39.
11. Atkinson, Susan E., Elizabeth S. Maywood, Johanna E. Chesham, Christian Wozny, Christopher S. Colwell, Michael H. Hastings, and Stephen R. Williams. 2011. “Cyclic AMP Signaling Control of Action Potential Firing Rate and Molecular Circadian Pacemaking in the Suprachiasmatic

Nucleus." *Journal of Biological Rhythms* 26(3):210–20.

12. Baden, Tom, Philipp Berens, Katrin Franke, Miroslav Román Rosón, Matthias Bethge, and Thomas Euler. 2016. "The Functional Diversity of Retinal Ganglion Cells in the Mouse." *Nature* 529(7586):345–50.
13. Baldridge, W. H., D. I. Vaney, and R. Weiler. 1998. "The Modulation of Intercellular Coupling in the Retina." *Seminars in Cell & Developmental Biology* 9(3):311–18.
14. Bansal, Anu, Joshua H. Singer, Bryan J. Hwang, Wei Xu, Art Beaudet, and Marla B. Feller. 2000. "Mice Lacking Specific Nicotinic Acetylcholine Receptor Subunits Exhibit Dramatically Altered Spontaneous Activity Patterns and Reveal a Limited Role for Retinal Waves in Forming ON and OFF Circuits in the Inner Retina." 20(20):7672–81.
15. Barkis, William B., Kevin J. Ford, and Marla B. Feller. 2010. "Non-Cell-Autonomous Factor Induces the Transition from Excitatory to Inhibitory GABA Signaling in Retina Independent of Activity." *Proceedings of the National Academy of Sciences of the United States of America* 107(51):22302–7.
16. Barrera, Kyrstle, Philip Chu, Jason Abramowitz, Robert Steger, Raddy L. Ramos, and Joshua C. Brumberg. 2013. "Organization of Myelin in the Mouse Somatosensory Barrel Cortex and the Effects of Sensory Deprivation." *Developmental Neurobiology* 73(4):297–314.
17. Baver, Scott B., Galen E Pickard, Patricia J. Sollars, and Gary E Pickard. 2008. "Two Types of Melanopsin Retinal Ganglion Cell Differentially Innervate the Hypothalamic Suprachiasmatic Nucleus and the Olivary Pretectal Nucleus." *The European Journal of Neuroscience* 27(7):1763–70.
18. Bedont, Joseph L. and Seth Blackshaw. 2015. "Constructing the Suprachiasmatic Nucleus: A Watchmaker's Perspective on the Central Clockworks." *Frontiers in Systems Neuroscience* 9:74.
19. Béïque, Jean-Claude, Youn Na, Dietmar Kuhl, Paul F. Worley, and Richard L. Huganir. 2011. "Arc-Dependent Synapse-Specific Homeostatic Plasticity." *Proceedings of the National Academy of Sciences of the United States of America* 108(2):816–21.
20. Belle, Mino D. C., Casey O. Diekman, Daniel B. Forger, and Hugh D. Piggins. 2009. "Daily Electrical Silencing in the Mammalian Circadian Clock." *Science (New York, N.Y.)* 326(5950):281–84.
21. Ben-Ari, Y., E. Cherubini, R. Corradetti, and J. L. Gaiarsa. 1989. "Giant Synaptic Potentials in Immature Rat CA3 Hippocampal Neurones." *The Journal of Physiology* 416:303–25.
22. Ben-Ari, Yehezkel, Jean-Luc Gaiarsa, Roman Tyzio, and Rustem Khazipov. 2007. "GABA: A Pioneer Transmitter That Excites Immature Neurons and Generates Primitive Oscillations."

Physiological Reviews 87(4):1215–84.

23. Benjumeda, Isabel, Augusto Escalante, Chris Law, Daniel Morales, Geraud Chauvin, Gerald Muça, Yaiza Coca, Joaquín Márquez, Guillermina López-Bendito, Artur Kania, Luis Martínez, and Eloísa Herrera. 2013. "Uncoupling of EphA/EphrinA Signaling and Spontaneous Activity in Neural Circuit Wiring." *The Journal of Neuroscience : The Official Journal of the Society for Neuroscience* 33(46):18208–18.
24. Berson, David M., Felice A. Dunn, and Motoharu Takao. 2002. "Phototransduction by Retinal Ganglion Cells That Set the Circadian Clock." *Science (New York, N.Y.)* 295(5557):1070–73.
25. Bevins, Nicholas, Greg Lemke, and Michaël Reber. 2011. "Genetic Dissection of EphA Receptor Signaling Dynamics during Retinotopic Mapping." *The Journal of Neuroscience : The Official Journal of the Society for Neuroscience* 31(28):10302–10.
26. Bickford, Martha E., Na Zhou, Thomas E. Krahe, Gubbi Govindaiah, and William Guido. 2015. "Retinal and Tectal 'Driver-Like' Inputs Converge in the Shell of the Mouse Dorsal Lateral Geniculate Nucleus." *The Journal of Neuroscience : The Official Journal of the Society for Neuroscience* 35(29):10523–34.
27. Blankenship, Aaron G., Aaron M. Hamby, Alana Firl, Shri Vyas, Stephan Maxeiner, Klaus Willecke, and Marla B. Feller. 2011. "The Role of Neuronal Connexins 36 and 45 in Shaping Spontaneous Firing Patterns in the Developing Retina." *The Journal of Neuroscience : The Official Journal of the Society for Neuroscience* 31(27):9998–10008.
28. Blazynski, Christine. 1989. "Displaced Cholinergic, GABAergic Amacrine Cells in the Rabbit Retina Also Contain Adenosine." *Visual Neuroscience* 3(5):425–31.
29. Bloomfield, S. A., D. Xin, and S. E. Persky. 1995. "A Comparison of Receptive Field and Tracer Coupling Size of Horizontal Cells in the Rabbit Retina." *Visual Neuroscience* 12(5):985–99.
30. Bonetti, Ciro and Enrico Maria Surace. 2010. "Mouse Embryonic Retina Delivers Information Controlling Cortical Neurogenesis." *PloS One* 5(12):e15211.
31. Borodinsky, Laura N., Cory M. Root, Julia A. Cronin, Sharon B. Sann, Xiaonan Gu, and Nicholas C. Spitzer. 2004. "Activity-Dependent Homeostatic Specification of Transmitter Expression in Embryonic Neurons." *Nature* 429(6991):523–30.
32. Bosler, O. and A. Beaudet. 1985. "VIP Neurons as Prime Synaptic Targets for Serotonin Afferents in Rat Suprachiasmatic Nucleus: A Combined Radioautographic and Immunocytochemical Study." *Journal of Neurocytology* 14(5):749–63.
33. Bouzioukh, Farima, Gaël Daoudal, Julien Falk, Dominique Debanne, Geneviève Rougon, and Valérie Castellani. 2006. "Semaphorin3A Regulates Synaptic Function of Differentiated

Hippocampal Neurons." *The European Journal of Neuroscience* 23(9):2247–54.

34. Branco, Tiago, Kevin Staras, Kevin J. Darcy, and Yukiko Goda. 2008. "Local Dendritic Activity Sets Release Probability at Hippocampal Synapses." *Neuron* 59(3):475–85.
35. Bronchti, G., N. Schönenberger, E. Welker, and H. Van der Loos. 1992. "Barrelfield Expansion after Neonatal Eye Removal in Mice." *Neuroreport* 3(6):489–92.
36. Brooks, Elisabeth, Dhruval Patel, and Maria Mercè Canal. 2014. "Programming of Mice Circadian Photic Responses by Postnatal Light Environment." *PloS One* 9(5):e97160.
37. Brooks, Justin M., Jianmin Su, Carl Levy, Jessica S. Wang, Tania A. Seabrook, William Guido, and Michael A. Fox. 2013. "A Molecular Mechanism Regulating the Timing of Corticogeniculate Innervation." *Cell Reports* 5(3):573–81.
38. Brown, Timothy M., Carlos Gias, Megumi Hatori, Sheena R. Keding, Ma'ayan Semo, Peter J. Coffey, John Gigg, Hugh D. Piggins, Satchidananda Panda, and Robert J. Lucas. 2010. "Melanopsin Contributions to Irradiance Coding in the Thalamo-Cortical Visual System." *PLoS Biology* 8(12):e1000558.
39. Brzezinski, Joseph A., Nadean L. Brown, Atsuhiro Tanikawa, Ronald A. Bush, Paul A. Sieving, Martha H. Vitaterna, Joseph S. Takahashi, and Tom Glaser. 2005. "Loss of Circadian Photoentrainment and Abnormal Retinal Electrophysiology in Math5 Mutant Mice." *Investigative Ophthalmology & Visual Science* 46(7):2540–51.
40. Buhusi, Mona, Galina P. Demyanenko, Karry M. Jannie, Jasbir Dalal, Eli P. B. Darnell, Joshua A. Weiner, and Patricia F. Maness. 2009. "ALCAM Regulates Mediolateral Retinotopic Mapping in the Superior Colliculus." *The Journal of Neuroscience : The Official Journal of the Society for Neuroscience* 29(50):15630–41.
41. Bunt, S. M. and R. D. Lund. 1981. "Development of a Transient Retino-Retinal Pathway in Hooded and Albino Rats." *Brain Research* 211(2):399–404.
42. Burbridge, Timothy J., Hong-Ping Xu, James B. Ackman, Xinxin Ge, Yueyi Zhang, Mei-Jun Ye, Z. Jimmy Zhou, Jian Xu, Anis Contractor, and Michael C. Crair. 2014. "Visual Circuit Development Requires Patterned Activity Mediated by Retinal Acetylcholine Receptors." *Neuron* 84(5):1049–64.
43. Burrone, Juan, Michael O. Byrne, and Venkatesh N. Murthy. 2002. "Multiple Forms of Synaptic Plasticity Triggered by Selective Suppression of Activity in Individual Neurons." 420(November).
44. Butts, D. A., M. B. Feller, C. J. Shatz, and D. S. Rokhsar. 1999. "Retinal Waves Are Governed by Collective Network Properties." *The Journal of Neuroscience : The Official Journal of the Society for Neuroscience* 19(9):3580–93.
45. Butts, Daniel A., Patrick O. Kanold, and Carla J. Shatz. 2007. "A Burst-Based 'Hebbian' Learning

Rule at Retinogeniculate Synapses Links Retinal Waves to Activity-Dependent Refinement." *PLoS Biology* 5(3):e61.

46. Cang, Jianhua, Lupeng Wang, Michael P. Stryker, and David a Feldheim. 2008. "Roles of Ephrin-as and Structured Activity in the Development of Functional Maps in the Superior Colliculus." *The Journal of Neuroscience : The Official Journal of the Society for Neuroscience* 28(43):11015–23.
47. Carmona-Alcocer, Vania, John H. Abel, Tao C. Sun, Linda R. Petzold, Francis J. Doyle, Carrie L. Simms, and Erik D. Herzog. 2018. "Ontogeny of Circadian Rhythms and Synchrony in the Suprachiasmatic Nucleus." *The Journal of Neuroscience : The Official Journal of the Society for Neuroscience* 38(6):1326–34.
48. Carreres, Maria Isabel, Augusto Escalante, Blanca Murillo, Geraud Chauvin, Patricia Gaspar, Celia Vegar, and Eloisa Herrera. 2011. "Transcription Factor Foxd1 Is Required for the Specification of the Temporal Retina in Mammals." *The Journal of Neuroscience : The Official Journal of the Society for Neuroscience* 31(15):5673–81.
49. Carrillo, Gabriela L., Jianmin Su, Aboozar Monavarfeshani, and Michael A. Fox. 2018. "F-Spondin Is Essential for Maintaining Circadian Rhythms." *Frontiers in Neural Circuits* 12:13.
50. Castel, M. and J. F. Morris. 2000. "Morphological Heterogeneity of the GABAergic Network in the Suprachiasmatic Nucleus, the Brain's Circadian Pacemaker." *Journal of Anatomy* 196 (Pt 1:1–13.
51. Catsicas, M., V. Bonness, D. Becker, and P. Mobbs. 1998. "Spontaneous Ca2+ Transients and Their Transmission in the Developing Chick Retina." *Current Biology : CB* 8(5):283–86.
52. Chalupa, Leo M. 2009. "Retinal Waves Are Unlikely to Instruct the Formation of Eye-Specific Retinogeniculate Projections." *Neural Development* 4:25.
53. Chandrasekaran, Anand R., Daniel T. Plas, Ernesto Gonzalez, and Michael C. Crair. 2005. "Evidence for an Instructive Role of Retinal Activity in Retinotopic Map Refinement in the Superior Colliculus of the Mouse." *The Journal of Neuroscience : The Official Journal of the Society for Neuroscience* 25(29):6929–38.
54. Chandrasekaran, Anand R., Ruchir D. Shah, and Michael C. Crair. 2007. "Developmental Homeostasis of Mouse Retinocollicular Synapses." *The Journal of Neuroscience : The Official Journal of the Society for Neuroscience* 27(7):1746–55.
55. Chen, C. and W. G. Regehr. 2000. "Developmental Remodeling of the Retinogeniculate Synapse." *Neuron* 28(3):955–66.
56. Chen, Lu, Anthony G. Lau, and Federica Sarti. 2014. "Synaptic Retinoic Acid Signaling and Homeostatic Synaptic Plasticity." *Neuropharmacology* 78:3–12.
57. Chen, Minggang, Shijun Weng, Qiudong Deng, Zhen Xu, and Shigang He. 2009. "Physiological

Properties of Direction-Selective Ganglion Cells in Early Postnatal and Adult Mouse Retina." *The Journal of Physiology* 587(Pt 4):819–28.

58. Chen, S. K., T. C. Badea, and S. Hattar. 2011. "Photoentrainment and Pupillary Light Reflex Are Mediated by Distinct Populations of IpRGCs." *Nature* 476(7358):92–96.
59. Chen, Xiao, Reazur Rahman, Fang Guo, and Michael Rosbash. 2016. "Genome-Wide Identification of Neuronal Activity-Regulated Genes in Drosophila." *ELife* 5.
60. Chen, Yachi and Anirvan Ghosh. 2005. "Regulation of Dendritic Development by Neuronal Activity." *Journal of Neurobiology* 64(1):4–10.
61. Chew, Kylie S., Jordan M. Renna, David S. McNeill, Diego C. Fernandez, William T. Keenan, Michael B. Thomsen, Jennifer L. Ecker, Gideon S. Loevinsohn, Cassandra VanDunk, Daniel C. Vicarel, Adele Tufford, Shijun Weng, Paul A. Gray, Michel Cayouette, Erik D. Herzog, Haiqing Zhao, David M. Berson, and Samer Hattar. 2017. "A Subset of IpRGCs Regulates Both Maturation of the Circadian Clock and Segregation of Retinogeniculate Projections in Mice." *ELife* 6.
62. Chung, Won-Suk, Laura E. Clarke, Gordon X. Wang, Benjamin K. Stafford, Alexander Sher, Chandrani Chakraborty, Julia Joung, Lynette C. Foo, Andrew Thompson, Chinfei Chen, Stephen J. Smith, and Ben A. Barres. 2013. "Astrocytes Mediate Synapse Elimination through MEGF10 and MERTK Pathways." *Nature* 504(7480):394–400.
63. Cohen-Cory, S., E. Escandón, and S. E. Fraser. 1996. "The Cellular Patterns of BDNF and TrkB Expression Suggest Multiple Roles for BDNF during Xenopus Visual System Development." *Developmental Biology* 179(1):102–15.
64. Colwell, Christopher S. 2011. "Linking Neural Activity and Molecular Oscillations in the SCN." *Nature Reviews. Neuroscience* 12(10):553–69.
65. Corlew, Rebekah, Martha M. Bosma, and William J. Moody. 2004. "Spontaneous, Synchronous Electrical Activity in Neonatal Mouse Cortical Neurones." *The Journal of Physiology* 560(Pt 2):377–90.
66. Cruz-Martín, Alberto, Rana N. El-Danaf, Fumitaka Osakada, Balaji Sriram, Onkar S. Dhande, Phong L. Nguyen, Edward M. Callaway, Anirvan Ghosh, and Andrew D. Huberman. 2014. "A Dedicated Circuit Links Direction-Selective Retinal Ganglion Cells to the Primary Visual Cortex." *Nature* 507(7492):358–61.
67. Dähne, Sven, Niko Wilbert, and Laurenz Wiskott. 2014. "Slow Feature Analysis on Retinal Waves Leads to V1 Complex Cells." *PLoS Computational Biology* 10(5):e1003564.
68. Dai, Jinxia, Jasbir S. Dalal, Sonal Thakar, Mark Henkemeyer, Vance P. Lemmon, Jill S. Harunaga, Monika C. Schlatter, Mona Buhusi, and Patricia F. Maness. 2012. "EphB Regulates L1

Phosphorylation during Retinocollicular Mapping." *Molecular and Cellular Neurosciences* 50(2):201–10.

69. Delwig, Anton, Anne M. Logan, David R. Copenhagen, and Andrew H. Ahn. 2012. "Light Evokes Melanopsin-Dependent Vocalization and Neural Activation Associated with Aversive Experience in Neonatal Mice." *PloS One* 7(9):e43787.
70. Demas, James A., Hannah Payne, and Hollis T. Cline. 2012. "Vision Drives Correlated Activity without Patterned Spontaneous Activity in Developing Xenopus Retina." *Developmental Neurobiology* 72(4):537–46.
71. Demas, Jay, Stephen J. Eglen, and Rachel O. L. Wong. 2003. "Developmental Loss of Synchronous Spontaneous Activity in the Mouse Retina Is Independent of Visual Experience." *The Journal of Neuroscience : The Official Journal of the Society for Neuroscience* 23(7):2851–60.
72. Demerens, C., B. Stankoff, M. Logak, P. Anglade, B. Allinquant, F. Couraud, B. Zalc, and C. Lubetzki. 1996. "Induction of Myelination in the Central Nervous System by Electrical Activity." *Proceedings of the National Academy of Sciences of the United States of America* 93(18):9887–92.
73. Denk, Winfried and Heinz Horstmann. 2004. "Serial Block-Face Scanning Electron Microscopy to Reconstruct Three-Dimensional Tissue Nanostructure." *PLoS Biology* 2(11):e329.
74. DeWoskin, Daniel, Jihwan Myung, Mino D. C. Belle, Hugh D. Piggins, Toru Takumi, and Daniel B. Forger. 2015. "Distinct Roles for GABA across Multiple Timescales in Mammalian Circadian Timekeeping." *Proceedings of the National Academy of Sciences of the United States of America* 112(29):E3911-9.
75. Dhande, Onkar S., Maureen E. Estevez, Lauren E. Quattrochi, Rana N. El-Danaf, Phong L. Nguyen, David M. Berson, and Andrew D. Huberman. 2013. "Genetic Dissection of Retinal Inputs to Brainstem Nuclei Controlling Image Stabilization." *The Journal of Neuroscience : The Official Journal of the Society for Neuroscience* 33(45):17797–813.
76. Dhande, Onkar S., Ethan W. Hua, Emily Guh, Jonathan Yeh, Shivani Bhatt, Yueyi Zhang, Edward S. Ruthazer, Marla B. Feller, and Michael C. Crair. 2011. "Development of Single Retinofugal Axon Arbors in Normal and β2 Knock-out Mice." *The Journal of Neuroscience : The Official Journal of the Society for Neuroscience* 31(9):3384–99.
77. Dhande, Onkar S. and Andrew D. Huberman. 2014. "Retinal Ganglion Cell Maps in the Brain: Implications for Visual Processing." *Current Opinion in Neurobiology* 24(1):133–42.
78. Do, Michael Tri Hoang and King-Wai Yau. 2010. "Intrinsically Photosensitive Retinal Ganglion Cells." *Physiological Reviews* 90(4):1547–81.

79. Dong, Wei and Carlos D. Aizenman. 2012. “A Competition-Based Mechanism Mediates Developmental Refinement of Tectal Neuron Receptive Fields.” *The Journal of Neuroscience : The Official Journal of the Society for Neuroscience* 32(47):16872–79.
80. Dräger, U. C. and D. H. Hubel. 1975. “Responses to Visual Stimulation and Relationship between Visual, Auditory, and Somatosensory Inputs in Mouse Superior Colliculus.” *Journal of Neurophysiology* 38(3):690–713.
81. Dräger, U. C. and D. H. Hubel. 1976. “Topography of Visual and Somatosensory Projections to Mouse Superior Colliculus.” *Journal of Neurophysiology* 39(1):91–101.
82. Dräger, U. C. and J. F. Olsen. 1980. “Origins of Crossed and Uncrossed Retinal Projections in Pigmented and Albino Mice.” *The Journal of Comparative Neurology* 191(3):383–412.
83. Duncan, M. J., M. J. Banister, and S. M. Reppert. 1986. “Developmental Appearance of Light-Dark Entrainment in the Rat.” *Brain Research* 369(1–2):326–30.
84. Dunn, Felice A., Luca Della Santina, Edward D. Parker, and Rachel O. L. Wong. 2013. “Sensory Experience Shapes the Development of the Visual System’s First Synapse.” *Neuron* 80(5):1159–66.
85. Ecker, Jennifer L., Olivia N. Dumitrescu, Kwoon Y. Wong, Nazia M. Alam, Shih-Kuo Chen, Tara LeGates, Jordan M. Renna, Glen T. Prusky, David M. Berson, and Samer Hattar. 2010. “Melanopsin-Expressing Retinal Ganglion-Cell Photoreceptors: Cellular Diversity and Role in Pattern Vision.” *Neuron* 67(1):49–60.
86. Ellis, Erika M., Gregory Gauvain, Benjamin Sivyer, and Gabe J. Murphy. 2016. “Shared and Distinct Retinal Input to the Mouse Superior Colliculus and Dorsal Lateral Geniculate Nucleus.” *Journal of Neurophysiology* 116(2):602–10.
87. Enoki, Ryosuke, Daisuke Ono, Shigeru Kuroda, Sato Honma, and Ken-Ichi Honma. 2017. “Dual Origins of the Intracellular Circadian Calcium Rhythm in the Suprachiasmatic Nucleus.” *Scientific Reports* 7:41733.
88. Estevez, Maureen E., P. Michelle Fogerson, Marissa C. Ilardi, Bart G. Borghuis, Eric Chan, Shijun Weng, Olivia N. Auferkorte, Jonathan B. Demb, and David M. Berson. 2012. “Form and Function of the M4 Cell, an Intrinsically Photosensitive Retinal Ganglion Cell Type Contributing to Geniculocortical Vision.” *The Journal of Neuroscience : The Official Journal of the Society for Neuroscience* 32(39):13608–20.
89. Evans, Jennifer A., Tanya L. Leise, Oscar Castanon-Cervantes, and Alec J. Davidson. 2011. “Intrinsic Regulation of Spatiotemporal Organization within the Suprachiasmatic Nucleus.” *PloS One* 6(1):e15869.

90. Failor, Samuel Wilson, Arash Ng, and Hwai-Jong Cheng. 2018. “Monocular Enucleation Alters Retinal Waves in the Surviving Eye.” *Neural Development* 13(1):4.
91. Faisal, A. Aldo, Luc P. J. Selen, and Daniel M. Wolpert. 2008. “Noise in the Nervous System.” *Nature Reviews Neuroscience* 9(4):292–303.
92. Feller, M. B., D. A. Butts, H. L. Aaron, D. S. Rokhsar, and C. J. Shatz. 1997. “Dynamic Processes Shape Spatiotemporal Properties of Retinal Waves.” *Neuron* 19(2):293–306.
93. Feller, M. B., D. P. Wellis, D. Stellwagen, F. S. Werblin, and C. J. Shatz. 1996. “Requirement for Cholinergic Synaptic Transmission in the Propagation of Spontaneous Retinal Waves.” *Science (New York, N.Y.)* 272(5265):1182–87.
94. Feller, Marla B. 2002. “The Role of NAChR-Mediated Spontaneous Retinal Activity in Visual System Development.” *Journal of Neurobiology* 53(4):556–67.
95. Fernandez, Diego Carlos, Yi-Ting Chang, Samer Hattar, and Shih-Kuo Chen. 2016. “Architecture of Retinal Projections to the Central Circadian Pacemaker.” *Proceedings of the National Academy of Sciences* 113(21):6047–52.
96. Fleming, M. D., R. M. Benca, and M. Behan. 2006. “Retinal Projections to the Subcortical Visual System in Congenic Albino and Pigmented Rats.” *Neuroscience* 143(3):895–904.
97. Ford, Kevin J., Aude L. Félix, and Marla B. Feller. 2012. “Cellular Mechanisms Underlying Spatiotemporal Features of Cholinergic Retinal Waves.” *The Journal of Neuroscience : The Official Journal of the Society for Neuroscience* 32(3):850–63.
98. Ford, Kevin J. and Marla B. Feller. 2012. “Assembly and Disassembly of a Retinal Cholinergic Network.” *Visual Neuroscience* 29(1):61–71.
99. Freeman, G. Mark, Rebecca M. Krock, Sara J. Aton, Paul Thaben, and Erik D. Herzog. 2013. “GABA Networks Destabilize Genetic Oscillations in the Circadian Pacemaker.” *Neuron* 78(5):799–806.
100. Frisén, J., P. A. Yates, T. McLaughlin, Glenn C. Friedman, D. D. O’Leary, and Mariano Barbacid. 1998. “Ephrin-A5 (AL-1/RAGS) Is Essential for Proper Retinal Axon Guidance and Topographic Mapping in the Mammalian Visual System.” *Neuron* 20(2):235–43.
101. Fuerst, Peter G., Freyja Bruce, Ryan P. Rounds, Lynda Erskine, and Robert W. Burgess. 2012. “Cell Autonomy of DSCAM Function in Retinal Development.” *Developmental Biology* 361(2):326–37.
102. Fujiyama, Fumino, Hiroyuki Hioki, Ryohei Tomioka, Kousuke Taki, Nobuaki Tamamaki, Sakashi Nomura, Keiko Okamoto, and Takeshi Kaneko. 2003. “Changes of Immunocytochemical Localization of Vesicular Glutamate Transporters in the Rat Visual System after the Retinofugal

Denervation." *The Journal of Comparative Neurology* 465(2):234–49.

103. Gale, N. W., S. J. Holland, D. M. Valenzuela, A. Flenniken, L. Pan, T. E. Ryan, M. Henkemeyer, K. Strebhardt, H. Hirai, D. G. Wilkinson, T. Pawson, S. Davis, and G. D. Yancopoulos. 1996. "Eph Receptors and Ligands Comprise Two Major Specificity Subclasses and Are Reciprocally Compartmentalized during Embryogenesis." *Neuron* 17(1):9–19.

104. Galli, L. and L. Maffei. 1988. "Spontaneous Impulse Activity of Rat Retinal Ganglion Cells in Prenatal Life." *Science (New York, N.Y.)* 242(4875):90–91.

105. Gamlin, Paul D. R. 2006. "The Pretectum: Connections and Oculomotor-Related Roles." *Progress in Brain Research* 151:379–405.

106. Garaschuk, O., E. Hanse, and A. Konnerth. 1998. "Developmental Profile and Synaptic Origin of Early Network Oscillations in the CA1 Region of Rat Neonatal Hippocampus." *The Journal of Physiology* 507 (Pt 1:219–36.

107. Garaschuk, O., J. Linn, J. Eilers, and A. Konnerth. 2000. "Large-Scale Oscillatory Calcium Waves in the Immature Cortex." *Nature Neuroscience* 3(5):452–59.

108. García-Frigola, Cristina and Eloísa Herrera. 2010. "Zic2 Regulates the Expression of Sert to Modulate Eye-Specific Refinement at the Visual Targets." *The EMBO Journal* 29(18):3170–83.

109. Godement, P., J. Salaün, and M. Imbert. 1984. "Prenatal and Postnatal Development of Retinogeniculate and Retinocollicular Projections in the Mouse." *The Journal of Comparative Neurology* 230(4):552–75.

110. Golding, Bruno, Gabrielle Pouchelon, Camilla Bellone, Sahana Murthy, Ariel A. Di Nardo, Subashika Govindan, Masahuro Ogawa, Tomomi Shimogori, Christian Lüscher, Alexandre Dayer, and Denis Jabaudon. 2014. "Retinal Input Directs the Recruitment of Inhibitory Interneurons into Thalamic Visual Circuits." *Neuron* 81(5):1057–69.

111. Gonzalez-Islas, Carlos and Peter Wenner. 2006. "Spontaneous Network Activity in the Embryonic Spinal Cord Regulates AMPAergic and GABAergic Synaptic Strength." *Neuron* 49(4):563–75.

112. Grubb, Matthew S., Francesco M. Rossi, Jean Pierre Changeux, and Ian D. Thompson. 2003. "Abnormal Functional Organization in the Dorsal Lateral Geniculate Nucleus of Mice Lacking the Beta 2 Subunit of the Nicotinic Acetylcholine Receptor." *Neuron* 40(6):1161–72.

113. Guillery, R. W. 1971. "Patterns of Synaptic Interconnections in the Dorsal Lateral Geniculate Nucleus of Cat and Monkey: A Brief Review." *Vision Research* Suppl 3:211–27.

114. Güler, Ali D., Jennifer L. Ecker, Gurprit S. Lall, Shafiqul Haq, Cara M. Altimus, Hsi-Wen Liao, Alun R. Barnard, Hugh Cahill, Tudor C. Badea, Haiqing Zhao, Mark W. Hankins, David M. Berson, Robert J. Lucas, King-Wai Yau, and Samer Hattar. 2008. "Melanopsin Cells Are the Principal

Conduits for Rod-Cone Input to Non-Image-Forming Vision." *Nature* 453(7191):102–5.

115. Gust, J., J. J. Wright, E. B. Pratt, and M. M. Bosma. 2003. "Development of Synchronized Activity of Cranial Motor Neurons in the Segmented Embryonic Mouse Hindbrain." *The Journal of Physiology* 550(Pt 1):123–33.

116. Guy, J., O. Bosler, G. Dusticier, G. Pelletier, and A. Calas. 1987. "Morphological Correlates of Serotonin-Neuropeptide Y Interactions in the Rat Suprachiasmatic Nucleus: Combined Radioautographic and Immunocytochemical Data." *Cell and Tissue Research* 250(3):657–62.

117. Hagihara, Kenta M., Tomonari Murakami, Takashi Yoshida, Yoshiaki Tagawa, and Kenichi Ohki. 2015. "Neuronal Activity Is Not Required for the Initial Formation and Maturation of Visual Selectivity." *Nature Neuroscience* 18(12):1780–88.

118. Hammer, Sarah, Aboozar Monavarfeshani, Tyler Lemon, Jianmin Su, and Michael Andrew Fox. 2015. "Multiple Retinal Axons Converge onto Relay Cells in the Adult Mouse Thalamus." *Cell Reports* 12(10):1575–83.

119. Hamos, James E., Susan C. Van Horn, Denis Raczkowski, and S. Murray Sherman. 1987. "Synaptic Circuits Involving an Individual Retinogeniculate Axon in the Cat." *The Journal of Comparative Neurology* 259(2):165–92.

120. Hansen, Kristi A., Christine L. Torborg, Justin Elstrott, and Marla B. Feller. 2005. "Expression and Function of the Neuronal Gap Junction Protein Connexin 36 in Developing Mammalian Retina." *The Journal of Comparative Neurology* 493(2):309–20.

121. Hanson, M. Gartz and Lynn T. Landmesser. 2004. "Normal Patterns of Spontaneous Activity Are Required for Correct Motor Axon Guidance and the Expression of Specific Guidance Molecules." *Neuron* 43(5):687–701.

122. Hastings, Michael H., Elizabeth S. Maywood, and Marco Brancaccio. 2018. "Generation of Circadian Rhythms in the Suprachiasmatic Nucleus." *Nature Reviews. Neuroscience* 19(8):453–69.

123. Hatori, Megumi, Hiep Le, Christopher Vollmers, Sheena Racheal Keding, Nobushige Tanaka, Thorsten Buch, Ari Waisman, Christian Schmedt, Timothy Jegla, and Satchidananda Panda. 2008. "Inducible Ablation of Melanopsin-Expressing Retinal Ganglion Cells Reveals Their Central Role in Non-Image Forming Visual Responses." *PloS One* 3(6):e2451.

124. Hattar, S., H. W. Liao, M. Takao, D. M. Berson, and K. W. Yau. 2002. "Melanopsin-Containing Retinal Ganglion Cells: Architecture, Projections, and Intrinsic Photosensitivity." *Science (New York, N.Y.)* 295(5557):1065–70.

125. Hattar, S., R. J. Lucas, N. Mrosovsky, S. Thompson, R. H. Douglas, M. W. Hankins, J. Lem, M. Biel,

F. Hofmann, R. G. Foster, and K. W. Yau. 2003. “Melanopsin and Rod-Cone Photoreceptive Systems Account for All Major Accessory Visual Functions in Mice.” *Nature* 424(6944):76–81.

126. Hattar, Samer, Monica Kumar, Alexander Park, Patrick Tong, Jonathan Tung, King-Wai Yau, and David M. Berson. 2006. “Central Projections of Melanopsin-Expressing Retinal Ganglion Cells in the Mouse.” *The Journal of Comparative Neurology* 497(3):326–49.

127. Häusser, M., N. Spruston, and G. J. Stuart. 2000. “Diversity and Dynamics of Dendritic Signaling.” *Science (New York, N.Y.)* 290(5492):739–44.

128. Hayter, Edward A. and Timothy M. Brown. 2018. “Additive Contributions of Melanopsin and Both Cone Types Provide Broadband Sensitivity to Mouse Pupil Control.” *BMC Biology* 16(1):83.

129. Heck, Nicolas, Antje Golbs, Therese Riedemann, Jyh-Jang Sun, Volkmar Lessmann, and Heiko J. Luhmann. 2008. “Activity-Dependent Regulation of Neuronal Apoptosis in Neonatal Mouse Cerebral Cortex.” *Cerebral Cortex (New York, N.Y. : 1991)* 18(6):1335–49.

130. Hennig, Matthias H., Christopher Adams, David Willshaw, and Evelyne Sernagor. 2009. “Early-Stage Waves in the Retinal Network Emerge Close to a Critical State Transition between Local and Global Functional Connectivity.” *The Journal of Neuroscience : The Official Journal of the Society for Neuroscience* 29(4):1077–86.

131. Hennig, Matthias H., John Grady, James van Coppenhagen, and Evelyne Sernagor. 2011. “Age-Dependent Homeostatic Plasticity of GABAergic Signaling in Developing Retinal Networks.” *The Journal of Neuroscience : The Official Journal of the Society for Neuroscience* 31(34):12159–64.

132. Herrera, Eloísa, Lucia Brown, Jun Aruga, Rivka A. Rachel, Gül Dolen, Katsuhiko Mikoshiba, Stephen Brown, and Carol A. Mason. 2003. “Zic2 Patterns Binocular Vision by Specifying the Uncrossed Retinal Projection.” *Cell* 114(5):545–57.

133. Herzog, Erik D., Tracey Hermanstyne, Nicola J. Smyllie, and Michael H. Hastings. 2017. “Regulating the Suprachiasmatic Nucleus (SCN) Circadian Clockwork: Interplay between Cell-Autonomous and Circuit-Level Mechanisms.” *Cold Spring Harbor Perspectives in Biology* 9(1).

134. Hicks, David. 2011. “Second Sight? Ecker JL, Dumitrescu ON, Wong KY, Alam NM, Chen SK, LeGates T, Renna JM, Prusky GT, Berson DM, Hattar S (2010) Melanopsin-Expressing Retinal Ganglion-Cell Photoreceptors: Cellular Diversity and Role in Pattern Vision. Neuron 67:49-60.” *Graefe’s Archive for Clinical and Experimental Ophthalmology = Albrecht von Graefes Archiv Fur Klinische Und Experimentelle Ophthalmologie* 249(3):313–14.

135. Hindges, Robert, Todd McLaughlin, Nicolas Genoud, Mark Henkemeyer, and Dennis D. M. O’Leary. 2002. “EphB Forward Signaling Controls Directional Branch Extension and Arborization Required for Dorsal-Ventral Retinotopic Mapping.” *Neuron* 35(3):475–87.

136. Hiramoto, Masaki and Hollis T. Cline. 2014. “Optic Flow Instructs Retinotopic Map Formation through a Spatial to Temporal to Spatial Transformation of Visual Information.” *Proceedings of the National Academy of Sciences of the United States of America* 111(47):E5105-13.

137. Hisano, S., M. Chikamori-Aoyama, S. Katoh, M. Maegawa, and S. Daikoku. 1987. “Immunohistochemical Evidence of Serotoninergic Regulation of Vasoactive Intestinal Polypeptide (VIP) in the Rat Suprachiasmatic Nucleus.” *Histochemistry* 86(6):573–78.

138. Hong, Y. Kate, Eliza F. Burr, Joshua R. Sanes, and Chinfei Chen. 2019. “Heterogeneity of Retinogeniculate Axon Arbors.” *The European Journal of Neuroscience* 49(7):948–56.

139. Hong, Y. Kate, In-Jung Kim, and Joshua R. Sanes. 2011. “Stereotyped Axonal Arbors of Retinal Ganglion Cell Subsets in the Mouse Superior Colliculus.” *The Journal of Comparative Neurology* 519(9):1691–1711.

140. Hooks, Bryan M. and Chinfei Chen. 2007. “Critical Periods in the Visual System: Changing Views for a Model of Experience-Dependent Plasticity.” *Neuron* 56(2):312–26.

141. Hou, Qingming, Dawei Zhang, Larissa Jarzylo, Richard L. Huganir, and Heng-Ye Man. 2008. “Homeostatic Regulation of AMPA Receptor Expression at Single Hippocampal Synapses.” *Proceedings of the National Academy of Sciences of the United States of America* 105(2):775–80.

142. Howarth, Michael, Lauren Walmsley, and Timothy M. Brown. 2014. “Binocular Integration in the Mouse Lateral Geniculate Nuclei.” *Current Biology : CB* 24(11):1241–47.

143. Hu, Edward H., Feng Pan, Béla Völgyi, and Stewart A. Bloomfield. 2010. “Light Increases the Gap Junctional Coupling of Retinal Ganglion Cells.” *The Journal of Physiology* 588(Pt 21):4145–63.

144. Huberman, Andrew D., Marla B. Feller, and Barbara Chapman. 2008. “Mechanisms Underlying Development of Visual Maps and Receptive Fields.” *Annual Review of Neuroscience* 31:479–509.

145. Huberman, Andrew D., Mihai Manu, Selina M. Koch, Michael W. Susman, Amanda Brosius Lutz, Erik M. Ullian, Stephen A. Baccus, and Ben A. Barres. 2008. “Architecture and Activity-Mediated Refinement of Axonal Projections from a Mosaic of Genetically Identified Retinal Ganglion Cells.” *Neuron* 59(3):425–38.

146. Huberman, Andrew D., Karl D. Murray, David K. Warland, David A. Feldheim, and Barbara Chapman. 2005. “Ephrin-As Mediate Targeting of Eye-Specific Projections to the Lateral Geniculate Nucleus.” *Nature Neuroscience* 8(8):1013–21.

147. Huberman, Andrew D. and Cristopher M. Niell. 2011. “What Can Mice Tell Us about How Vision Works?” *Trends in Neurosciences* 34(9):464–73.

148. Huberman, Andrew D., David Stellwagen, and Barbara Chapman. 2002. “Decoupling Eye-Specific

Segregation from Lamination in the Lateral Geniculate Nucleus." *The Journal of Neuroscience : The Official Journal of the Society for Neuroscience* 22(21):9419–29.

149. Huberman, Andrew D., Guo-Yong Wang, Lauren C. Liets, Odell A. Collins, Barbara Chapman, and Leo M. Chalupa. 2003. "Eye-Specific Retinogeniculate Segregation Independent of Normal Neuronal Activity." *Science (New York, N.Y.)* 300(5621):994–98.

150. Huberman, Andrew D., Wei Wei, Justin Elstrott, Ben K. Stafford, Marla B. Feller, and Ben A. Barres. 2009. "Genetic Identification of an On-Off Direction-Selective Retinal Ganglion Cell Subtype Reveals a Layer-Specific Subcortical Map of Posterior Motion." *Neuron* 62(3):327–34.

151. Hutchins, J. B. and V. A. Casagrande. 1990. "Development of the Lateral Geniculate Nucleus: Interactions between Retinal Afferent, Cytoarchitectonic, and Glial Cell Process Lamination in Ferrets and Tree Shrews." *The Journal of Comparative Neurology* 298(1):113–28.

152. Ibata, Y., Y. Takahashi, H. Okamura, F. Kawakami, H. Terubayashi, T. Kubo, and N. Yanaihara. 1989. "Vasoactive Intestinal Peptide (VIP)-like Immunoreactive Neurons Located in the Rat Suprachiasmatic Nucleus Receive a Direct Retinal Projection." *Neuroscience Letters* 97(1–2):1–5.

153. Ikonomidou, C., F. Bosch, M. Miksa, P. Bittigau, J. Vöckler, K. Dikranian, T. I. Tenkova, V. Stefovska, L. Turski, and J. W. Olney. 1999. "Blockade of NMDA Receptors and Apoptotic Neurodegeneration in the Developing Brain." *Science (New York, N.Y.)* 283(5398):70–74.

154. James, Gregory, Simon R. Foster, Brian Key, and Annemiek Beverdam. 2013. "The Expression Pattern of EVA1C, a Novel Slit Receptor, Is Consistent with an Axon Guidance Role in the Mouse Nervous System." *PloS One* 8(9):e74115.

155. Jaubert-Miazza, Lisa, Erick Green, Fu-Sun Lo, Kim Bui, Jeremy Mills, and William Guido. 2005. "Structural and Functional Composition of the Developing Retinogeniculate Pathway in the Mouse." *Visual Neuroscience* 22(5):661–76.

156. Jetti, Suresh Kumar, Nuria Vendrell-Llopis, and Emre Yaksi. 2014. "Spontaneous Activity Governs Olfactory Representations in Spatially Organized Habenular Microcircuits." *Current Biology : CB* 24(4):434–39.

157. Jiang, Yu-Qiu, Boubker Zaaimi, and John H. Martin. 2016. "Competition with Primary Sensory Afferents Drives Remodeling of Corticospinal Axons in Mature Spinal Motor Circuits." *The Journal of Neuroscience : The Official Journal of the Society for Neuroscience* 36(1):193–203.

158. Johnson-Venkatesh, Erin M., Mudassar N. Khan, Geoffrey G. Murphy, Michael A. Sutton, and Hisashi Umemori. 2015. "Excitability Governs Neural Development in a Hippocampal Region-Specific Manner." *Development (Cambridge, England)* 142(22):3879–91.

159. Johnson, Juliette, Ning Tian, Matthew S. Caywood, Richard J. Reimer, Robert H. Edwards, and

David R. Copenhagen. 2003. “Vesicular Neurotransmitter Transporter Expression in Developing Postnatal Rodent Retina: GABA and Glycine Precede Glutamate.” *The Journal of Neuroscience : The Official Journal of the Society for Neuroscience* 23(2):518–29.

160. Johnson, Juliette, Vincent Wu, Michael Donovan, Sriparna Majumdar, René C. Rentería, Travis Porco, Russell N. Van Gelder, and David R. Copenhagen. 2010. “Melanopsin-Dependent Light Avoidance in Neonatal Mice.” *Proceedings of the National Academy of Sciences of the United States of America* 107(40):17374–78.

161. Juárez, Claudia, Elvira Morgado, Enrique Meza, Stefan M. Waliszewski, Raúl Aguilar-Roblero, and Mario Caba. 2013. “Development of Retinal Projections and Response to Photic Input in the Suprachiasmatic Nucleus of New Zealand White Rabbits.” *Brain Research* 1499:21–28.

162. Kalamatianos, Theodosis, Imre Kalló, Hugh D. Piggins, and Clive W. Coen. 2004. “Expression of VIP and/or PACAP Receptor MRNA in Peptide Synthesizing Cells within the Suprachiasmatic Nucleus of the Rat and in Its Efferent Target Sites.” *The Journal of Comparative Neurology* 475(1):19–35.

163. Karlen, Sarah J. and Leah Krubitzer. 2009. “Effects of Bilateral Enucleation on the Size of Visual and Nonvisual Areas of the Brain.” *Cerebral Cortex (New York, N.Y. : 1991)* 19(6):1360–71.

164. Kato, I., K. Harada, T. Hasegawa, T. Igarashi, Y. Koike, and T. Kawasaki. 1986. “Role of the Nucleus of the Optic Tract in Monkeys in Relation to Optokinetic Nystagmus.” *Brain Research* 364(1):12–22.

165. Kay, Jeremy N., Irina De la Huerta, In-Jung Kim, Yifeng Zhang, Masahito Yamagata, Monica W. Chu, Markus Meister, and Joshua R. Sanes. 2011. “Retinal Ganglion Cells with Distinct Directional Preferences Differ in Molecular Identity, Structure, and Central Projections.” *The Journal of Neuroscience : The Official Journal of the Society for Neuroscience* 31(21):7753–62.

166. Kenet, Tal, Dmitri Bibitchkov, Misha Tsodyks, Amiram Grinvald, and Amos Arieli. 2003. “Spontaneously Emerging Cortical Representations of Visual Attributes.” *Nature* 425(6961):954–56.

167. Kerschensteiner, Daniel. 2016. “Glutamatergic Retinal Waves.” *Frontiers in Neural Circuits* 10(May):1–7.

168. Kim, In-Jung, Yifeng Zhang, Markus Meister, and Joshua R. Sanes. 2010. “Laminar Restriction of Retinal Ganglion Cell Dendrites and Axons: Subtype-Specific Developmental Patterns Revealed with Transgenic Markers.” *The Journal of Neuroscience : The Official Journal of the Society for Neuroscience* 30(4):1452–62.

169. Kim, In-Jung, Yifeng Zhang, Masahito Yamagata, Markus Meister, and Joshua R. Sanes. 2008.

"Molecular Identification of a Retinal Cell Type That Responds to Upward Motion." *Nature* 452(7186):478–82.

170. Kim, Keun-Young, Luis C. Rios, Hiep Le, Alex J. Perez, Sébastien Phan, Eric A. Bushong, Thomas J. Deerinck, Yu Hsin Liu, Maya A. Ellisman, Varda Lev-Ram, Suyeon Ju, Sneha A. Panda, Sanghee Yoon, Masatoshi Hirayama, Ludovic S. Mure, Megumi Hatori, Mark H. Ellisman, and Satchidananda Panda. 2019. "Synaptic Specializations of Melanopsin-Retinal Ganglion Cells in Multiple Brain Regions Revealed by Genetic Label for Light and Electron Microscopy." *Cell Reports* 29(3):628-644.e6.

171. Kirkby, Lowry a and Marla B. Feller. 2013. "Intrinsically Photosensitive Ganglion Cells Contribute to Plasticity in Retinal Wave Circuits." *Proceedings of the National Academy of Sciences of the United States of America* (16):1–6.

172. Kiss, J., C. Léránth, and B. Halász. 1984. "Serotoninergic Endings on VIP-Neurons in the Suprachiasmatic Nucleus and on ACTH-Neurons in the Arcuate Nucleus of the Rat Hypothalamus. A Combination of High Resolution Autoradiography and Electron Microscopic Immunocytochemistry." *Neuroscience Letters* 44(2):119–24.

173. Koch, Selina M., Cassandra G. Dela Cruz, Thomas S. Hnasko, Robert H. Edwards, Andrew D. Huberman, and Erik M. Ullian. 2011. "Pathway-Specific Genetic Attenuation of Glutamate Release Alters Select Features of Competition-Based Visual Circuit Refinement." *Neuron* 71(2):235–42.

174. Kolodziejczak, Marta, Catherine Béchade, Nicolas Gervasi, Theano Irinopoulou, Sophie M. Banas, Corinne Cordier, Alexandra Rebsam, Anne Roumier, and Luc Maroteaux. 2015. "Serotonin Modulates Developmental Microglia via 5-HT2B Receptors: Potential Implication during Synaptic Refinement of Retinogeniculate Projections." *ACS Chemical Neuroscience* 6(7):1219–30.

175. Kothmann, W. Wade, Stephen C. Massey, and John O'Brien. 2009. "Dopamine-Stimulated Dephosphorylation of Connexin 36 Mediates AII Amacrine Cell Uncoupling." *The Journal of Neuroscience : The Official Journal of the Society for Neuroscience* 29(47):14903–11.

176. Koulakov, Alexei A. and Dmitry N. Tsigankov. 2004. "A Stochastic Model for Retinocollicular Map Development." *BMC Neuroscience* 5:30.

177. Kozorovitskiy, Yevgenia, Arpiar Saunders, Caroline A. Johnson, Bradford B. Lowell, and Bernardo L. Sabatini. 2012. "Recurrent Network Activity Drives Striatal Synaptogenesis." *Nature* 485(7400):646–50.

178. Krahe, Thomas E. and William Guido. 2011. "Homeostatic Plasticity in the Visual Thalamus by Monocular Deprivation." *The Journal of Neuroscience : The Official Journal of the Society for Neuroscience* 31(18):6842–49.

179.Krout, K. E., J. Kawano, T. C. Mettenleiter, and A. D. Loewy. 2002. “CNS Inputs to the Suprachiasmatic Nucleus of the Rat.” *Neuroscience* 110(1):73–92.

180.Kubota, T., M. Morimoto, T. Kanaseki, and H. Inomata. 1987. “Projection from the Pretectal Nuclei to the Dorsal Lateral Geniculate Nucleus in the Cat: A Wheat Germ Agglutinin-Horseradish Peroxidase Study.” *Brain Research* 421(1–2):30–40.

181.Kutsarova, Elena, Martin Munz, and Edward S. Ruthazer. 2017. “Rules for Shaping Neural Connections in the Developing Brain.” *Frontiers in Neural Circuits* 10(January):1–16.

182.Lacoste, Baptiste, Cesar H. Comin, Ayal Ben-Zvi, Pascal S. Kaeser, Xiaoyin Xu, Luciano da F. Costa, and Chenghua Gu. 2014. “Sensory-Related Neural Activity Regulates the Structure of Vascular Networks in the Cerebral Cortex.” *Neuron* 83(5):1117–30.

183.Landmesser, L. T. and M. J. O’Donovan. 1984. “Activation Patterns of Embryonic Chick Hind Limb Muscles Recorded in Ovo and in an Isolated Spinal Cord Preparation.” *The Journal of Physiology* 347:189–204.

184.Leard, L. E., E. S. Macdonald, H. C. Heller, and T. S. Kilduff. 1994. “Ontogeny of Photic-Induced c-Fos MRNA Expression in Rat Suprachiasmatic Nuclei.” *Neuroreport* 5(18):2683–87.

185.Lee, Philip R., Jonathan E. Cohen, Dumitru A. Iacobas, Sanda Iacobas, and R. Douglas Fields. 2017. “Gene Networks Activated by Specific Patterns of Action Potentials in Dorsal Root Ganglia Neurons.” *Scientific Reports* 7:43765.

186.LeGates, Tara A., Diego C. Fernandez, and Samer Hattar. 2014. “Light as a Central Modulator of Circadian Rhythms, Sleep and Affect.” *Nature Reviews. Neuroscience* 15(7):443–54.

187.LeSauter, J., L. J. Kriegsfeld, J. Hon, and R. Silver. 2002. “Calbindin-D(28K) Cells Selectively Contact Intra-SCN Neurons.” *Neuroscience* 111(3):575–85.

188.Liang, Liang, Alex Fratzl, Glenn Goldey, Rohan N. Ramesh, Arthur U. Sugden, Josh L. Morgan, Chinfei Chen, and Mark L. Andermann. 2018. “A Fine-Scale Functional Logic to Convergence from Retina to Thalamus.” *Cell* 173(6):1343-1355.e24.

189.Liets, Lauren C., Bruno A. Olshausen, Guo-Yong Wang, and Leo M. Chalupa. 2003. “Spontaneous Activity of Morphologically Identified Ganglion Cells in the Developing Ferret Retina.” *The Journal of Neuroscience : The Official Journal of the Society for Neuroscience* 23(19):7343–50.

190.Lim, Yoo-Shick, Todd McLaughlin, Tsung-Chang Sung, Alicia Santiago, Kuo-Fen Lee, and Dennis D. M. O’Leary. 2008. “P75(NTR) Mediates Ephrin-A Reverse Signaling Required for Axon Repulsion and Mapping.” *Neuron* 59(5):746–58.

191.London, Michael and Michael Häusser. 2005. “Dendritic Computation.” *Annual Review of Neuroscience* 28:503–32.

192. Luhmann, Heiko J., Anne Sinning, Jenq-Wei Yang, Vicente Reyes-Puerta, Maik C. Stüttgen, Sergei Kirischuk, and Werner Kilb. 2016. "Spontaneous Neuronal Activity in Developing Neocortical Networks: From Single Cells to Large-Scale Interactions." *Frontiers in Neural Circuits* 10:40.

193. Lüscher, Christian and Robert C. Malenka. 2012. "NMDA Receptor-Dependent Long-Term Potentiation and Long-Term Depression (LTP/LTD)." *Cold Spring Harbor Perspectives in Biology* 4(6).

194. Maccione, Alessandro, Matthias H. Hennig, Mauro Gandolfo, Oliver Muthmann, James van Coppenhagen, Stephen J. Eglen, Luca Berdondini, and Evelyne Sernagor. 2014. "Following the Ontogeny of Retinal Waves: Pan-Retinal Recordings of Population Dynamics in the Neonatal Mouse." *The Journal of Physiology* 592(7):1545–63.

195. Magee, J. C. 2000. "Dendritic Integration of Excitatory Synaptic Input." *Nature Reviews. Neuroscience* 1(3):181–90.

196. Mao, Chai-An, Hongyan Li, Zhijing Zhang, Takae Kiyama, Satchidananda Panda, Samer Hattar, Christophe P. Ribelayga, Stephen L. Mills, and Steven W. Wang. 2014. "T-Box Transcription Regulator Tbr2 Is Essential for the Formation and Maintenance of Opn4/Melanopsin-Expressing Intrinsically Photosensitive Retinal Ganglion Cells." *The Journal of Neuroscience : The Official Journal of the Society for Neuroscience* 34(39):13083–95.

197. Marcucci, Florencia, Célia A. Soares, and Carol Mason. 2019. "Distinct Timing of Neurogenesis of Ipsilateral and Contralateral Retinal Ganglion Cells." *The Journal of Comparative Neurology* 527(1):212–24.

198. Marler, Katharine J., Philipp Suetterlin, Asha Dopplapudi, Aine Rubikaite, Jihad Adnan, Nicola A. Maiorano, Andrew S. Lowe, Ian D. Thompson, Manav Pathania, Angelique Bordey, Tudor Fulga, David L. Van Vactor, Robert Hindges, and Uwe Drescher. 2014. "BDNF Promotes Axon Branching of Retinal Ganglion Cells via MiRNA-132 and P250GAP." *The Journal of Neuroscience : The Official Journal of the Society for Neuroscience* 34(3):969–79.

199. Marques, K. M. and R. J. Clarke. 1990. "The Development of the Retinal Projection to the Olivary Pretectal Nucleus in Normal and Monocularly Enucleated Hamsters." *Brazilian Journal of Medical and Biological Research = Revista Brasileira de Pesquisas Medicas e Biologicas* 23(6–7):601–3.

200. Martin, P. R. 1986. "The Projection of Different Retinal Ganglion Cell Classes to the Dorsal Lateral Geniculate Nucleus in the Hooded Rat." *Experimental Brain Research* 62(1):77–88.

201. Martini, Francisco J., Verónica Moreno-Juan, Anton Filipchuk, Miguel Valdeolmillos, and Guillermina López-Bendito. 2018. "Impact of Thalamocortical Input on Barrel Cortex Development." *Neuroscience* 368:246–55.

202. Masland, R. H. 1977. “Maturation of Function in the Developing Rabbit Retina.” *The Journal of Comparative Neurology* 175(3):275–86.

203. Masland, Richard H. 2012. “The Neuronal Organization of the Retina.” *Neuron* 76(2):266–80.

204. Maywood, Elizabeth S., Johanna E. Chesham, John A. O’Brien, and Michael H. Hastings. 2011. “A Diversity of Paracrine Signals Sustains Molecular Circadian Cycling in Suprachiasmatic Nucleus Circuits.” *Proceedings of the National Academy of Sciences of the United States of America* 108(34):14306–11.

205. McLaughlin, Todd, Robert Hindges, and Dennis Dm O’Leary. 2003. “Regulation of Axial Patterning of the Retina and Its Topographic Mapping in the Brain.” *Current Opinion in Neurobiology* 13(1):57–69.

206. McLaughlin, Todd, Yoo-Shick Lim, Alicia Santiago, and Dennis D. M. O’Leary. 2014. “Multiple EphB Receptors Mediate Dorsal-Ventral Retinotopic Mapping via Similar Bi-Functional Responses to Ephrin-B1.” *Molecular and Cellular Neurosciences* 63:24–30.

207. McNeill, David S., Catherine J. Sheely, Jennifer L. Ecker, Tudor C. Badea, Duncan Morhardt, William Guido, and Samer Hattar. 2011. “Development of Melanopsin-Based Irradiance Detecting Circuitry.” *Neural Development* 6(1):2–11.

208. Meister, M., R. O. Wong, D. A. Baylor, and C. J. Shatz. 1991. “Synchronous Bursts of Action Potentials in Ganglion Cells of the Developing Mammalian Retina.” *Science (New York, N.Y.)* 252(5008):939–43.

209. Migliarini, S., G. Pacini, B. Pelosi, G. Lunardi, and M. Pasqualetti. 2013. “Lack of Brain Serotonin Affects Postnatal Development and Serotonergic Neuronal Circuitry Formation.” *Molecular Psychiatry* 18(10):1106–18.

210. Mills, S. L. and S. C. Massey. 1995. “Differential Properties of Two Gap Junctional Pathways Made by AII Amacrine Cells.” *Nature* 377(6551):734–37.

211. Mills, Stephen L., Xiao-Bo Xia, Hideo Hoshi, Sally I. Firth, Margaret E. Rice, Laura J. Frishman, and David W. Marshak. 2007. “Dopaminergic Modulation of Tracer Coupling in a Ganglion-Amacrine Cell Network.” *Visual Neuroscience* 24(4):593–608.

212. Ming, G., J. Henley, M. Tessier-Lavigne, H. Song, and M. Poo. 2001. “Electrical Activity Modulates Growth Cone Guidance by Diffusible Factors.” *Neuron* 29(2):441–52.

213. Moore, R. Y. and M. E. Bernstein. 1989. “Synaptogenesis in the Rat Suprachiasmatic Nucleus Demonstrated by Electron Microscopy and Synapsin I Immunoreactivity.” *The Journal of Neuroscience : The Official Journal of the Society for Neuroscience* 9(6):2151–62.

214. Moreno-Juan, Verónica, Anton Filipchuk, Noelia Antón-Bolaños, Cecilia Mezzera, Henrik Gezelius,

Belen Andrés, Luis Rodríguez-Malmierca, Rafael Susín, Olivier Schaad, Takuji Iwasato, Roland Schüle, Michael Rutlin, Sacha Nelson, Sebastien Ducret, Miguel Valdeolmillos, Filippo M. Rijli, and Guillermina López-Bendito. 2017. "Prenatal Thalamic Waves Regulate Cortical Area Size Prior to Sensory Processing." *Nature Communications* 8.

215. Morgan, Josh Lyskowski, Daniel Raimund Berger, Arthur Willis Wetzel, and Jeff William Lichtman. 2016. "The Fuzzy Logic of Network Connectivity in Mouse Visual Thalamus." *Cell* 165(1):192–206.

216. Morin, Lawrence P. 2007. "SCN Organization Reconsidered." *Journal of Biological Rhythms* 22(1):3–13.

217. Morin, Lawrence P. and Keith M. Studholme. 2014. "Retinofugal Projections in the Mouse." *The Journal of Comparative Neurology* 522(16):3733–53.

218. Mouland, Joshua W., Adam R. Stinchcombe, Daniel B. Forger, Timothy M. Brown, and Robert J. Lucas. 2017. "Responses to Spatial Contrast in the Mouse Suprachiasmatic Nuclei." *Current Biology : CB* 27(11):1633-1640.e3.

219. Mrsic-Flogel, Thomas D., Sonja B. Hofer, Claire Creutzfeldt, Isabelle Cloëz-Tayarani, Jean-Pierre Changeux, Tobias Bonhoeffer, and Mark Hübener. 2005. "Altered Map of Visual Space in the Superior Colliculus of Mice Lacking Early Retinal Waves." *The Journal of Neuroscience : The Official Journal of the Society for Neuroscience* 25(29):6921–28.

220. Muñoz Llamosas, M., J. J. Huerta, R. Cernuda-Cernuda, and J. M. García-Fernández. 2000. "Ontogeny of a Photic Response in the Retina and Suprachiasmatic Nucleus in the Mouse." *Brain Research. Developmental Brain Research* 120(1):1–6.

221. Munteanu, Teona, Katelyn J. Noronha, Amanda C. Leung, Simon Pan, Jasmine A. Lucas, and Tiffany M. Schmidt. 2018. "Light-Dependent Pathways for Dopaminergic Amacrine Cell Development and Function." *ELife* 7.

222. Murata, Yasunobu and Matthew T. Colonnese. 2016. "An Excitatory Cortical Feedback Loop Gates Retinal Wave Transmission in Rodent Thalamus." *ELife* 5.

223. Murcia-Belmonte, Verónica, Yaiza Coca, Celia Vegar, Santiago Negueruela, Camino de Juan Romero, Arturo José Valiño, Salvador Sala, Ronan DaSilva, Artur Kania, Víctor Borrell, Luis M. Martinez, Lynda Erskine, and Eloísa Herrera. 2019a. "A Retino-Retinal Projection Guided by Unc5c Emerged in Species with Retinal Waves." *Current Biology : CB* 29(7):1149-1160.e4.

224. Murcia-Belmonte, Verónica, Yaiza Coca, Celia Vegar, Santiago Negueruela, Camino de Juan Romero, Arturo José Valiño, Salvador Sala, Ronan DaSilva, Artur Kania, Víctor Borrell, Luis M. Martinez, Lynda Erskine, and Eloísa Herrera. 2019b. "A Retino-Retinal Projection Guided by Unc5c Emerged in Species with Retinal Waves." *Current Biology : CB* 29(7):1149-1160.e4.

225. Muscat, Louise, Andrew D. Huberman, Cynthia L. Jordan, and Lawrence P. Morin. 2003. “Crossed and Uncrossed Retinal Projections to the Hamster Circadian System.” *The Journal of Comparative Neurology* 466(4):513–24.

226. Nakamoto, Chizu, Elaine Durward, Masato Horie, and Masaru Nakamoto. 2019. “Nell2 Regulates the Contralateral-versus-Ipsilateral Visual Projection as a Domain-Specific Positional Cue.” *Development (Cambridge, England)* 146(4).

227. Nakashima, Ai, Naoki Ihara, Mayo Shigeta, Hiroshi Kiyonari, Yuji Ikegaya, and Haruki Takeuchi. 2019. “Structured Spike Series Specify Gene Expression Patterns for Olfactory Circuit Formation.” *Science (New York, N.Y.)* 365(6448).

228. Nicol, Xavier, Sylvie Voyatzis, Aude Muzerelle, Nicolas Narboux-Nême, Thomas C. Südhof, Richard Miles, and Patricia Gaspar. 2007. “CAMP Oscillations and Retinal Activity Are Permissive for Ephrin Signaling during the Establishment of the Retinotopic Map.” *Nature Neuroscience* 10(3):340–47.

229. Noseda, Rodrigo and Rami Burstein. 2011. “Advances in Understanding the Mechanisms of Migraine-Type Photophobia.” *Current Opinion in Neurology* 24(3):197–202.

230. Noutel, Joao, Y. Kate Hong, Byunghee Leu, Erin Kang, and Chinfei Chen. 2011. “Experience-Dependent Retinogeniculate Synapse Remodeling Is Abnormal in MeCP2-Deficient Mice.” *Neuron* 70(1):35–42.

231. Ono, Daisuke, Sato Honma, and Ken-ichi Honma. 2013. “Cryptochromes Are Critical for the Development of Coherent Circadian Rhythms in the Mouse Suprachiasmatic Nucleus.” *Nature Communications* 4:1666.

232. Ono, Daisuke, Sato Honma, and Ken-Ichi Honma. 2016. “Differential Roles of AVP and VIP Signaling in the Postnatal Changes of Neural Networks for Coherent Circadian Rhythms in the SCN.” *Science Advances* 2(9):e1600960.

233. Osterhout, Jessica A., Rana N. El-Danaf, Phong L. Nguyen, and Andrew D. Huberman. 2014. “Birthdate and Outgrowth Timing Predict Cellular Mechanisms of Axon Target Matching in the Developing Visual Pathway.” *Cell Reports* 8(4):1006–17.

234. Owens, Melinda T., David a Feldheim, Michael P. Stryker, Jason W. Triplett, Melinda T. Owens, David a Feldheim, Michael P. Stryker, and Jason W. Triplett. 2015. “Stochastic Interaction between Neural Activity and Molecular Cues in the Formation of Topographic Article Stochastic Interaction between Neural Activity and Molecular Cues.” *Neuron* 87(6):1261–73.

235. Pak, Winnie, Robert Hindges, Yoo-Shick Lim, Samuel L. Pfaff, and Dennis D. M. O’Leary. 2004. “Magnitude of Binocular Vision Controlled by Islet-2 Repression of a Genetic Program That

Specifies Laterality of Retinal Axon Pathfinding." *Cell* 119(4):567–78.

236. Panda, Satchidananda, Ignacio Provencio, Daniel C. Tu, Susana S. Pires, Mark D. Rollag, Ana Maria Castrucci, Mathew T. Pletcher, Trey K. Sato, Tim Wiltshire, Mary Andahazy, Steve A. Kay, Russell N. Van Gelder, and John B. Hogenesch. 2003. "Melanopsin Is Required for Non-Image-Forming Photic Responses in Blind Mice." *Science (New York, N.Y.)* 301(5632):525–27.

237. Paul, Jodi R., Daniel DeWoskin, Laura J. McMeekin, Rita M. Cowell, Daniel B. Forger, and Karen L. Gamble. 2016. "Regulation of Persistent Sodium Currents by Glycogen Synthase Kinase 3 Encodes Daily Rhythms of Neuronal Excitability." *Nature Communications* 7:13470.

238. Penn, Anna A., Patricio A. Riquelme, Marla B. Feller, and Carla J. Shatz. 1998. "Competition in Retinogeniculate Patterning Driven by Spontaneous Activity." 279(March).

239. Pérez-Otaño, Isabel and Michael D. Ehlers. 2005. "Homeostatic Plasticity and NMDA Receptor Trafficking." *Trends in Neurosciences* 28(5):229–38.

240. Perry, V. H. and A. Cowey. 1984. "Retinal Ganglion Cells That Project to the Superior Colliculus and Pretectum in the Macaque Monkey." *Neuroscience* 12(4):1125–37.

241. Petrof, Iraklis and S. Murray Sherman. 2013. "Functional Significance of Synaptic Terminal Size in Glutamatergic Sensory Pathways in Thalamus and Cortex." *The Journal of Physiology* 591(13):3125–31.

242. Petros, Timothy J., Alexandra Rebsam, and Carol a Mason. 2008. "Retinal Axon Growth at the Optic Chiasm: To Cross or Not to Cross." *Annual Review of Neuroscience* 31:295–315.

243. Pfeiffenberger, Cory, Tyler Cutforth, Georgia Woods, Jena Yamada, René C. Rentería, David R. Copenhagen, John G. Flanagan, and David a Feldheim. 2005. "Ephrin-As and Neural Activity Are Required for Eye-Specific Patterning during Retinogeniculate Mapping." *Nature Neuroscience* 8(8):1022–27.

244. Pfeiffenberger, Cory, Jena Yamada, and David a Feldheim. 2006. "Ephrin-As and Patterned Retinal Activity Act Together in the Development of Topographic Maps in the Primary Visual System." *The Journal of Neuroscience : The Official Journal of the Society for Neuroscience* 26(50):12873–84.

245. Pham, T. A., J. L. Rubenstein, A. J. Silva, D. R. Storm, and M. P. Stryker. 2001. "The CRE/CREB Pathway Is Transiently Expressed in Thalamic Circuit Development and Contributes to Refinement of Retinogeniculate Axons." *Neuron* 31(3):409–20.

246. Pozo, Karine and Yukiko Goda. 2010. "Unraveling Mechanisms of Homeostatic Synaptic Plasticity." *Neuron* 66(3):337–51.

247. Pratt, Kara G. and Carlos D. Aizenman. 2007. "Homeostatic Regulation of Intrinsic Excitability and

Synaptic Transmission in a Developing Visual Circuit." *The Journal of Neuroscience : The Official Journal of the Society for Neuroscience* 27(31):8268–77.

248. Prigge, Cameron L., Po-Ting Yeh, Nan-Fu Liou, Chi-Chan Lee, Shih-Feng You, Lei-Lei Liu, David S. McNeill, Kylie S. Chew, Samer Hattar, Shih-Kuo Chen, and Dao-Qi Zhang. 2016. "M1 IpRGCs Influence Visual Function through Retrograde Signaling in the Retina." *The Journal of Neuroscience : The Official Journal of the Society for Neuroscience* 36(27):7184–97.

249. Prosser, R. A., D. M. Edgar, H. C. Heller, and J. D. Miller. 1994. "A Possible Glial Role in the Mammalian Circadian Clock." *Brain Research* 643(1–2):296–301.

250. Prusky, G. T. and R. M. Douglas. 2004. "Characterization of Mouse Cortical Spatial Vision." *Vision Research* 44(28):3411–18.

251. Quattrochi, Lauren E., Maureen E. Stabio, Inkyu Kim, Marissa C. Ilardi, P. Michelle Fogerson, Megan L. Leyrer, and David M. Berson. 2019. "The M6 Cell: A Small-Field Bistratified Photosensitive Retinal Ganglion Cell." *The Journal of Comparative Neurology* 527(1):297–311.

252. Rao, Sujata, Christina Chun, Jieqing Fan, J. Matthew Kofron, Michael B. Yang, Rashmi S. Hegde, Napoleone Ferrara, David R. Copenhagen, and Richard A. Lang. 2013. "A Direct and Melanopsin-Dependent Fetal Light Response Regulates Mouse Eye Development." *Nature* 494(7436):243–46.

253. Reber, Michaël, Patrick Burrola, and Greg Lemke. 2004. "A Relative Signalling Model for the Formation of a Topographic Neural Map." *Nature* 431(7010):847–53.

254. Reese, B. E. n.d. "'Hidden Lamination' in the Dorsal Lateral Geniculate Nucleus: The Functional Organization of This Thalamic Region in the Rat." *Brain Research* 472(2):119–37.

255. Renier, Nicolas, Zhuhao Wu, David J. Simon, Jing Yang, Pablo Ariel, and Marc Tessier-lavigne. 2014. "Resource IDISCO : A Simple , Rapid Method to Immunolabel Large Tissue Samples for Volume Imaging." *Cell* 159(4):896–910.

256. Renna, Jordan M., Shijun Weng, and David M. Berson. 2011. "Light Acts through Melanopsin to Alter Retinal Waves and Segregation of Retinogeniculate Afferents." *Nature Neuroscience* 14:827.

257. Rheaume, Bruce A., Amyeo Jereen, Mohan Bolisetty, Muhammad S. Sajid, Yue Yang, Kathleen Renna, Lili Sun, Paul Robson, and Ephraim F. Trakhtenberg. 2018. "Single Cell Transcriptome Profiling of Retinal Ganglion Cells Identifies Cellular Subtypes." *Nature Communications* 9(1):2759.

258. Rice, D. S., R. W. Williams, and D. Goldowitz. 1995. "Genetic Control of Retinal Projections in Inbred Strains of Albino Mice." *The Journal of Comparative Neurology* 354(3):459–69.

259. Rivlin-Etzion, Michal, Kaili Zhou, Wei Wei, Justin Elstrott, Phong L. Nguyen, Ben A. Barres, Andrew D. Huberman, and Marla B. Feller. 2011. "Transgenic Mice Reveal Unexpected Diversity of On-off Direction-Selective Retinal Ganglion Cell Subtypes and Brain Structures Involved in Motion

Processing." *The Journal of Neuroscience : The Official Journal of the Society for Neuroscience* 31(24):8760–69.

260. Rockhill, Wendy, Jennifer L. Kirkman, and Martha M. Bosma. 2009. "Spontaneous Activity in the Developing Mouse Midbrain Driven by an External Pacemaker." *Developmental Neurobiology* 69(11):689–704.

261. Romano, Sebastián A., Thomas Pietri, Verónica Pérez-Schuster, Adrien Jouary, Mathieu Haudrechy, and Germán Sumbre. 2015. "Spontaneous Neuronal Network Dynamics Reveal Circuit's Functional Adaptations for Behavior." *Neuron* 85(5):1070–85.

262. Rompani, Santiago B., Fiona E. Müllner, Adrian Wanner, Chi Zhang, Chiara N. Roth, Keisuke Yonehara, and Botond Roska. 2017. "Different Modes of Visual Integration in the Lateral Geniculate Nucleus Revealed by Single-Cell-Initiated Transsynaptic Tracing." *Neuron* 93(4):767-776.e6.

263. Rosa, Juliana M., Ryan D. Morrie, Hans C. Baertsch, and Marla B. Feller. 2016. "Contributions of Rod and Cone Pathways to Retinal Direction Selectivity Through Development." *The Journal of Neuroscience : The Official Journal of the Society for Neuroscience* 36(37):9683–95.

264. Rossi, F. M., T. Pizzorusso, V. Porciatti, L. M. Marubio, L. Maffei, and J. P. Changeux. 2001. "Requirement of the Nicotinic Acetylcholine Receptor Beta 2 Subunit for the Anatomical and Functional Development of the Visual System." *Proceedings of the National Academy of Sciences of the United States of America* 98(11):6453–58.

265. Sahay, Amar, Chong-Hyun Kim, Jehuda P. Sepkuty, Edward Cho, Richard L. Huganir, David D. Ginty, and Alex L. Kolodkin. 2005. "Secreted Semaphorins Modulate Synaptic Transmission in the Adult Hippocampus." *The Journal of Neuroscience : The Official Journal of the Society for Neuroscience* 25(14):3613–20.

266. Sand, Andrea, Tiffany M. Schmidt, and Paulo Kofuji. 2012. "Diverse Types of Ganglion Cell Photoreceptors in the Mammalian Retina." *Progress in Retinal and Eye Research* 31(4):287–302.

267. Sanes, Joshua R. and Richard H. Masland. 2015. "The Types of Retinal Ganglion Cells: Current Status and Implications for Neuronal Classification." *Annual Review of Neuroscience* 38:221–46.

268. Schafer, Dorothy P., Emily K. Lehrman, Amanda G. Kautzman, Ryuta Koyama, Alan R. Mardinly, Ryo Yamasaki, Richard M. Ransohoff, Michael E. Greenberg, Ben A. Barres, and Beth Stevens. 2012. "Microglia Sculpt Postnatal Neural Circuits in an Activity and Complement-Dependent Manner." *Neuron* 74(4):691–705.

269. Schindelin, Johannes, Ignacio Arganda-Carreras, Erwin Frise, Verena Kaynig, Mark Longair, Tobias Pietzsch, Stephan Preibisch, Curtis Rueden, Stephan Saalfeld, Benjamin Schmid, Jean

Yves Tinevez, Daniel James White, Volker Hartenstein, Kevin Eliceiri, Pavel Tomancak, and Albert Cardona. 2012. “Fiji: An Open-Source Platform for Biological-Image Analysis.” *Nature Methods* 9(7):676–82.

270. Schmidt, Tiffany M., Nazia M. Alam, Shan Chen, Paulo Kofuji, Wei Li, Glen T. Prusky, and Samer Hattar. 2014. “A Role for Melanopsin in Alpha Retinal Ganglion Cells and Contrast Detection.” *Neuron* 82(4):781–88.

271. Schmidt, Tiffany M., Michael Tri H. Do, Dennis Dacey, Robert Lucas, Samer Hattar, and Anna Matynia. 2011. “Melanopsin-Positive Intrinsically Photosensitive Retinal Ganglion Cells: From Form to Function.” *The Journal of Neuroscience : The Official Journal of the Society for Neuroscience* 31(45):16094–101.

272. Schmidt, Tiffany M. and Paulo Kofuji. 2009. “Functional and Morphological Differences among Intrinsically Photosensitive Retinal Ganglion Cells.” *The Journal of Neuroscience : The Official Journal of the Society for Neuroscience* 29(2):476–82.

273. Schmidt, Tiffany M. and Paulo Kofuji. 2011. “Structure and Function of Bistratified Intrinsically Photosensitive Retinal Ganglion Cells in the Mouse.” *The Journal of Comparative Neurology* 519(8):1492–1504.

274. Schmitt, Adam M., Jun Shi, Alex M. Wolf, Chin-Chun Lu, Leslie A. King, and Yimin Zou. 2006. “Wnt-Ryk Signalling Mediates Medial-Lateral Retinotectal Topographic Mapping.” *Nature* 439(7072):31–37.

275. Schroeder, Melanie M., Krystal R. Harrison, Elizabeth R. Jaeckel, Hunter N. Berger, Xiwu Zhao, Michael P. Flannery, Emma C. St Pierre, Nancy Pateqi, Agnieszka Jachimska, Andrew P. Chervenak, and Kwoon Y. Wong. 2018. “The Roles of Rods, Cones, and Melanopsin in Photoresponses of M4 Intrinsically Photosensitive Retinal Ganglion Cells (IpRGCs) and Optokinetic Visual Behavior.” *Frontiers in Cellular Neuroscience* 12:203.

276. Schwartz, Neil, Anne Schohl, and Edward S. Ruthazer. 2011. “Activity-Dependent Transcription of BDNF Enhances Visual Acuity during Development.” *Neuron* 70(3):455–67.

277. Seabrook, Tania A., Timothy J. Burbridge, Michael C. Crair, and Andrew D. Huberman. 2017. “Architecture, Function, and Assembly of the Mouse Visual System.” *Annual Review of Neuroscience* 40:499–538.

278. Seabrook, Tania A., Rana N. El-Danaf, Thomas E. Krahe, Michael A. Fox, and William Guido. 2013. “Retinal Input Regulates the Timing of Corticogeniculate Innervation.” *The Journal of Neuroscience : The Official Journal of the Society for Neuroscience* 33(24):10085–97.

279. Sekaran, S., D. Lupi, S. L. Jones, C. J. Sheely, S. Hattar, K. W. Yau, R. J. Lucas, R. G. Foster, and

M. W. Hankins. 2005. “Melanopsin-Dependent Photoreception Provides Earliest Light Detection in the Mammalian Retina.” *Current Biology : CB* 15(12):1099–1107.

280. Sekaran, Sumathi, Russell G. Foster, Robert J. Lucas, and Mark W. Hankins. 2003. “Calcium Imaging Reveals a Network of Intrinsically Light-Sensitive Inner-Retinal Neurons.” *Current Biology : CB* 13(15):1290–98.

281. Sernagor, E., S. J. Eglen, and R. O. Wong. 2001. “Development of Retinal Ganglion Cell Structure and Function.” *Progress in Retinal and Eye Research* 20(2):139–74.

282. Sernagor, E. and N. M. Grzywacz. 1996. “Influence of Spontaneous Activity and Visual Experience on Developing Retinal Receptive Fields.” *Current Biology : CB* 6(11):1503–8.

283. Sernagor, Evelyne. 2005. “Retinal Development: Second Sight Comes First.” *Current Biology : CB* 15(14):R556-9.

284. Shah, Ruchir D. and Michael C. Crair. 2008. “Retinocollicular Synapse Maturation and Plasticity Are Regulated by Correlated Retinal Waves.” *The Journal of Neuroscience : The Official Journal of the Society for Neuroscience* 28(1):292–303.

285. Shanks, James A., Shinya Ito, Laura Schaevitz, Jena Yamada, Bin Chen, Alan Litke, and David A. Feldheim. 2016. “Corticothalamic Axons Are Essential for Retinal Ganglion Cell Axon Targeting to the Mouse Dorsal Lateral Geniculate Nucleus.” *The Journal of Neuroscience : The Official Journal of the Society for Neuroscience* 36(19):5252–63.

286. Shen, Wanhua, Han-Hsuan Liu, Lucio Schiapparelli, Daniel McClatchy, Hai-Yan He, John R. Yates, and Hollis T. Cline. 2014. “Acute Synthesis of CPEB Is Required for Plasticity of Visual Avoidance Behavior in Xenopus.” *Cell Reports* 6(4):737–47.

287. Sherry, David M., Meng M. Wang, Jason Bates, and Laura J. Frishman. 2003. “Expression of Vesicular Glutamate Transporter 1 in the Mouse Retina Reveals Temporal Ordering in Development of Rod vs. Cone and ON vs. OFF Circuits.” *The Journal of Comparative Neurology* 465(4):480–98.

288. Shigeoka, Toshiaki, Hosung Jung, Jane Jung, Benita Turner-Bridger, Jiyeon Ohk, Julie Qiaojin Lin, Paul S. Amieux, and Christine E. Holt. 2016. “Dynamic Axonal Translation in Developing and Mature Visual Circuits.” *Cell* 166(1):181–92.

289. Shinohara, K., S. Honma, Y. Katsuno, H. Abe, and K. Honma. 1995. “Two Distinct Oscillators in the Rat Suprachiasmatic Nucleus in Vitro.” *Proceedings of the National Academy of Sciences of the United States of America* 92(16):7396–7400.

290. Shoykhet, Michael and Jason W. Middleton. 2016. “Cardiac Arrest-Induced Global Brain Hypoxia-Ischemia during Development Affects Spontaneous Activity Organization in Rat Sensory and

Motor Thalamocortical Circuits during Adulthood." *Frontiers in Neural Circuits* 10:68.

291. Simmons, Aaron B., Samuel J. Bloomsburg, Samuel A. Billingslea, Morgan M. Merrill, Shuai Li, Marshall W. Thomas, and Peter G. Fuerst. 2016. "Pou4f2 Knock-in Cre Mouse: A Multifaceted Genetic Tool for Vision Researchers." *Molecular Vision* 22:705–17.

292. Singer, J. H., R. R. Mirotznik, and M. B. Feller. 2001. "Potentiation of L-Type Calcium Channels Reveals Nonsynaptic Mechanisms That Correlate Spontaneous Activity in the Developing Mammalian Retina." *The Journal of Neuroscience* 21(21):8514–22.

293. Spitzer, Nicholas C. 2006. "Electrical Activity in Early Neuronal Development." *Nature* 444(7120):707–12.

294. Sretavan, D. W. and C. J. Shatz. 1987. "Axon Trajectories and Pattern of Terminal Arborization during the Prenatal Development of the Cat's Retinogeniculate Pathway." *The Journal of Comparative Neurology* 255(3):386–400.

295. Stabio, Maureen E., Shai Sabbah, Lauren E. Quattrochi, Marissa C. Ilardi, P. Michelle Fogerson, Megan L. Leyrer, Min Tae Kim, Inkyu Kim, Matthew Schiel, Jordan M. Renna, Kevin L. Briggman, and David M. Berson. 2018. "The M5 Cell: A Color-Opponent Intrinsically Photosensitive Retinal Ganglion Cell." *Neuron* 97(1):150-163.e4.

296. Stacy, Rebecca C., Jay Demas, Robert W. Burgess, Joshua R. Sanes, and Rachel O. L. Wong. 2005. "Disruption and Recovery of Patterned Retinal Activity in the Absence of Acetylcholine." *The Journal of Neuroscience : The Official Journal of the Society for Neuroscience* 25(41):9347–57.

297. Stafford, Ben K., Alexander Sher, Alan M. Litke, and David a Feldheim. 2009. "Spatial-Temporal Patterns of Retinal Waves Underlying Activity-Dependent Refinement of Retinofugal Projections." *Neuron* 64(2):200–212.

298. Stella, Salvatore L., Stefanie Li, Andrea Sabatini, Alejandro Vila, and Nicholas C. Brecha. 2008. "Comparison of the Ontogeny of the Vesicular Glutamate Transporter 3 (VGLUT3) with VGLUT1 and VGLUT2 in the Rat Retina." *Brain Research* 1215:20–29.

299. Stellwagen, D. and C. J. Shatz. 2002. "An Instructive Role for Retinal Waves in the Development of Retinogeniculate Connectivity." 33:357–67.

300. Stellwagen, D., C. J. Shatz, and M. B. Feller. 1999. "Dynamics of Retinal Waves Are Controlled by Cyclic AMP." *Neuron* 24(3):673–85.

301. Stephan, Alexander H., Ben A. Barres, and Beth Stevens. 2012. "The Complement System: An Unexpected Role in Synaptic Pruning during Development and Disease." *Annual Review of Neuroscience* 35:369–89.

302. Stinchcombe, Adam R., Joshua W. Mouland, Kwoon Y. Wong, Robert J. Lucas, and Daniel B.

Forger. 2017. “Multiplexing Visual Signals in the Suprachiasmatic Nuclei.” *Cell Reports* 21(6):1418–25.

303. Stryker, M. P. and P. H. Schiller. 1975. “Eye and Head Movements Evoked by Electrical Stimulation of Monkey Superior Colliculus.” *Experimental Brain Research* 23(1):103–12.

304. Su, Jianmin, Cheryl V Haner, Terence E. Imbery, Justin M. Brooks, Duncan R. Morhardt, Karen Gorse, William Guido, and Michael a Fox. 2011. “Reelin Is Required for Class-Specific Retinogeniculate Targeting.” *The Journal of Neuroscience : The Official Journal of the Society for Neuroscience* 31(2):575–86.

305. Su, Jianmin, Michael A. Klemm, Anne M. Josephson, and Michael A. Fox. 2013. “Contributions of VLDLR and LRP8 in the Establishment of Retinogeniculate Projections.” *Neural Development* 8:11.

306. Suh, Joowon and F. Rob Jackson. 2007. “Drosophila Ebony Activity Is Required in Glia for the Circadian Regulation of Locomotor Activity.” *Neuron* 55(3):435–47.

307. Sun, Chao, David K. Warland, Jose M. Ballesteros, Deborah van der List, and Leo M. Chalupa. 2008. “Retinal Waves in Mice Lacking the Beta2 Subunit of the Nicotinic Acetylcholine Receptor.” *Proceedings of the National Academy of Sciences of the United States of America* 105(36):13638–43.

308. Sweeney, Neal T., Hannah Tierney, and David A. Feldheim. 2014. “Tbr2 Is Required to Generate a Neural Circuit Mediating the Pupillary Light Reflex.” *The Journal of Neuroscience : The Official Journal of the Society for Neuroscience* 34(16):5447–53.

309. Syed, Mohsin Md, Seunghoon Lee, Jijian Zheng, and Z. Jimmy Zhou. 2004. “Stage-Dependent Dynamics and Modulation of Spontaneous Waves in the Developing Rabbit Retina.” *The Journal of Physiology* 560(Pt 2):533–49.

310. Tanaka, M., Y. Ichitani, H. Okamura, Y. Tanaka, and Y. Ibata. 1993. “The Direct Retinal Projection to VIP Neuronal Elements in the Rat SCN.” *Brain Research Bulletin* 31(6):637–40.

311. Thompson, I. D. and J. E. Morgan. 1993. “The Development of Retinal Ganglion Cell Decussation Patterns in Postnatal Pigmented and Albino Ferrets.” *The European Journal of Neuroscience* 5(4):341–56.

312. Tian, Ning and David R. Copenhagen. 2003. “Visual Stimulation Is Required for Refinement of ON and OFF Pathways in Postnatal Retina.” *Neuron* 39(1):85–96.

313. Tien, Nai-Wen and Daniel Kerschensteiner. 2018. “Homeostatic Plasticity in Neural Development.” *Neural Development* 13(1):9.

314. Tiriac, Alexandre, Benjamin E. Smith, and Marla B. Feller. 2018. “Light Prior to Eye Opening Promotes Retinal Waves and Eye-Specific Segregation.” *Neuron* 100(5):1059-1065.e4.

315. Tolhurst D. Movshon, J. A. and A. Dean. 1983. “The Statistical Reliability of Single Neurons in Cat and Monkey Visual Cortex.” *Vision Research* 23:775–85.

316. Torborg, Christine L. and Marla B. Feller. 2004. “Unbiased Analysis of Bulk Axonal Segregation Patterns.” *Journal of Neuroscience Methods* 135(1–2):17–26.

317. Torborg, Christine L. and Marla B. Feller. 2005. “Spontaneous Patterned Retinal Activity and the Refinement of Retinal Projections.” *Progress in Neurobiology* 76(4):213–35.

318. Torborg, Christine L., Kristi A. Hansen, and Marla B. Feller. 2005. “High Frequency, Synchronized Bursting Drives Eye-Specific Segregation of Retinogeniculate Projections.” *Nature Neuroscience* 8(1):72–78.

319. Triplett, Jason W. 2014. “Molecular Guidance of Retinotopic Map Development in the Midbrain.” *Current Opinion in Neurobiology* 24(1):7–12.

320. Triplett, Jason W. and David A. Feldheim. 2012. “Eph and Ephrin Signaling in the Formation of Topographic Maps.” *Seminars in Cell & Developmental Biology* 23(1):7–15.

321. Triplett, Jason W., Melinda T. Owens, Jena Yamada, Greg Lemke, Jianhua Cang, Michael P. Stryker, and David a Feldheim. 2009. “Retinal Input Instructs Alignment of Visual Topographic Maps.” *Cell* 139(1):175–85.

322. Tritsch, Nicolas X., Eunyoung Yi, Jonathan E. Gale, Elisabeth Glowatzki, and Dwight E. Bergles. 2007. “The Origin of Spontaneous Activity in the Developing Auditory System.” *Nature* 450(7166):50–55.

323. Tsigankov, Dmitry and Alexei A. Koulakov. 2010. “Sperry versus Hebb: Topographic Mapping in Isl2/EphA3 Mutant Mice.” *BMC Neuroscience* 11:155.

324. Tsigankov, Dmitry N. and Alexei A. Koulakov. 2006. “A Unifying Model for Activity-Dependent and Activity-Independent Mechanisms Predicts Complete Structure of Topographic Maps in Ephrin-A Deficient Mice.” *Journal of Computational Neuroscience* 21(1):101–14.

325. Tu, Daniel C., Dongyang Zhang, Jay Demas, Elon B. Slutsky, Ignacio Provencio, Timothy E. Holy, and Russell N. Van Gelder. 2005. “Physiologic Diversity and Development of Intrinsically Photosensitive Retinal Ganglion Cells.” *Neuron* 48(6):987–99.

326. Turrigiano, Gina G. 2008. “The Self-Tuning Neuron: Synaptic Scaling of Excitatory Synapses.” *Cell* 135(3):422–35.

327. Upton, A. L., A. Ravary, N. Salichon, R. Moessner, K. P. Lesch, R. Hen, I. Seif, and P. Gaspar. 2002. “Lack of 5-HT(1B) Receptor and of Serotonin Transporter Have Different Effects on the Segregation of Retinal Axons in the Lateral Geniculate Nucleus Compared to the Superior Colliculus.” *Neuroscience* 111(3):597–610.

328. Upton, A. L., N. Salichon, C. Lebrand, A. Ravary, R. Blakely, I. Seif, and P. Gaspar. 1999. "Excess of Serotonin (5-HT) Alters the Segregation of Ispilateral and Contralateral Retinal Projections in Monoamine Oxidase A Knock-out Mice: Possible Role of 5-HT Uptake in Retinal Ganglion Cells during Development." *The Journal of Neuroscience : The Official Journal of the Society for Neuroscience* 19(16):7007–24.

329. Vuong, Helen E., Claudia N. Hardi, Steven Barnes, and Nicholas C. Brecha. 2015. "Parallel Inhibition of Dopamine Amacrine Cells and Intrinsically Photosensitive Retinal Ganglion Cells in a Non-Image-Forming Visual Circuit of the Mouse Retina." *The Journal of Neuroscience : The Official Journal of the Society for Neuroscience* 35(48):15955–70.

330. Walmsley, Lauren, Lydia Hanna, Josh Mouland, Franck Martial, Alexander West, Andrew R. Smedley, David A. Bechtold, Ann R. Webb, Robert J. Lucas, and Timothy M. Brown. 2015. "Colour as a Signal for Entraining the Mammalian Circadian Clock." *PLoS Biology* 13(4):e1002127.

331. Wang, Han Chin and Dwight E. Bergles. 2015. "Spontaneous Activity in the Developing Auditory System." *Cell and Tissue Research* 361(1):65–75.

332. Wang, Qing, Florencia Marcucci, Isadora Cerullo, and Carol Mason. 2016. "Ipsilateral and Contralateral Retinal Ganglion Cells Express Distinct Genes during Decussation at the Optic Chiasm." *ENeuro* 3(6).

333. Warland, David K., Andrew D. Huberman, and Leo M. Chalupa. 2006. "Dynamics of Spontaneous Activity in the Fetal Macaque Retina during Development of Retinogeniculate Pathways." *The Journal of Neuroscience : The Official Journal of the Society for Neuroscience* 26(19):5190–97.

334. Watt, Alanna J., Hermann Cuntz, Masahiro Mori, Zoltan Nusser, P. Jesper Sjöström, and Michael Häusser. 2009. "Traveling Waves in Developing Cerebellar Cortex Mediated by Asymmetrical Purkinje Cell Connectivity." *Nature Neuroscience* 12(4):463–73.

335. Weaver, D. R. 1998. "The Suprachiasmatic Nucleus: A 25-Year Retrospective." *Journal of Biological Rhythms* 13(2):100–112.

336. Weaver, D. R. and S. M. Reppert. 1995. "Definition of the Developmental Transition from Dopaminergic to Photic Regulation of C-Fos Gene Expression in the Rat Suprachiasmatic Nucleus." *Brain Research. Molecular Brain Research* 33(1):136–48.

337. Welsh, David K., Joseph S. Takahashi, and Steve A. Kay. 2010. "Suprachiasmatic Nucleus: Cell Autonomy and Network Properties." *Annual Review of Physiology* 72:551–77.

338. White, L. E., D. M. Coppola, and D. Fitzpatrick. 2001. "The Contribution of Sensory Experience to the Maturation of Orientation Selectivity in Ferret Visual Cortex." *Nature* 411(6841):1049–52.

339. Whiteus, Christina, Catarina Freitas, and Jaime Grutzendler. 2014. "Perturbed Neural Activity

Disrupts Cerebral Angiogenesis during a Postnatal Critical Period." *Nature* 505(7483):407–11.

340. Williams, Scott E., Fanny Mann, Lynda Erskine, Takeshi Sakurai, Shiniu Wei, Derrick J. Rossi, Nicholas W. Gale, Christine E. Holt, Carol A. Mason, and Mark Henkemeyer. 2003. "Ephrin-B2 and EphB1 Mediate Retinal Axon Divergence at the Optic Chiasm." *Neuron* 39(6):919–35.

341. Williams, Stephen R. and Greg J. Stuart. 2002. "Dependence of EPSP Efficacy on Synapse Location in Neocortical Pyramidal Neurons." *Science (New York, N.Y.)* 295(5561):1907–10.

342. Wong, R. O. 1999. "Retinal Waves and Visual System Development." *Annual Review of Neuroscience* 22:29–47.

343. Wong, R. O., A. Chernjavsky, S. J. Smith, and C. J. Shatz. 1995. "Early Functional Neural Networks in the Developing Retina." *Nature* 374(6524):716–18.

344. Wong, R. O., M. Meister, and C. J. Shatz. 1993. "Transient Period of Correlated Bursting Activity during Development of the Mammalian Retina." *Neuron* 11(5):923–38.

345. Wong, W. T., K. L. Myhr, E. D. Miller, and R. O. Wong. 2000. "Developmental Changes in the Neurotransmitter Regulation of Correlated Spontaneous Retinal Activity." *The Journal of Neuroscience : The Official Journal of the Society for Neuroscience* 20(1):351–60.

346. Wu, G. Y., R. Malinow, and H. T. Cline. 1996. "Maturation of a Central Glutamatergic Synapse." *Science* 274(5289):972–76.

347. Xu, H., M. Furman, YS Mineur, and H. Chen. 2011. "An Instructive Role for Patterned Spontaneous Retinal Activity in Mouse Visual Map Development." *Neuron* 70(6):1115–27.

348. Yamaguchi, Shun, Hiromi Isejima, Takuya Matsuo, Ryusuke Okura, Kazuhiro Yagita, Masaki Kobayashi, and Hitoshi Okamura. 2003. "Synchronization of Cellular Clocks in the Suprachiasmatic Nucleus." *Science (New York, N.Y.)* 302(5649):1408–12.

349. Yamamoto, Nobuhiko and Guillermina López-Bendito. 2012. "Shaping Brain Connections through Spontaneous Neural Activity." *The European Journal of Neuroscience* 35(10):1595–1604.

350. Yee, Ada X., Yu-Tien Hsu, and Lu Chen. 2017. "A Metaplasticity View of the Interaction between Homeostatic and Hebbian Plasticity." *Philosophical Transactions of the Royal Society of London. Series B, Biological Sciences* 372(1715).

351. Yonehara, Keisuke, Hiroshi Ishikane, Hiraki Sakuta, Takafumi Shintani, Kayo Nakamura-Yonehara, Nilton L. Kamiji, Shiro Usui, and Masaharu Noda. 2009. "Identification of Retinal Ganglion Cells and Their Projections Involved in Central Transmission of Information about Upward and Downward Image Motion." *PloS One* 4(1):e4320.

352. Young, M. J. and R. D. Lund. 1994. "The Anatomical Substrates Subserving the Pupillary Light Reflex in Rats: Origin of the Consensual Pupillary Response." *Neuroscience* 62(2):481–96.

353.Young, M. J. and R. D. Lund. 1998. “The Retinal Ganglion Cells That Drive the Pupilloconstrictor Response in Rats.” *Brain Research* 787(2):191–202.

354.Young, R. W. 1984. “Cell Death during Differentiation of the Retina in the Mouse.” *The Journal of Comparative Neurology* 229(3):362–73.

355.Yu, C. Ron, Jennifer Power, Gilad Barnea, Sean O’Donnell, Hannah E. V. Brown, Joseph Osborne, Richard Axel, and Joseph A. Gogos. 2004. “Spontaneous Neural Activity Is Required for the Establishment and Maintenance of the Olfactory Sensory Map.” *Neuron* 42(4):553–66.

356.Yu, Yao-Qing, Devin M. Barry, Yan Hao, Xue-Ting Liu, and Zhou-Feng Chen. 2017. “Molecular and Neural Basis of Contagious Itch Behavior in Mice.” *Science (New York, N.Y.)* 355(6329):1072–76.

357.Zhang, Dao-Qi, Kwoon Y. Wong, Patricia J. Sollars, David M. Berson, Gary E. Pickard, and Douglas G. McMahon. 2008. “Intraretinal Signaling by Ganglion Cell Photoreceptors to Dopaminergic Amacrine Neurons.” *Proceedings of the National Academy of Sciences of the United States of America* 105(37):14181–86.

358.Zhang, Jiayi, James B. Ackman, Hong-Ping Xu, and Michael C. Crair. 2011. “Visual Map Development Depends on the Temporal Pattern of Binocular Activity in Mice.” *Nature Neuroscience* 15(2):298–307.

359.Zhang, Ling-Li, Hemal R. Pathak, Douglas A. Coulter, Michael A. Freed, and Noga Vardi. 2006. “Shift of Intracellular Chloride Concentration in Ganglion and Amacrine Cells of Developing Mouse Retina.” *Journal of Neurophysiology* 95(4):2404–16.

360.Zhang, Rong-Wei, Xiao-Quan Li, Koichi Kawakami, and Jiu-Lin Du. 2016. “Stereotyped Initiation of Retinal Waves by Bipolar Cells via Presynaptic NMDA Autoreceptors.” *Nature Communications* 7:12650.

361.Zhao, Xinyu, Hui Chen, Xiaorong Liu, and Jianhua Cang. 2013. “Orientation-Selective Responses in the Mouse Lateral Geniculate Nucleus.” *The Journal of Neuroscience : The Official Journal of the Society for Neuroscience* 33(31):12751–63.

362.Zheng, Ji-jian, Seunghoon Lee, and Z. Jimm. Zhou. 2004. “A Developmental Switch in the Excitability and Function of the Starburst Network in the Mammalian Retina.” *Neuron* 44(5):851–64.

363.Zheng, Jijian, Seunghoon Lee, and Z. Jimmy Zhou. 2006. “A Transient Network of Intrinsically Bursting Starburst Cells Underlies the Generation of Retinal Waves.” *Nature Neuroscience* 9(3):363–71.

364.Zhou, Z. J. 1998. “Direct Participation of Starburst Amacrine Cells in Spontaneous Rhythmic Activities in the Developing Mammalian Retina.” *The Journal of Neuroscience : The Official Journal of the Society for Neuroscience* 18(11):4155–65.

365.Zhou, Z. J. 2001a. “A Critical Role of the Strychnine-Sensitive Glycinergic System in Spontaneous Retinal Waves of the Developing Rabbit.” *The Journal of Neuroscience : The Official Journal of the Society for Neuroscience* 21(14):5158–68.

366.Zhou, Z. J. 2001b. “The Function of the Cholinergic System in the Developing Mammalian Retina.” *Progress in Brain Research* 131:599–613.

367.Zhou, Z. J. and D. Zhao. 2000. “Coordinated Transitions in Neurotransmitter Systems for the Initiation and Propagation of Spontaneous Retinal Waves.” *The Journal of Neuroscience : The Official Journal of the Society for Neuroscience* 20(17):6570–77.

368.Ziburkus, Jok**ū**bas, Emily K. Dilger, Fu-Sun Lo, and William Guido. 2009. “LTD and LTP at the Developing Retinogeniculate Synapse.” *Journal of Neurophysiology* 102(6):3082–90.

ARTÍCULO ADJUNTADO COMO INDICIO DE CALIDAD:

A Retino-retinal Projection Guided by Unc5c Emerged in Species with Retinal Waves

Verónica Murcia-Belmonte, Yaiza Coca, Celia Vegar, Santiago Negueruela, Camino de Juan Romero, Arturo José Valiño, Salvador Sala, Ronan DaSilva, Artur Kania, Víctor Borrell, Luis M. Martinez, Lynda Erskine, Eloísa Herrera

Summary

The existence of axons extending from one retina to the other has been reported during perinatal development in different vertebrates. However, it has been thought that these axons are either a labeling artifact or misprojections. Here, we show unequivocally that a small subset of retinal ganglion cells (RGCs) project to the opposite retina and that the guidance receptor Unc5c, expressed in the retinal region where the retinal-retinal (R-R) RGCs are located, is necessary and sufficient to guide axons to the opposite retina. In addition, Netrin1, an Unc5c ligand, is expressed in the ventral diencephalon in a pattern that is consistent with impeding the growth of Unc5c-positive retinal axons into the brain. We also have generated a mathematical model to explore the formation of retinotopic maps in the presence and absence of a functional connection between both eyes. This model predicts that an R-R connection is required for the bilateral coordination of axonal refinement in species where refinement depends upon spontaneous retinal waves. Consistent with this idea, the retinal expression of Unc5c correlates with the existence and size of an R-R projection in different species and with the extent of axonal refinement in visual targets. These findings demonstrate that active guidance drives the formation of the R-R projection and suggest an important role for these projections in visual mapping to ensure congruent bilateral refinement.

Introduction

Visual information is perceived by each retina and transmitted to the brain through retinal ganglion cell (RGC) axons. RGC axons extend from each eye via the optic nerves and meet at the ventral diencephalon to form the optic chiasm. Here, axons in all species cross the midline to join the contralateral tract. In species with stereoscopic vision, a number of RGCs do not cross at the chiasm but project, together with contralateral axons from the other eye, to the superior colliculus (SC) and the lateral geniculate nucleus

in a topographical and eye-specific manner. The topographic arrangement at the targets allows the perception of a continuous visual field image on the target [1, 2, 3, 4] and is established initially through molecular recognition mediated mainly by Ephs and ephrins, followed by an activity-dependent local refinement of exuberant terminals influenced by electrical activity waves generated spontaneously in the retina before eye opening [5, 6, 7, 8].

In addition to the RGC axons that connect each retina with targets in the brain, a direct connection between both retinas (R-R projection) has been reported in different vertebrates [6, 9, 10, 11, 12, 13, 14, 15, 16, 17, 18, 19]. However, R-R axons have been detected in only very low numbers and seem to be largely absent in adult animals [11, 14, 15]. As a consequence, they have been considered artifacts of the axonal tracing method or a consequence of axonal projection errors during development. The recent visualization of a subset of calcium waves traveling from the retina to the SC in a simultaneous bilateral manner raised the hypothesis that interactions brought about by an R-R projection could be responsible for synchronizing retinal waves [6]. This idea is further supported by recent results demonstrating that enucleation of one eye alters retinal waves in the remaining eye [20].

Here, we demonstrate unequivocally the existence of an R-R projection that emerges predominately from the central part of the ventral-nasal retina, a region that transiently expresses the axon guidance receptor Unc5c. Loss-of-function experiments revealed that Unc5c, a receptor for Netrin1 that is expressed at the optic chiasm, is required for RGCs to extend their axons into the contralateral optic nerve. Conversely, ectopic expression of Unc5c forces axons to join the contralateral optic nerve. In addition, Zic2, a transcription factor that specifies ipsilateral RGCs [21], represses Unc5c expression in ipsilateral axons, supporting the idea that Unc5c needs to be downregulated in RGC axons to facilitate growth into the optic tracts. We also found that retinal expression of Unc5c in different species is consistent with a computational model in which R-R projections synchronize retinal spontaneous activity in bilateral species that undergo an important axon refinement process during the maturation of the visual system.

Results

Characterization of the R-R Projection in the Mouse Visual System

To characterize the development of the R-R projection in the mouse visual system, embryonic day (E) 13.5 embryos were electroporated in one eye with EGFP-encoding plasmids (CAG-EGFP), and three (E16.5), five (E18.5), seven (postnatal day 2 [P2]), or nine (P4) days later, axon trajectories at the chiasm were analyzed (Figure 1). This labeling method eliminates the possibility of labeling artifacts resulting from transfer between cells. At E16.5, although the majority of EGFP-axons projected to the contralateral optic tract, some axons entered the contralateral optic nerve (Figures 1A and 1B). By E18.5, more EGFP-

positive axons were found in the contralateral optic nerve and most had reached the contralateral retina (Figures 1C and 1D).

To visualize the trajectory of EGFP axons in the opposite retina, we analyzed whole-mount retinal preparations from E18.5 embryos electroporated at E13.5 and found EGFP axons all over the retina. The number of labeled axon terminals decreased at P2, and very few were detected at P4 (Figures 1E and 1F). The two main types of neurons located in the RGC layer are RGCs and starburst amacrine cells. Labeling of these cells with antibodies against Brn3b, Tuj1 (Figure S1A) and choline-acetyl-transferase (ChAT), respectively, in retinas containing EGFP-R-R axon terminals revealed that amacrine prolongations embrace R-R axons at several sights (Figures 1G and 1H). These experiments confirm the existence of a subpopulation of retinal neurons whose axons reach the opposite retina at perinatal stages and progressively vanish during the first postnatal week. Although further work is required to determine whether R-R axons directly contact starburst amacrine cells, our findings support the hypothesis that these two types of neurons could establish some type of communication.

Next, we mapped the retinal location of R-R neurons. We monocularly injected the retrograde tracer cholera toxin subunit B (CTB)-Alexa-Fluor-594 in newborn mice at several postnatal stages and analyzed the opposite retina 2 days later (Figure 1I). At P3–P5, retrogradely labeled cells were found into the RGC layer (Figure 1I), were positive for RGC markers (Brn3a and Isl1/2), and located predominately in the ventro-nasal retina (Figure 1J). By P30, no retrogradely labeled cells were found. In an attempt to label a larger number of R-R cells, we injected AAV5-RFP viruses [22] into the eye of E13.5 mouse embryos and analyzed the opposite retina postnatally. We found more cells retrogradely labeled than using CTB, and again, most of them were detected in the ventro-nasal quadrant (Figure S1B). Because the number of retrogradely labeled cells appears to depend on the technique and the timing of injection, it was not possible to quantify the total number of R-R cells. Nevertheless, these experiments demonstrate that R-R RGCs are mainly located in the ventro-nasal region of the retina.

To determine whether R-R axons are collateral branches of RGCs that project to visual targets in the brain, newborn mice were injected with CTB-488 and CTB-647 in the eye and the ipsilateral superior colliculus, respectively. The retina contralateral to the injections side was analyzed 2 days later. None of the CTB-488 cells analyzed were positive for CTB-647 (25 CTB-488 cells from three different pups; Figure 1K). Together with previous studies reporting that retrograde labeling from the eye and the thalamus do not yield double-labeled cells in the retina [23, 24], these results demonstrate that R-R cells are not collateral branches of brain-projecting RGCs.

Netrin1 Is Expressed in the Ventral Diencephalon at the Time that RGC Axons Transverse the Chiasmatic Region

In contrast to all the other RGC axons, R-R axons do not grow into the ventral region of the optic chiasm. Possible explanations for this behavior include the expression of attractive guidance cues from the contralateral optic nerve and/or repulsive signals at the ventral diencephalon. Among the guidance cues known to be expressed in the ventral diencephalon, Netrin1 has an expression pattern compatible with a putative function as a repellant for R-R RGC axons [25]. *In situ* hybridization on coronal and horizontal sections during the period when RGC axons are navigating through the optic chiasm (E12.5–E14.5) confirmed that *Netrin1* is expressed ventrally in the chiasm at E12.5 and detected strongly at the level of the future optic tracts (Figure 2). At E14.5, *Netrin1* continues to be expressed at the chiasm region and surrounds RGC axons at their most ventral aspect. Thus, the expression of *Netrin1* mRNA is consistent with a role in preventing R-R RGC axons from entering the prospective optic tracts and growing to the brain.

Unc5c Is Expressed in a Subpopulation of Ventral RGCs

Netrin1 acts through two types of receptors: deleted in colorectal cancer (Dcc) or its homolog Neogenin and Unc5 [26, 27, 28, 29, 30, 31], but only Unc5 receptors mediate repulsion [27, 32, 33, 34]. The expression patterns in the developing mouse retina of three of the four mammalian Unc5c homologs (Unc5a, Unc5b, and Unc5d) have been reported, and none show a pattern consistent with a putative role in the guidance of R-R projections [35]. We therefore analyzed the expression of the remaining family member, Unc5c, which has not been reported previously. Using *in situ* hybridization, *Unc5c* was not detected in the retina at E13.5 but by E14.5 was expressed specifically in the ventral region (Figures 3A and 3B). Immunostaining for Brn3a confirmed that *Unc5c* mRNA is expressed in the RGC layer (Figure S2A). Expression of both Unc5c mRNA and protein was maintained in ventral retina from E14.5 to E18.5 but switched off after birth (Figures 3A–3F). *In situ* hybridization on coronal and horizontal retinal sections confirmed that *Unc5c* is highly expressed in ventral areas and weakly in the dorsal retina. Furthermore, *Unc5c* is detected at higher levels in the nasal than in the temporal quadrant (Figures 3G and 3H). This expression pattern contrasted with that of Dcc, which was expressed in RGCs in all retinal regions [25] (Figure S2B). Importantly, the spatial-temporal expression pattern of *Unc5c* mRNA coincides with the location of R-R RGCs in the retina and with the timing of RGCs extending their axons across the optic chiasm. Together with the expression of Netrin1 at the ventral diencephalon, this expression pattern of Unc5c (Figure 3I) strongly suggested an instructive role for Unc5c in the development of R-R projections.

Unc5c Is Required for the Formation of the R-R Projection

To elucidate whether Unc5c is involved in the development of the R-R pathway, we performed *in vivo* loss-of-function experiments. Labeling of all axons from one eye of E17.5 Unc5c-knockout embryos (Unc5c−/−) and control (Unc5c+/+) littermates with the lipophilic tracer DiI revealed a clear reduction in the labeling of the contralateral optic nerve in Unc5c−/− embryos compared with the controls (Unc5c+/+; Figures 4A–4D). This finding supports the idea that Unc5c is essential for the formation of the R-R projection. Retrograde tracing by depositing a DiI crystal in one optic nerve and analyzing the opposite retina resulted in many labeled RGCs in the retinas of E17.5 Unc5c+/+ embryos but very few in Unc5c−/− littermates (Figures 4E–4H).

To confirm these results, and determine the cell-autonomous function of Unc5c in guiding the R-R projection, we carried out additional loss-of-function experiments by specifically downregulating Unc5c in RGCs using short hairpin RNAs (shRNAs). Plasmids encoding *Unc5c* shRNA or control scrambled shRNA were monocularly electroporated in the central retina of E13.5 embryos together with EGFP-encoding reporter plasmids and the axons from targeted RGCs analyzed at E16.5 or E18.5. The downregulation of *Unc5c* mRNA in retinas electroporated with *Unc5c* shRNAs confirmed the efficiency of these shRNAs (Figure S3). As expected, in control embryos, most axons crossed the midline and projected into the contralateral optic tract and a small proportion extended into the contralateral optic nerve (Figures 4I and 4I'). However, embryos electroporated with *Unc5c* shRNAs showed a dramatic reduction in the number of EGFP axons projecting into the contralateral optic nerve (Figures 4J and 4J'). In addition, a number of labeled axons projected to the ipsilateral optic tract of *Unc5c* shRNA-electroporated embryos (Figures 4I–4K), a phenotype that was not detected in DiI-labeled Unc5c−/− embryos likely because the endogenous ipsilateral projection masked those R-R axons that changed their trajectories to project ventrally. This unexpected result suggests that Unc5c-deficient axons are not repelled away from the ventral diencephalon and, consequently, enter the optic tracts.

Unc5c Is Not Expressed in Ipsilaterally Projecting RGCs

In retinal sections, Unc5c appeared to be consistently excluded from the most peripheral region of the ventral retina (Figures 3C and 3G), which is the location of the RGCs that project ipsilaterally and express the transcription factor Zic2 [21]. *In situ* hybridization for Unc5c combined with immunostaining for Zic2 in E16.5 retinal sections demonstrated that Unc5c and Zic2 are expressed in mutually exclusive patterns (Figure 5A). In addition, *in situ* hybridization for Unc5c in Zic2-knockdown embryos (Zic2kd/kd) revealed that Unc5c expression expanded into the peripheral ventro-temporal territory (Figure 5B), the area where Zic2 is normally expressed [21], suggesting that Zic2 represses Unc5c expression. Accordingly, ectopic electroporation of Zic2 into the retina of E13.5 embryos led to downregulation of Unc5c (Figures 5C and

5D). Furthermore, axons from RGCs that ectopically express Zic2 never projected into the contralateral optic nerve (Figures 5E–5G). Altogether, these results suggest that Zic2 represses the expression of Unc5c in the ventro-temporal retina, making ipsilateral axons insensitive to repulsive signaling from the ventral diencephlon, enabling projection to ipsilateral targets.

Unc5c Is Sufficient to Guide Retinal Axons to the Contralateral Retina

We next asked whether Unc5c is sufficient to guide RGC axons to the contralateral retina. Plasmids encoding Unc5c (CAG-Unc5c) together with CAG-EGFP plasmids, or CAG-EGFP plasmids alone, were electroporated *in utero* into the retinas of E13.5 mouse embryos, and 3 (E16.5) or 5 (E18.5) days later, the projection phenotype of the targeted RGCs was analyzed (Figure 6A). As in previous experiments, a small proportion of control EGFP axons entered the contralateral optic nerve (more at E18.5 than at E16.5; Figures 6B and 6D). In embryos electroporated with Unc5c-encoding plasmids, fewer EGFP axons reached the chiasm region compared with controls. This may occur because some axons ectopically expressing Unc5c misproject intraretinally (Figure S4), likely as a consequence of Netrin1 expression at the optic disc [36] (Figures S4C and S4C'). However, most Unc5c-misexpressing axons were still able to exit the retina by passing through the ring of Netrin1 expression at the optic disc (Figures S4D and S4D'). Importantly, a large percentage of the Unc5c-missexpressing axons that reached the optic chiasm grew into the contralateral optic nerve (Figures 6C and 6E), demonstrating that Unc5c is sufficient to redirect RGC axons to the contralateral retina. These gain-of-function experiments demonstrate that Unc5c-expressing axons are able to transverse the optic disc, despite Netrin1 expression in this region, and that Unc5c is sufficient to redirect axons to the contralateral optic nerve.

The R-R Projection May Synchronize Retinal Waves to Modulate Bilateral Alignment of Topographic Visual Maps

Our data confirm the existence of an R-R projection and identify guidance mechanisms by which this connection is established. However, although it has been suggested that an R-R projection may help synchronize retinal waves, its specific function remains unknown. To shed some light on this question, we used a simplified version of the classical self-organizing map (SOM) model [37, 38, 39]. In the previously proposed SOM model, neighboring neurons compete through lateral interactions to develop into a spatially organized "topographic map." Although this powerful self-organizing principle can produce a reasonable local distribution of receptive fields, it is necessary to lower the levels of randomness in order to achieve a global order that characterizes the correct orientation of the retinotopic map. This can be accomplished either by introducing some initial order in the early connectivity weights between neurons of the pre- and postsynaptic layer or by structuring the input that the postsynaptic layer receives (see STAR Methods and Figures S5 and S6 for additional details on the mathematical model).

In the model proposed here, when the sizes of the pre- (retina) and postsynaptic (SC or tectum) tissues are similar (low **σ**-molecular values), a congruent map may be established by using a symmetric gradient of molecular guidance cues, one that determines a point-to-point mapping with adequate precision (Figures 7A, S5, and S6). However, when the size of the target tissue is larger than that of the retina (high **σ**-molecular values), the final map cannot be established with only a simple molecular gradient because errors in topology and folding accumulate. In this latter case, the proper layout of the bilateral retinotopic map critically depends on the synchronization of activity in both maps, particularly in the form of coordinated waves (Figures 7B and S6).

Thus, this mathematical model predicts that the establishment of congruent visual maps in image-forming visual targets may be determined by a point-to-point tagging mechanism in species where the retina and the target tissue have a similar size but that a synchronizing factor must exist in species where RGC axons first create a rough map based on tags and then later undergo a wide refinement process dependent on retinal spontaneous activity. This synchronizing factor may be the R-R connection, and in its absence, topological and unfolding errors increase when the target tissue is bigger than the retina.

The retina and the tectum of lower vertebrates have similar sizes by the time that retinal axons project into this target. Furthermore, it is known that visual mapping in these vertebrates is established according to a fairly accurate axonal targeting, with only modest further refinement [40] (Figure 7A). In contrast, the target tissue is larger than the retina in amniotes, and the initial collection of arbors reaching the visual targets is loosely organized around the position of the future terminal. A substantial degree of local remodeling then takes place, including the elimination of overshooting portions of RGC axons as well as the removal of inappropriately located branches, to establish the final map [40] (Figure 7B). This local axonal remodeling depends on the action of retinal spontaneous activity [5, 7, 41, 42], and according to our predictive model, both retinas should be connected to assure the synchronization of this activity and promote a bilaterally congruent refinement. Otherwise, axonal refinement would occur independently in each side and thereby create a fractured visual field.

Retinal Expression of Unc5c Correlates with the Existence of an R-R Projection and the Extent of Axonal Refinement at the Visual Targets in Different Species

In zebrafish, retinal axons directly travel to their final locations on the optic tectum, and axon refinement at these visual nuclei is very modest [40]. However, both chickens and mice use an “overshoot and refine” strategy for axons to establish proper connections at the targets in the brain. This occurs upon axons extending into the caudal regions of the tectum in the case of chickens and posterior superior colliculus in the case of mice. To assess a putative correlation between the expression of Unc5c in the retina and the existence of an R-R projection and its function in refinement, we analyzed Unc5c

expression in the developing retinas of zebrafish and chickens. Expression of *Unc5c* was not detected in the developing zebrafish retina at the time that RGC axons grow to reach their targets (36–48 h postfertilization [hpf]; Figures 7C and 7D) [43]. Accordingly, monocular injections of DiI in zebrafish embryos did not reveal R-R projections (Figures 7E and 7E'). In chickens, the existence of a transient R-R projection has been reported previously [17]. In agreement with this, we detected *Unc5c* in the RGC layer of the developing chicken retina (Figure S7). In ferrets, the period of retinal wave-dependent axon refinement is extended for several weeks after birth. We analyzed the expression of *Unc5c* mRNA in ferrets and found it is expressed in the RGC layer of the ventral retina both embryonically (E34) and postnatally (P1) (data not shown; Figures 7F and 7G). An R-R projection has not been reported previously in ferrets, and to investigate whether they have it, we monocularly injected DiI into a newborn ferret and followed the traced axons. High fluorescence intensity was detected in the contralateral optic nerve, indicating the presence of axons projecting to the opposite retina (Figure 7H). Retrograde labeling by CTB injection into one eye of P1 ferrets demonstrated the existence of R-R neurons in the ventral retina matching the expression of *Unc5c*, with the extent of these neurons being greater than in mice (Figure 7I). Moreover, as in mice, the expression pattern of Zic2 in the developing retina was complementary to Unc5c expression in ferret (Figure 7J). These results in mouse, zebrafish, chick, and ferret strongly support a conserved evolutionary role for the Zic2-Unc5c-Netrin1 axis in regulating the formation of the R-R projection, which may be essential for the correct functioning of the visual system in amniotes.

Discussion

The existence of an R-R projection that connects both eyes has been a controversial issue for some time. Here, monocular electroporation of EGFP-reporter plasmids during embryonic stages definitively demonstrates the existence of an R-R projection that is established during embryogenesis and early postnatal stages. The formation of this visual pathway depends on Unc5c-mediated signaling in RGC axons and, likely, on its ligand Netrin1, which is expressed at the ventral aspect of the developing diencephalon. Species without R-R projections (e.g., zebrafish) do not express Unc5c in the retina, whereas species with R-R-projecting neurons (e.g., mouse, chick, and ferret) express Unc5c in the RGC layer when retinal axons are passing through the optic chiasm region. These observations uncover a conserved role for Unc5c in controlling the formation of R-R projections in the developing retina and indicate a positive selection for this mechanism through evolution. Together with functional experiments and a computational model, our results suggest that the R-R projection play an important role in the congruency of visual maps in species that undergo intensive retinal wave-dependent axon refinement during development.

Unc5c/Netrin1 Repulsive Signaling as a Candidate to Direct R-R Axons to the Contralateral Optic Nerve

Although our data are consistent with a repulsive role for Netrin/Unc5c signaling in directing navigation of R-R axons at the chiasm, further experiments are crucial to confirm this idea. Conditional removal of Netrin1 from the chiasm region would be necessary to uncover the role of Netrin1 in the formation of the R-R. Also, because (1) EphB2 is expressed in the ventral retina [44], (2) Netrin and ephrins play a synergistic effect in axons expressing EphBs and Unc5 receptors [45], and (3) ephrinB2 is expressed at the midline [46], further work is needed to establish whether EphB2 and/or ephrinB2 is involved in modulating Unc5c-mediated guidance of R-R axons.

The Function of the R-R Projection in Different Species

A simple, single-retina SOM model, when stimulated randomly with a uniform distribution, can readily generate postsynaptic maps that reproduce the geometry of the presynaptic layer (Figures 7 and S6). These maps, however, are rarely oriented correctly because there are four different ways in which two square grids can be oriented relative to each other, and only one of these orientations is topologically correct. Thus, the probability of generating the correct map between the retina and its targets in the brain is only 1/24 (~4%). Furthermore, if we consider that two independent retinas must be correctly laid out at the same time, the probability drops even further to (1/24)2 (~0.02%). Our modeling results show that the concurrent contribution of the gradients of molecular guidance cues and the bilateral coordination of retinal activity afforded by an R-R projection helps avoid such an orientation error.

Retinal waves have been proposed as an evolutionary adaptation in animals with extended periods of visual development [47] to help set a functional visual system before eye opening. Coordinated waves of spontaneous activity occur in the visual system before the onset of visual experience in all amniote species that have been examined to date (turtles, chicks, rats, mice, ferrets, cats, and monkeys) [7, 48]. In mice, the number of R-R axons seems to peak at perinatal stages, a period that coincides with the cholinergic phase of spontaneous retinal activity (see [49] for a recent review). Compared with mice, ferrets experience an extended period of spontaneous retinal waves that last several weeks after birth [5, 50, 51, 52]. Non-amniote vertebrates only have a brief gestational period before the beginning of vision, and as such, the role of spontaneous patterned activity in these species is likely assumed by sensory experience. Interestingly, spontaneous waves have not been found in non-amniotes [47, 53]. Our results demonstrating that ferrets have more R-R axons than mice, and zebrafish lack an R-R projection, support the hypothesis that, in amniotes, both retinas must be connected to ensure a correct bilateral refinement. The fact that chickens have Unc5c, but not Zic2 [21], also argues that R-R projections emerged during evolution to match axonal refinement in the visual targets at both sides of the brain and suggests that stereoscopic vision, which depends on Zic2-driven ipsilateral projection,

emerged on top of this feature. Adams and Horton theorized years ago that spontaneous waves would need to occur simultaneously in both eyes to generate the striking symmetry observed in the global patterns of dominance columns [54]. The results shown here provide an avenue by which spontaneous retinal waves could be synchronized in order to fine-tune bilateral topographic maps and give rise to a congruent visual image in direct visual nuclei, as well as in the visual cortex of animals that have a particularly elaborated visual system.

Contact for Reagent and Resource Sharing

Further information and requests for resources and reagents should be directed to and will fulfilled by the Lead Contact, Eloísa Herrera (e.herrera@umh.es).

Experimental Model and Subject Details

B6D2F1 (DBA2—C57BL/6) mice used for electroporation, *in situ* hybridization, immunofluorescence or DiI tracing experiments were housed in a timed-pregnancy breeding colony at the Instituto de Neurociencias de Alicante, Spain. Zic2 knockdown mice (Zic2kd/kd mice) were originally obtained from the RIKEN Repository. Unc5c knockout mice (*Unc5crcm*) were obtained from Jackson Laboratories (Stock Number: 001607). Females were checked for vaginal plugs at approximately noon each day. E0.5 corresponds to the day when the vaginal plug was detected, with the assumption that conception took place at approximately midnight. Conditions and procedures were approved by the IN Animal Care and Use Committee and met European (2013/63/UE) and Spanish regulations (RD 53/2013).

Fertilized chicken embryos were obtained from Granja Santa Isabel, Córdoba, Spain. Eggs were incubated on their sides in a humidified incubator at 37°C until the desired embryological stage. All embryos were staged according to Hamburger and Hamilton [60].

Zebrafish were maintained at 28°C under standard conditions, and the embryos were staged as described previously [61].

Pigmented sable ferrets (Mustela putorius furo) were obtained from Euroferret (Copenhagen, Denmark) and kept at the Animal Facilities of the Universidad Miguel Hernández on a 16:08 h light:dark cycle. Ferrets were treated according to Spanish and European Union regulations, and experimental protocols were approved by the Institutional Animal Care and Use Committee of the University.

Method Details

Plasmids

Unc5c coding sequence was cloned in the mammalian expression plasmid pCAG. Unc5c shRNA target sequence were designed using the GenScript siRNA Target Finder tool located at https://www.genscript.com/ssl-bin/app/rnai and cloned into the pSilencer2.1 plasmid using the pSilencer Kit (Thermo Fisher Scientific) in accordance with the manufacturer's recommendations. Mouse Unc5c RNAi target sequence was cloned using the following primers:

5′-GATCCGAACCACCGTGACTTTGAGTTCAAGAGACTCAAAGTCACGGTGGTTCTTTTTTGGAA-3′ and 5′-AGCTTTTCCAAAAAAGAACCACCGTGACTTTGAGTCTCTTGAACTCAAAGTCACGGTGGTTCG-3′.

In utero electroporation and DiI tracing

Plasmidic DNA solution was injected into embryonic retinas as described previously [59, 62]. Forward DiI labeling in P0 ferret and E16.5 mice was performed as described previously [63]. After 6 days at 37°C for mice and 45 days at 37°C for ferrets, brains were removed and the optic chiasm exposed in whole mount under a fluorescence dissenting microscope. DiI crystals were dissolved in dimethyl sulfoxide and injected into the retina of 36-48 hours postfertilization (hpf) zebrafish embryos using a micropipette.

CTB injections and adenovirus infection

Cholera toxin B subunit (CTB)-Alexa 594, 647 or 488 (Thermo Fisher Scientific) retrograde injections in P1, P3 and P28 in mouse and P1 ferret were performed as described [64]. For viral infection into the embryonic mouse retinas adenoviruses encoding for tdTomato (pAAV-CAG-tdTomato, Addgen#59462-AAV5) were injected into the retinas of E13.5 embryos following a surgical protocol similar to that used for in utero electroporation.

Western Blot

Immunoblotting was performed to assess the presence of Unc5c and DCC across retinal development. HEK cells transfected with a Unc5c encoding plasmid and retinas from E13.5, E14.5, E15.5, E16.5, E18.5 and P2 were dissected and homogenized in lysis buffer (IGEPAL, cOmplete Mini EDTA-free protease inhibitor cocktail tablets (Sigma-Aldrich) in PBS 1x pH 7.4) and passed through a 1 mL insulin syringe with a 20G needle. Insoluble materials were incubated (30 min on ice) and pelleted by centrifugation at

16000 g for 15 min at 4°C. Protein concentration was assayed with protein assay dye reagent concentrate (BioRad) and samples were boiled in Laemmli's buffer (Sigma-Aldrich) and loaded in a gel according to standard protocols. Antibodies anti-β-actin (Sigma-Aldrich), anti-DCC (santa cruz), anti-Unc5c (Abcam) were used.

In situ hybridization and immunohistochemistry

E12.5 mouse embryos were extracted from the pregnant mother and fixed by immersion with 4% paraformaldehyde (PFA) in phosphate buffer saline (PBS, pH 7.4). Later stages embryos were intracardially perfused. Mouse and ferret heads, chicken embryos and zebrafish were post-fixed in the same fixative for 4 hours, and washed in PBS three times. The tissue was cryoprotected in 30% (w/v) sucrose in PBS and frozen in dry ice. Coronal sections (20 μm) were obtained with a cryostat (SLEE medical GmbH, Mainz) and stored at −20°C until used. *In situ* hybridization was performed according to reported methods [65]. A riboprobe to detect mouse and ferret Unc5c mRNA was synthetized using the following primers: 5′-CGGCCCCGAAGAATGGAGGC-3′ and 5′-GGTCAGCACAACGGGTCGGG-3′ from E14.5 mouse embryos cDNA. To detect zebrafish Unc5c mRNA we used a riboprobe cloned in a TOPO plasmid (Thermo Fisher Scientific) from zebrafish cDNA at 36-48 hpf using the following primers: 5′-GACACGCAGGACGCACTCAAG-3′ and 5′-CCCACAGGTCCAGGATCACTC-5. To detect chicken Unc5c mRNA a riboprobe, cloned in a TOPO plasmid, was synthetized using the following primers: 5′-CGGCCCCGAAGAATGGAGGC-3′ and 5′-GGTCAGCACAACGGGTCGGG-3′ from E7 chicken embryos.

Netrin1 was detected using a specific antisense riboprobe (gift of Prof. Orly Reiner (Weizmann Institute of Science, Rehovot, Israel)). For immunohistochemistry, antigen retrieval was performed before blocking and incubation with specific primary antibodies. The following primary antibodies were used: chicken anti-GFP (Aves Labs); rabbit anti-Zic2 (Herrera's lab [55, 56, 57, 58];), mouse anti-Tuj1 (Covance), rabbit anti-Tuj1 (Abcam), mouse anti-Brn3a (Chemicon), rabbit anti-calbindin (Swant), goat anti-ChAT (Millipore). For immunofluorescence detection, Alexa 488, Alexa 546, and Alexa 647 (Invitrogen, Molecular Probes) secondary antibodies were used. A DAPI staining solution was used to visualize nuclei (2 μg/mL).

Microscopy setup

Images were captured with an Olympus FV1000 confocal IX81 microscope/FV10-ASW software. Deconvoluted z stack images data acquired from tissue section by confocal microscopy were rendered in three dimensions using IMARIS 9.2.1 (Bitplane, Zurich, Switzerland). Chiasm images were acquired using a Leica MZ16F stereoscope.

Mathematical Model

We generated a simplified version of the self-organizing map (SOM) model originally described by [37, 38, 39]. The topography of the RGCs is represented by a regular square mesh of size 11 by 11 with the cells in the nodes. Those cells project to a postsynaptic layer of the same size, initially with synapses connecting all pre- and postsynaptic neurons in a non-specific manner. Thus, a representation of the location of the center of mass (CM) of the normalized weights, *w*, of the synaptic connections results in a mesh contained in a unit square (Figure S5). The model incorporates the role of the gradients of molecular guidance cues in establishing topography as a Gaussian function which sets the strength of the initial weights of the synaptic connections, based on the proximity between the presynaptic and postsynaptic neurons as,

where MG is the weight of the molecular gradient for each presynaptic neuron respect to all of the postsynaptic neurons, σmolecular determines the specificity or strength of the molecular gradient and rnoise introduces a level of normally distributed noise between connections, with mean 0 and standard deviation σnoise (Figure S5).

By stimulating the retina with different stimuli (see below), the synaptic weights change according to a Hebbian rule as follows:

where δwi is the change in the *i* synaptic weight *wi*, λ is the weight decay term, *t* is the time expressed in number of iterations, τ is the time constant for the λ decay, *X* and *Y* are the arrays holding the coordinates of retinal ganglion cells, *xw* and *yw* are the coordinates of the cell closest to the stimulus location which will receive the strongest effect, σ gives the extent to which the activation propagates to neighboring cells, and finally, *rs* is the vector containing the positions of the stimulus.

The different types of retinal activity used are shown in Figure S6. First, random patterns activate each retina with a sequence of independent uniform random stimuli. This stimulus class models the emergence of retinotopic topography in the absence of R-R projections. Second, locally coupled stimuli activate synchronously a small subset of RGCs retinotopically matched in both retinas for the first few iterations (100) of the model. Afterward, the activation of both retinas followed a sequence of independent uniform random stimuli as in the previous scenario. Last, binocularly matched retinal waves were triggered near the center of a retinal mesh and travel toward the periphery at the same speed in both retinas. The radius of the wave of stimulation increased at a rate of 2 10^{-}4 (per iteration), and stimuli were applied randomly around that radius following a Gaussian distribution of mean 0 and sigma 0.04. In each case, the final synaptic strength onto each postsynaptic neuron Ni is the normalized average of all of its weighted connections. By modeling the development of the right and left postsynaptic targets simultaneously, we

were able to study how the presence or absence of R-R connections, and the different patterns of coordinated activity that they afford, could affect the establishment of bilaterally congruent retinotopic maps in visual structures receiving direct retinal inputs (Figure S6). The model returns correct results, i.e., perfectly matched left and right retinotopic layouts, only when the unfolding and orientation of both postsynaptic sheets is the same as the orientation in the presynaptic RGC layer. On the other hand, incorrect results could come in the form of different orientations between pre and postsynaptic sheets or incorrect unfolding, which produce disruptions on the topographic map. Model parameters and code are provided in Table S1 of the accompanying Supplemental Information and Sofware and Algorithms in the STAR Methods section.

Quantification and Statistical Analysis

To quantify retinal projections at the optic chiasm level, squared regions of interest (ROI) were superimposed on the width of the optic nerve close to the electroporated retina, the opposite optic nerve, the contralateral optic tract and the ipsilateral optic tract in regions proximal to the chiasm. Fluorescence intensity within each ROI was measured using ImageJ Software and normalized with respect to the background. The percentage of fluorescence intensity in each ROI relative to the optic nerve ROI on the electroporated side was then represented in a graph. Statistical analyses were performed when appropriate, error bars indicate ± SEM (*$p < 0.05$, **$p < 0.01$, ***$p < 0.001$, Student's unpaired t test).

Acknowledgments

We thank D. Baeza and M. Herrera for mouse breeding, genotyping and E. Llorens and J. Mullet for technical help in experiments involving ferrets. We also thank A. Barco for discussion and comments on the manuscript. The laboratory of E.H. is funded with the following grants: BFU2016-77605 from the National Grant Research Program; PROMETEO Program [2016/026] from Generalitat Valenciana; PCIN2015-192-C02-02 from ERA-Net Program; and ERC-282329 from the European Research Council. Work in the laboratory of L.M.M. and S.S. was supported by the National Grant Research Program (grant BFU2014-58776), co-financed by the European Regional Development Fund (ERDF). V.M.-B. holds a postdoctoral contract from the Generalitat Valenciana. A.J.V. is the recipient of a FPI fellowship from the National Grant Research Program. We also acknowledge the financial support received from the "Severo Ochoa" Program for Centers of Excellence in R&D (SEV-2013-0317). A.K. was supported by the Canadian Institutes of Health Research operating grants MOP-77556 and MOP-97758, as well as Brain Canada, Canadian Foundation for Innovation, and the W. Garfield Weston Foundation.

Author Contributions

V.M.B. performed and analyzed most of the experiments. C.V. made the initial observations on the expression of Unc5c in the developing retina and performed some gain-of-function experiments. Y.C. has performed in utero electroporations and axon tracer injections assisted by S.N. R.D. and A.K. provided the Unc5c mice. C.d.J. and V.B. provided and performed in situ hybridization and immunohistochemistry in ferret embryos; A.J.V., S.S., and L.M.M. generated the computation model. E.H. wrote the original draft and conceived and supervised the study. A.K., V.B., and L.M.M. revised subsequent versions of the manuscript. L.E. helped with experimental design and revisited critically the manuscript for important intellectual content.

Declaration of Interests

The authors declare no competing interests.

FIGURES

Figure 1. Characterization of Retino-retinal Cells in Mice

(A) Labeled axons from embryos monocularly electroporated with EGFP-encoding plasmids at E13.5 were analyzed at E16.5 or E18.5.

(B–D) At E16.5, EGFP-labeled axons are present within the contralateral optic nerve (cON) (arrowheads, B) and by E18.5 have reached the contralateral optic disc (asterisk, C and D).

(E) Targeted cells (green dots) in retinas electroporated at E13.5 (white flat-mounted retinas) and tracings of EGFP-labeled axons in the contralateral retina (gray flat-mounted retinas) at E18.5–P4.

(F) Mean (± SEM) number of R-R axons in E18.5–P4 retinas after electroporation of the opposite eye at E13.5. These numbers do not represent the total number of R-R neurons, as not all cells are targeted by electroporation.

(G) Diagram of a P2 retina containing R-R axons labeled from the opposite eye. (G'–G''') Image of boxed area in (G) showing an EGFP R-R axon and starburst amacrine cells labeled with ChAT antibodies.

(H) 3D reconstruction of z-projection with a z-step of 1.5 μm captured from boxed region in (G) showing ChAT+ cells embracing the axon terminal (red arrows).

(I) Middle: diagram of monocular injection of CTB. Left: retinal sections of injected P3 and P30 mice injected with CTB 2 days earlier are shown. Right: retinal sections of contralateral retinas from same animals are shown. Note two retrogradely labeled cells in the RGC layer at P3.

(J) Top: diagrams of whole-mount retinas retrogradely labeled with CTB at P3, P5, or P30. Boxed region of P3 retina shows retrogradely labeled cells (red) combined with antibody staining for Brn3a or Islet1/2 (green). Graph shows mean (± SEM) number of labeled cells/retina quadrant. At perinatal stages, most CTB-positive cells are in the ventral quadrants (ventronasal [VN] and ventrotemporal [VT]). At P30, no CTB cells were found.

(K) CTB-488 (green) and CTB-647 (red) were injected in the retina and the ipsilateral superior colliculus (SC), respectively, of newborn mice. The opposite whole-mounted retina was analyzed 2 days later. Right: images from the boxed area show a representative CTB-488 cell negative for CTB-647.

Error bars indicate ± SEM.

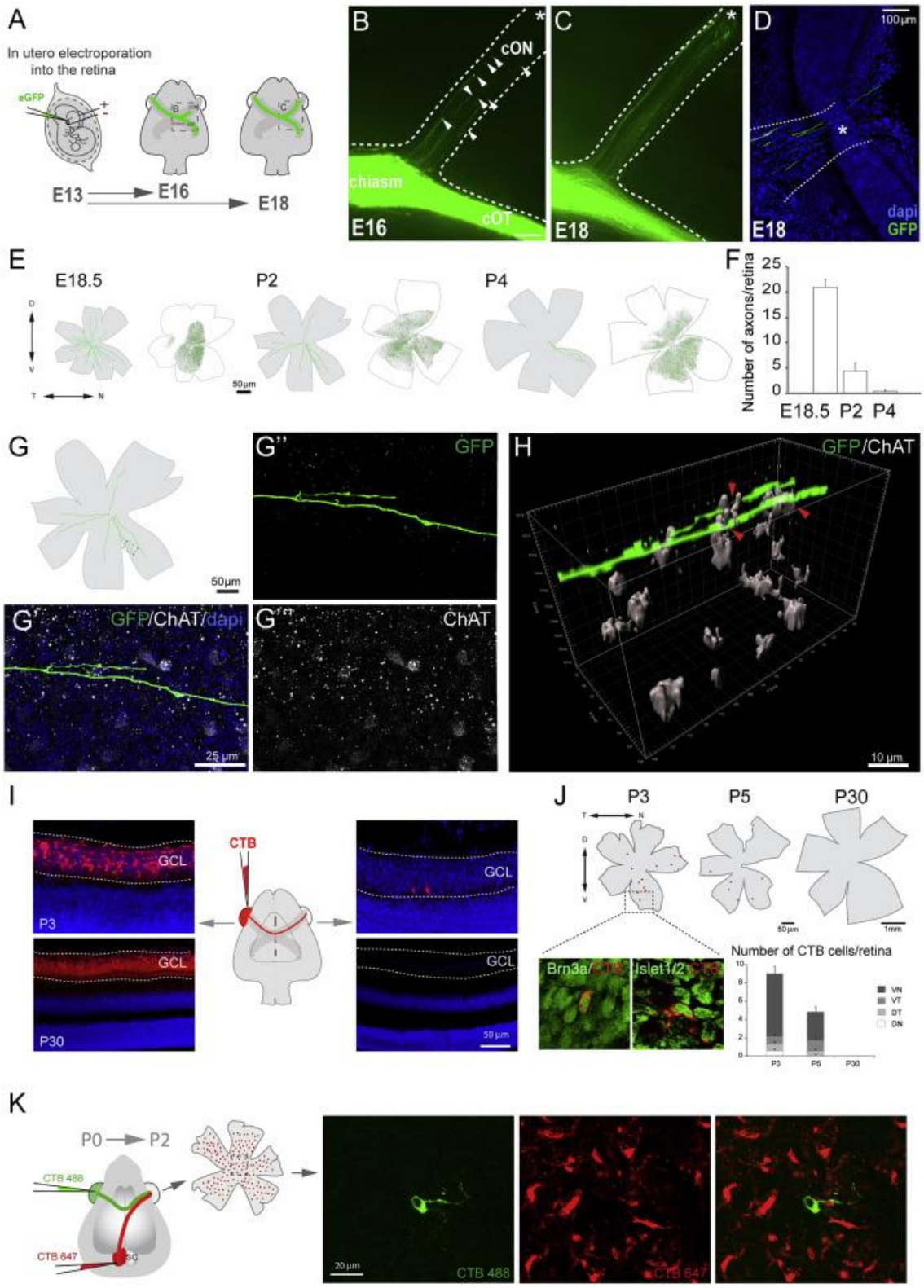
A
In utero electroporation into the retina
eGFP
E13
E16
E18
B
cON
chiasm
cOT
E16
C
E18
D
100 µm
dapi
GFP
E18
E
E18.5
P2
P4
50µm
F
Number of axons/retina
25
20
15
10
5
0
E18.5 P2 P4
G
G''
GFP
50µm
G'
GFP/ChAT/dapi
25 µm
G'''
ChAT
H
GFP/ChAT
10 µm
I
CTB
GCL
P3
GCL
P30
GCL
GCL
50 µm
J
P3
P5
P30
50µm
1mm
Brn3a/CTB
Islet1/2 CTB
Number of CTB cells/retina
VN
VT
DT
DN
P3
P5
P30
K
P0 P2
CTB 488
CTB 647
sc
20 µm
CTB 488
CTB 647

Figure 2. Netrin1 Is Expressed at the Developing Ventral Chiasm

(A–D) Horizontal (A–B'') and coronal (C–D'') serial sections of E12.5 (A–A'' and C–C'') and E14.5 (B–B'' and D–D'') embryos at the level of the optic chiasm region stained by ISH for Netrin1 (red) combined with immunofluorescence for Tuj1 (green) to label retinal axons.

(E) Diagram summarizing the spatiotemporal expression of Netrin1 at the optic chiasm (red). RGC axons projecting to the brain (light green) or to the opposite optic nerve (dark green) are also represented. At E12.5, when RGC axons have not yet arrived at the chiasm, Netrin1 mRNA is expressed predominately in two patches on both sides of the ventral diencephalon. At E14.5, when axons are at the chiasm region, Netrin1 mRNA surrounds the optic tracts.

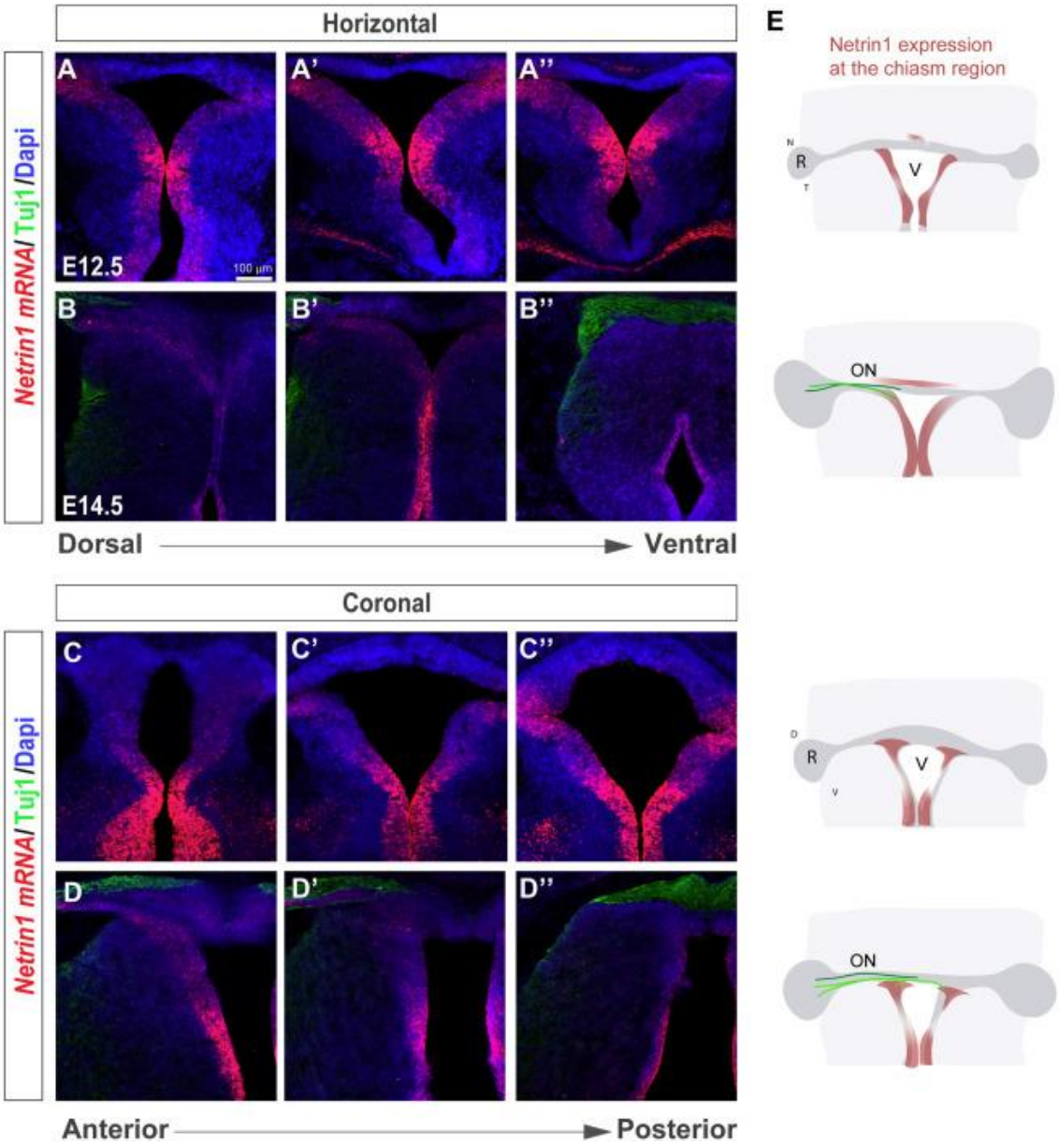

Figure 3. Unc5c Is Expressed in Ventral-Central Retina

(A–E) In situ hybridization (ISH) for Unc5c in coronal retinal sections at E13.5 (A), E14.5 (B), E16.5 (C), E18.5 (D), and P2 (E) mice.

(F) Immunoblot detection of Unc5c and Dcc in control (CT) HEK cells and HEK transfected with Unc5c encoding plasmids and in E13.5–P2 retinal lysates. β-actin was used as a loading control. Graphs show levels of Unc5c and Dcc normalized to actin levels. Peak of Unc5c expression is at E14.5.

(G) Representative images of Unc5c expression (red) in coronal (upper) and horizontal (bottom) retinal sections from E16.5 mouse embryos stained with DAPI (gray).

(H) Mean (± SEM) fluorescent intensity of Unc5c in each quadrant of E16.5 retinas.

(I) Diagram of a whole-mounted retina summarizing the expression of Unc5c (red).

Error bars indicate ± SEM.

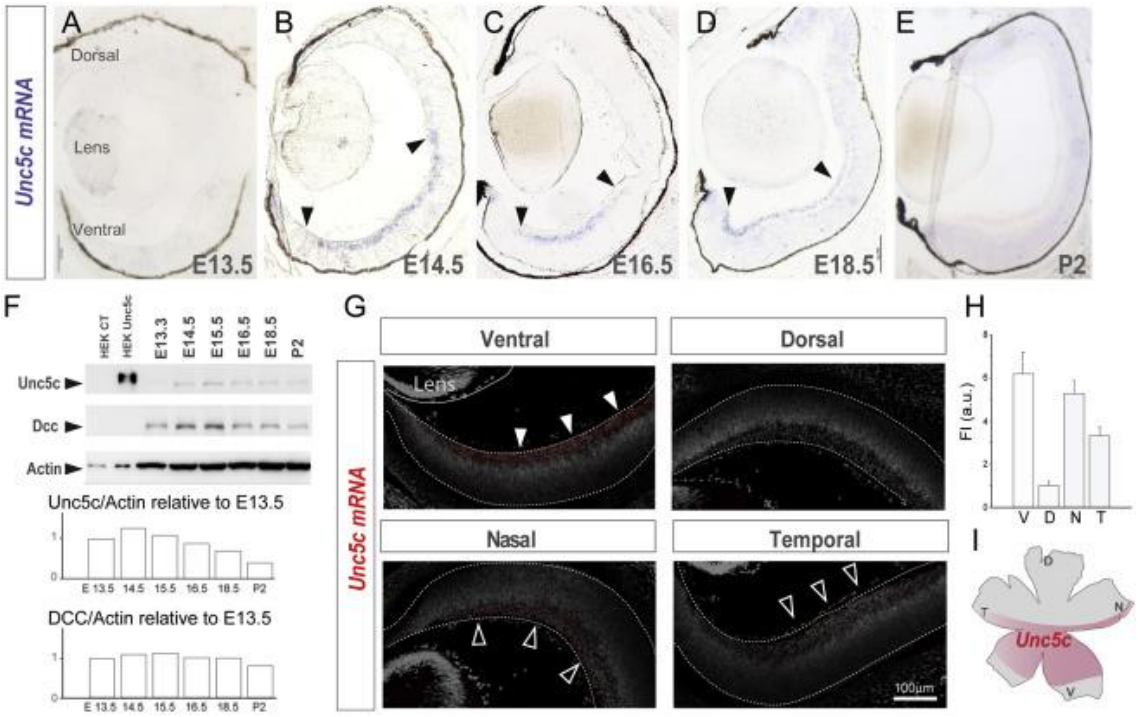

Figure 4. Unc5c Is Necessary for Establishment of the Retino-retinal Projection

(A–C) DiI was placed into one eye and the labeled axons viewed at the chiasm (A).

(B and C) DiI-labeled E17.5 Unc5c+/+ and Unc5c−/− embryos. The fluorescence intensity in the contralateral optic nerve of the Unc5c−/− embryo is decreased compared with the control littermate (arrowhead).

(B' and C') Higher magnification of the boxed regions in (B) and (C).

(D) Mean (± SEM) normalized fluorescence intensity (FI) in the contralateral optic nerve of E17.5 Unc5c−/− and wild-type embryos monocularly injected with DiI.

(E–G) DiI was applied to one optic nerve and the opposite retina analyzed (E).

(F and G) Whole-mounted retinas from E17.5 Unc5c+/+ and Unc5c−/− embryos retrogradely labeled with DiI. Inserts: tracings of the labeled cells are shown.

(H) Mean (± SEM) number of retrogradely labeled cells in each quadrant of E17.5 wild-type and Unc5c mutant retinas.

(I and J) E16.5 embryos electroporated at E13.5 with control or Unc5c shRNAs plus EGFP-encoding plasmids. Insert: corresponding whole-mounted electroporated retina is shown. EGFP-positive axons were present in the contralateral optic nerve of control (I and I'), but not Unc5c shRNA electroporated, embryos (open arrowhead, J and J'). Unc5c electroporated embryos also displayed an ectopic ipsilateral projection (orange arrowhead).

(K) Mean (± SEM) normalized fluorescence intensity in the contralateral optic nerve and ipsilateral optic tract of E16.5 embryos electroporated at E13.5 with Unc5c shRNA or control shRNA.

cON, contralateral optic nerve c; cOT, contralateral optic tract; D, dorsal; iON, ipsilateral optic nerve; iOT, ipsilateral optic tract; N, nasal; T, temporal; V, ventral. Error bars indicate ± SEM. (**$p < 0.01$, ***$p < 0.001$, Student's unpaired t test).

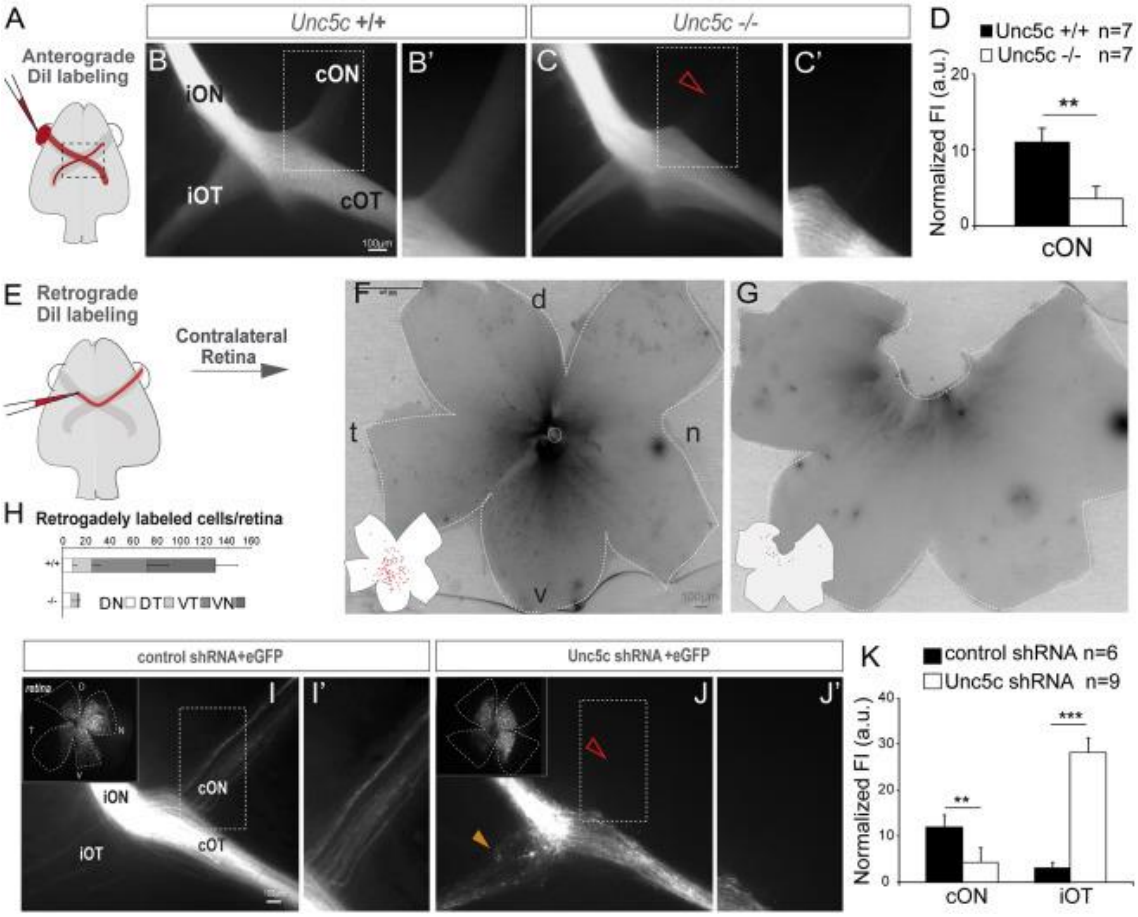
A
Anterograde
DiI labeling
Unc5c +/+
Unc5c -/-
B
iON
cON
iOT
cOT
B'
C
C'
D
Unc5c +/+ n=7
Unc5c -/- n=7
Normalized FI (a.u.)
cON
E
Retrograde
DiI labeling
Contralateral
Retina
F
d
t
n
v
G
H
Retrogadely labeled cells/retina
DN DT VT VN
control shRNA+eGFP
Unc5c shRNA +eGFP
I
I'
J
J'
K
control shRNA n=6
Unc5c shRNA n=9
Normalized FI (a.u.)
cON
iOT

Figure 5. Ipsilateral RGCs Do Not Express Unc5c

(A–A'') ISH for Unc5c (red) in an E16.5 retinal section shown as a single channel (A') or in combination with immunohistochemistry for Zic2 (green, A and A''). Red arrowheads indicate peripheral limit of Unc5c expression, green arrowheads central limit of Zic2 expression, and white arrowhead the region where the neural retina meets the ciliary margin zone (CMZ).

(B) ISH for Unc5c (red) combined with immunohistochemistry for Zic2 in Zic2 mutant embryos. Red arrowhead marks the most peripheral limit of Unc5c mRNA expression and white arrowhead the region where the neural retina meets the CMZ.

(C and D) ISH for Unc5c (red) in retinal sections electroporated with EGFP-encoding (C) or Zic2/EGFP-encoding (D) plasmids. Unc5c mRNA expression is reduced after ectopic expression of Zic2.

(E and F) Optic chiasms from E16.5 embryos electroporated with plasmids encoding Zic2/EGFP (F) or EGFP alone (E). Red arrowhead indicates the ectopic ipsilateral projection in embryos electroporated with Zic2 and empty arrowhead the reduced number of EGFP-labeled axons in the contralateral optic nerve of Zic2 electroporated embryos compared to the control.

(G) Mean (± SEM) normalized fluorescence intensity in the contralateral optic nerve and the ipsilateral optic tract of E16.5 embryos electroporated with plasmids encoding Zic2/EGFP or EGFP alone.

Error bars indicate ± SEM. (**$p < 0.01$, ***$p < 0.001$, Student's unpaired t test).

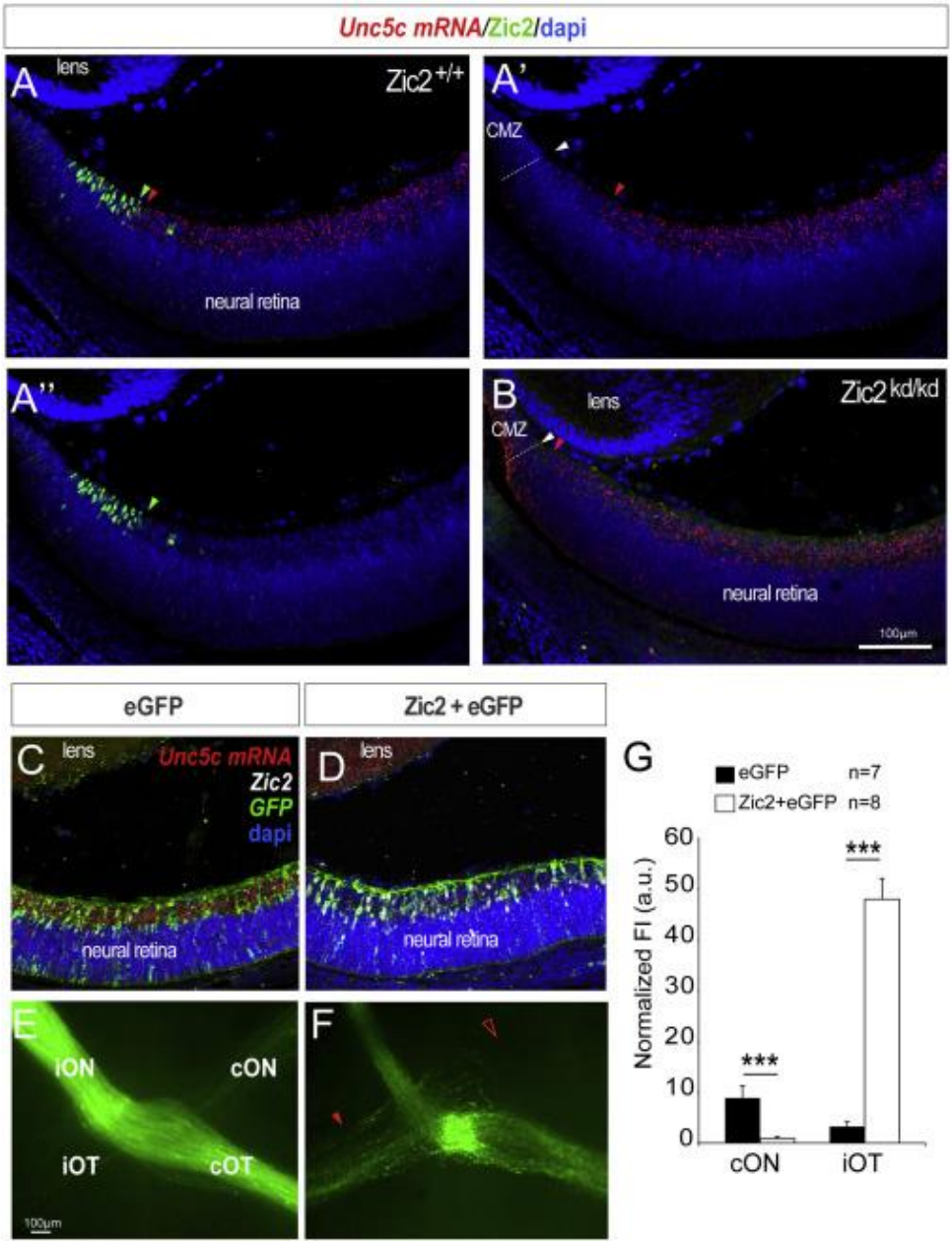
Unc5c mRNA/Zic2/dapi
A
lens
Zic2+/+
neural retina
A'
CMZ
A''
B
lens
CMZ
Zic2 kd/kd
neural retina
100μm
eGFP
Zic2 + eGFP
C
lens
Unc5c mRNA
Zic2
GFP
dapi
neural retina
D
lens
neural retina
E
lON
cON
lOT
cOT
100μm
F
G
eGFP n=7
Zic2+eGFP n=8
Normalized FI (a.u.)
60
50
40
30
20
10
0
***
***
cON
lOT

Figure 6. Unc5c Is Sufficient to Guide RGC Axons into the Opposite Optic Nerve

(A) EGFP or Unc5c/GFP-encoding plasmids were electroporated into one eye of E13.5 embryos and axons growing into the opposite optic nerve analyzed at E16.5 or E18.5.

(B–E) E16.5 (B and C) and E18.5 (D and E) embryos electroporated with Unc5c-encoding plasmids (C and E) display an increase in the number of R-R axons (arrowheads) compared to age-matched controls (B and D).

(F) Mean (± SEM) normalized fluorescence intensity in the cON of E16.5 embryos after electroporation of EGFP or Unc5c/GFP-encoding plasmids.

Error bars indicate ± SEM. (***p < 0.001, Student's unpaired t test).

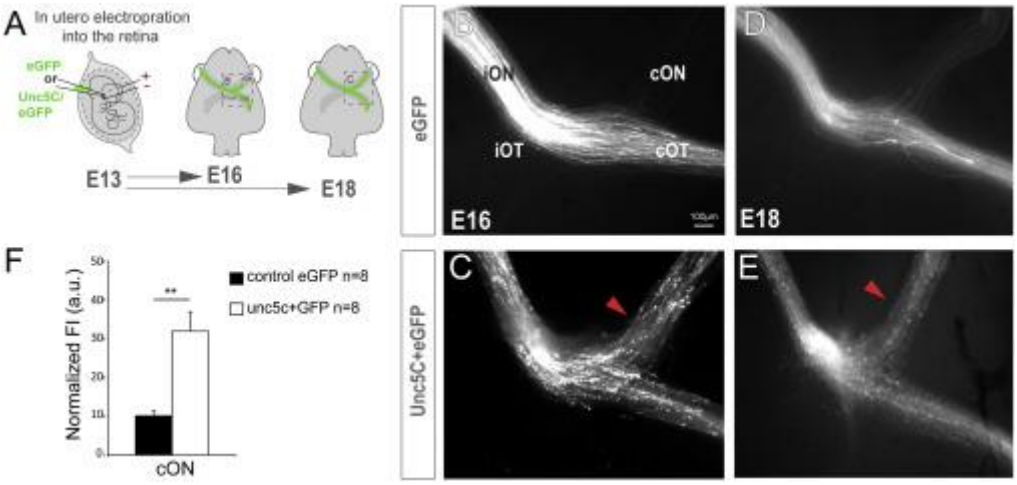

Figure 7. The R-R Connection through Evolution

(A) Working model of the function of R-R in different species. In species where the size of the tectum and retina is similar, the establishment of bilaterally congruent maps may rely on point-to-point molecular tagging mechanisms.

(B) In species where the size of the visual target is larger than the retina, map topography relies both on a molecular tagging mechanism and a later refinement process, dependent on waves of spontaneous activity. The presence of an R-R connection may enable the synchronization of retinal waves from each eye, driving symmetrical refinement in both hemispheres.

(C and D) ISH for Unc5c in horizontal (C) and coronal (D) sections of the zebrafish retina revealed no expression of Unc5c.

(E and E') A 36- to 48-h post fertilization (hpf) zebrafish embryo stained with DAPI and monocularly injected with DiI shows no retinal axons entering into the contralateral retina.

(F and G) ISH for Unc5c mRNA in horizontal (F) and coronal (G) sections from P0 ferret retinas. Unc5c mRNA is expressed in the RGC layer of ventral and temporal retina.

(H) Schematic diagram representing monocular DiI anterograde labeling. Optic chiasm of a DiI-labeled P0 ferret is shown. White arrowhead points to the axons into the contralateral optic nerve.

(I) Schematic diagram representing retrograde CTB-labeling. CTB injection was performed at P1, and labeled RGCs were visualized by red fluorescence in whole-mount retinas 1 day later.

(J–J'') ISH for Unc5c mRNA and immunohistochemistry for Zic2 in a coronal retinal section from an E34.5 ferret embryo counterstained with DAPI. Red arrowheads mark the most peripheral limit of Unc5c mRNA expression and green arrowheads the central limit of Zic2 expression. Zic2 and Unc5c mRNA expression is mostly complementary.

CTB, cholera toxin subunit B-Alexa594; RGCl, retinal ganglion cell layer. See also Figures S5, S6, and S7 and Table S1.

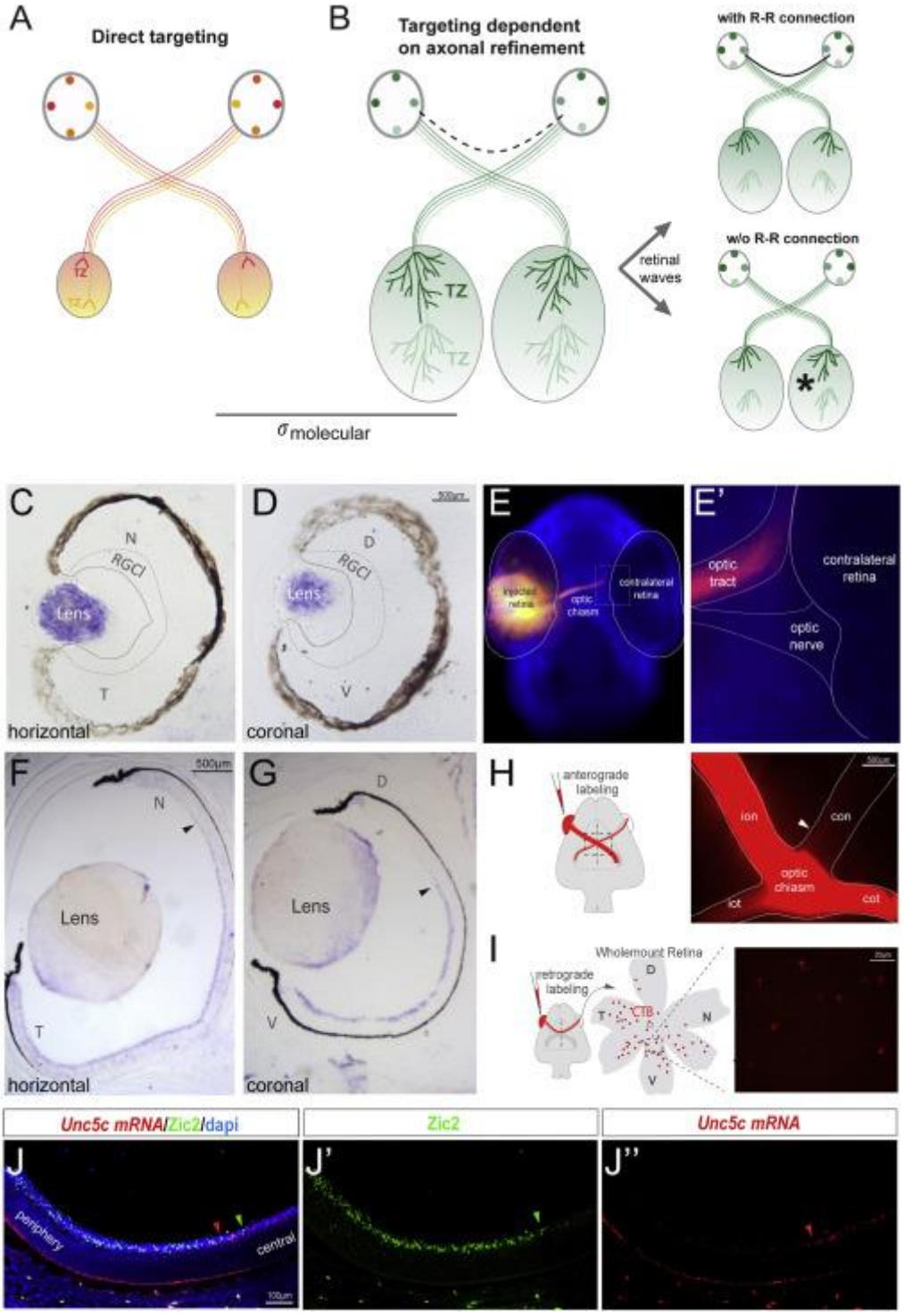
A
Direct targeting
B
Targeting dependent
on axonal refinement
with R-R connection
w/o R-R connection
retinal
waves
TZ
σ molecular
C
N
RGCl
Lens
T
horizontal
D
D
RGCl
Lens
V
coronal
E
injected retina
optic chiasm
contralateral retina
E'
optic tract
contralateral retina
optic nerve
F
500μm
N
Lens
T
horizontal
G
D
Lens
V
coronal
H
anterograde labeling
ion
con
optic chiasm
iot
cot
I
Wholemount Retina
retrograde labeling
D
T
CTB
N
V
Unc5c mRNA/Zic2/dapi
Zic2
Unc5c mRNA
J
periphery
central
J'
J''

References

1. J. Cang, C.M. Niell, X. Liu, C. Pfeiffenberger, D.A. Feldheim, M.P. Stryker. Selective disruption of one Cartesian axis of cortical maps and receptive fields by deficiency in ephrin-As and structured activity. Neuron, 57 (2008), pp. 511-523
2. P. Godement, J. Salaün, M. Imbert. Prenatal and postnatal development of retinogeniculate and retinocollicular projections in the mouse. J. Comp. Neurol., 230 (1984), pp. 552-575
3. G. Lemke, M. Reber. Retinotectal mapping: new insights from molecular genetics. Annu. Rev. Cell Dev. Biol., 21 (2005), pp. 551-580
4. H. Nakamura, D.D. O'Leary. Inaccuracies in initial growth and arborization of chick retinotectal axons followed by course corrections and axon remodeling to develop topographic order. J. Neurosci., 9 (1989), pp. 3776-3795
5. A.D. Huberman, M.B. Feller, B. Chapman. Mechanisms underlying development of visual maps and receptive fields. Annu. Rev. Neurosci., 31 (2008), pp. 479-509
6. J.B. Ackman, T.J. Burbridge, M.C. Crair. Retinal waves coordinate patterned activity throughout the developing visual system. Nature, 490 (2012), pp. 219-225
7. J.B. Ackman, M.C. Crair. Role of emergent neural activity in visual map development. Curr. Opin. Neurobiol., 24 (2014), pp. 166-175
8. L. Erskine, E. Herrera. Connecting the retina to the brain. ASN Neuro, 6 (2014),
9. R.C. Bohn, D.J. Stelzner. The aberrant retino-retinal projection during optic nerve regeneration in the frog. II. Anterograde labeling with horseradish peroxidase. J. Comp. Neurol., 196 (1981), pp. 621-632
10. C.R. Braekevelt, L.D. Beazley, S.A. Dunlop, J.E. Darby. Numbers of axons in the optic nerve and of retinal ganglion cells during development in the marsupial Setonix brachyurus. Brain Res., 390 (1986), pp. 117-125
11. S.M. Bunt, R.D. Lund. Development of a transient retino-retinal pathway in hooded and albino rats. Brain Res., 211 (1981), pp. 399-404
12. M.F. Humphrey, L.D. Beazley. Retinal ganglion cell death during optic nerve regeneration in the frog Hyla moorei. J. Comp. Neurol., 236 (1985), pp. 382-402
13. S.C. McLoon, R.D. Lund. Transient retinofugal pathways in the developing chick. Exp. Brain Res., 45 (1982), pp. 277-284
14. M. Müller, H. Holländer. A small population of retinal ganglion cells projecting to the retina of the other eye. An experimental study in the rat and the rabbit. Exp. Brain Res., 71 (1988), pp. 611-617
15. F.M. Nadal-Nicolás, F.J. Valiente-Soriano, M. Salinas-Navarro, M. Jiménez-López, M. Vidal-Sanz, M. Agudo-Barriuso. Retino-retinal projection in juvenile and young adult rats and mice. Exp. Eye Res., 134 (2015), pp. 47-52
16. M. Tennant, S.R. Bruce, L.D. Beazley. Survival of ganglion cells which form the retino-retinal projection during optic nerve regeneration in the frog. Vis. Neurosci., 10 (1993), pp. 681-686
17. S. Thanos. Genesis, neurotrophin responsiveness, and apoptosis of a pronounced direct connection between the two eyes of the chick embryo: a natural error or a meaningful developmental event? J. Neurosci., 19 (1999), pp. 3900-3917
18. P. Tóth, C. Straznicky. Retino-retinal projections in three anuran species. Neurosci. Lett., 104 (1989), pp. 43-47
19. X. Tang, R. Tzekov, C.L. Passaglia. Retinal cross talk in the mammalian visual system. J. Neurophysiol., 115 (2016), pp. 3018-3029
20. S.W. Failor, A. Ng, H.J. Cheng. Monocular enucleation alters retinal waves in the surviving eye. Neural Dev., 13 (2018), p. 4
21. E. Herrera, L. Brown, J. Aruga, R.A. Rachel, G. Dolen, K. Mikoshiba, S. Brown, C.A. Mason. Zic2 patterns binocular vision by specifying the uncrossed retinal projection. Cell, 114 (2003), pp. 545-557
22. D.F. Aschauer, S. Kreuz, S. Rumpel. Analysis of transduction efficiency, tropism and axonal transport of AAV serotypes 1, 2, 5, 6, 8 and 9 in the mouse brain. PLoS ONE, 8 (2013), p. e76310

23. T. Pratt, C.D. Conway, N.M. Tian, D.J. Price, J.O. Mason. Heparan sulphation patterns generated by specific heparan sulfotransferase enzymes direct distinct aspects of retinal axon guidance at the optic chiasm. J. Neurosci., 26 (2006), pp. 6911-6923
24. T. Pratt, N.M. Tian, T.I. Simpson, J.O. Mason, D.J. Price. The winged helix transcription factor Foxg1 facilitates retinal ganglion cell axon crossing of the ventral midline in the mouse. Development, 131 (2004), pp. 3773-3784
25. M.S. Deiner, D.W. Sretavan. Altered midline axon pathways and ectopic neurons in the developing hypothalamus of netrin-1- and DCC-deficient mice. J. Neurosci., 19 (1999), pp. 9900-9912.
26. S.L. Ackerman, L.P. Kozak, S.A. Przyborski, L.A. Rund, B.B. Boyer, B.B. Knowles. The mouse rostral cerebellar malformation gene encodes an UNC-5-like protein. Nature, 386 (1997), pp. 838-842
27. M. Hamelin, Y. Zhou, M.W. Su, I.M. Scott, J.G. Culotti. Expression of the UNC-5 guidance receptor in the touch neurons of C. elegans steers their axons dorsally. Nature, 364 (1993), pp. 327-330
28. K. Hong, L. Hinck, M. Nishiyama, M.M. Poo, M. Tessier-Lavigne, E. Stein. A ligand-gated association between cytoplasmic domains of UNC5 and DCC family receptors converts netrin-induced growth cone attraction to repulsion. Cell, 97 (1999), pp. 927-941
29. E.D. Leonardo, L. Hinck, M. Masu, K. Keino-Masu, S.L. Ackerman, M. Tessier-Lavigne. Vertebrate homologues of C. elegans UNC-5 are candidate netrin receptors. Nature, 386 (1997), pp. 833-838
30. C. Leung-Hagesteijn, A.M. Spence, B.D. Stern, Y. Zhou, M.W. Su, E.M. Hedgecock, J.G. Culotti. UNC-5, a transmembrane protein with immunoglobulin and thrombospondin type 1 domains, guides cell and pioneer axon migrations in C. elegans. Cell, 71 (1992), pp. 289-299
31. J. Vielmetter, J.F. Kayyem, J.M. Roman, W.J. Dreyer. Neogenin, an avian cell surface protein expressed during terminal neuronal differentiation, is closely related to the human tumor suppressor molecule deleted in colorectal cancer. J. Cell Biol., 127 (1994), pp. 2009-2020
32. S.A. Colamarino, M. Tessier-Lavigne. The axonal chemoattractant netrin-1 is also a chemorepellent for trochlear motor axons. Cell, 81 (1995), pp. 621-629

A. Fazeli, S.L. Dickinson, M.L. Hermiston, R.V. Tighe, R.G. Steen, C.G. Small, E.T. Stoeckli, K. Keino-Masu, M. Masu, H. Rayburn, et al. Phenotype of mice lacking functional Deleted in colorectal cancer (Dcc) gene. Nature, 386 (1997), pp. 796-804

33. E.M. Hedgecock, J.G. Culotti, D.H. Hall. The unc-5, unc-6, and unc-40 genes guide circumferential migrations of pioneer axons and mesodermal cells on the epidermis in C. elegans. Neuron, 4 (1990), pp. 61-85
34. D. Engelkamp. Cloning of three mouse Unc5 genes and their expression patterns at mid-gestation. Mech. Dev., 118 (2002), pp. 191-197
35. M.S. Deiner, T.E. Kennedy, A. Fazeli, T. Serafini, M. Tessier-Lavigne, D.W. Sretavan. Netrin-1 and DCC mediate axon guidance locally at the optic disc: loss of function leads to optic nerve hypoplasia. Neuron, 19 (1997), pp. 575-589
36. T. Kohonen. Self-organized formation of topologically correct feature maps. Biol. Cybern., 43 (1982), pp. 59-69
37. T. Kohonen. Essentials of the self-organizing map. Neural Netw., 37 (2013), pp. 52-65
38. D.J. Willshaw, C. von der Malsburg, H.C. Longuet-Higgins
39. How patterned neural connections can be set up by self-organization. Proc. R. Soc. Lond. B. Biol. Sci., 194 (1976), pp. 431-445
40. T. McLaughlin, D.D. O'Leary. Molecular gradients and development of retinotopic maps. Annu. Rev. Neurosci., 28 (2005), pp. 327-355
41. R.S. Erzurumlu, P.C. Kind. Neural activity: sculptor of 'barrels' in the neocortex. Trends Neurosci., 24 (2001), pp. 589-595

42. C.S. Goodman, C.J. Shatz. Developmental mechanisms that generate precise patterns of neuronal connectivity. Cell, 72 (Suppl) (1993), pp. 77-98
43. K.S. Dingwell, C.E. Holt, W.A. Harris. The multiple decisions made by growth cones of RGCs as they navigate from the retina to the tectum in Xenopus embryos. J. Neurobiol., 44 (2000), pp. 246-259
44. S. Thakar, G. Chenaux, M. Henkemeyer. Critical roles for EphB and ephrin-B bidirectional signalling in retinocollicular mapping. Nat. Commun., 2 (2011), p. 431
45. S. Poliak, D. Morales, L.P. Croteau, D. Krawchuk, E. Palmesino, S. Morton, J.F. Cloutier, F. Charron, M.B. Dalva, S.L. Ackerman, et al.. Synergistic integration of Netrin and ephrin axon guidance signals by spinal motor neurons. eLife, 4 (2015), p. e10841
46. S.E. Williams, C.A. Mason, E. Herrera. The optic chiasm as a midline choice point. Curr. Opin. Neurobiol., 14 (2004), pp. 51-60
47. J.A. Demas, H. Payne, H.T. Cline. Vision drives correlated activity without patterned spontaneous activity in developing Xenopus retina. Dev. Neurobiol., 72 (2012), pp. 537-546
48. R.O. Wong. Retinal waves and visual system development. Annu. Rev. Neurosci., 22 (1999), pp. 29-47
49. A.H. Leighton, C. Lohmann. The wiring of developing sensory circuits-from patterned spontaneous activity to synaptic plasticity mechanisms. Front. Neural Circuits, 10 (2016), p. 71
50. D.A. Arroyo, M.B. Feller. Spatiotemporal features of retinal waves instruct the wiring of the visual circuitry. Front. Neural Circuits, 10 (2016), p. 54
51. J.E. Bennett, W. Bair. Refinement and pattern formation in neural circuits by the interaction of traveling waves with spike-timing dependent plasticity. PLoS Comput. Biol., 11 (2015), p. e1004422
52. P.Y. Burgi, N.M. Grzywacz. Model for the pharmacological basis of spontaneous synchronous activity in developing retinas. J. Neurosci., 14 (1994), pp. 7426-7439
53. R.W. Zhang, X.Q. Li, K. Kawakami, J.L. Du.Stereotyped initiation of retinal waves by bipolar cells via presynaptic NMDA autoreceptors. Nat. Commun., 7 (2016), p. 12650
54. D.L. Adams, J.C. Horton. Capricious expression of cortical columns in the primate brain. Nat. Neurosci., 6 (2003), pp. 113-114
55. F. Marcucci, V. Murcia-Belmonte, Q. Wang, Y. Coca, S. Ferreiro-Galve, T. Kuwajima, S. Khalid, M.E. Ross, C. Mason, E. Herrera. The ciliary margin zone of the mammalian retina generates retinal ganglion cells. Cell Rep., 17 (2016), pp. 3153-3164
56. V. Murcia-Belmonte, G. Expósito, E. Herrera. Time-lapse imaging and cell tracking of migrating cells in slices and flattened telencephalic vesicles. Curr. Protoc. Neurosci., 79 (2017), pp. 3.31.1-3.31.12
57. B. Murillo, N. Ruiz-Reig, M. Herrera, A. Fairén, E. Herrera. Zic2 controls the migration of specific neuronal populations in the developing forebrain. J. Neurosci., 35 (2015), pp. 11266-11280
58. M.C. Tiveron, C. Beclin, S. Murgan, S. Wild, A. Angelova, J. Marc, N. Coré, A. de Chevigny, E. Herrera, A. Bosio, et al.. Zic-proteins are repressors of dopaminergic forebrain fate in mice and C. elegans. J. Neurosci., 37 (2017), pp. 10611-10623
59. C. Garcia-Frigola, M.I. Carreres, C. Vegar, E. Herrera. Gene delivery into mouse retinal ganglion cells by in utero electroporation. BMC Dev. Biol., 7 (2007), p. 103
60. V. Hamburger, H.L. Hamilton. A series of normal stages in the development of the chick embryo. J. Morphol., 88 (1951), pp. 49-92
61. C.B. Kimmel, W.W. Ballard, S.R. Kimmel, B. Ullmann, T.F. Schilling. Stages of embryonic development of the zebrafish. Dev. Dyn., 203 (1995), pp. 253-310

62. M. Scandaglia, E. Benito, C. Morenilla-Palao, A. Fiorenza, B. Del Blanco, Y. Coca, E. Herrera, A. Barco. Fine-tuned SRF activity controls asymmetrical neuronal outgrowth: implications for cortical migration, neural tissue lamination and circuit assembly. Sci. Rep., 5 (2015), p. 17470
63. A.S. Plump, L. Erskine, C. Sabatier, K. Brose, C.J. Epstein, C.S. Goodman, C.A. Mason, M. Tessier-Lavigne. Slit1 and Slit2 cooperate to prevent premature midline crossing of retinal axons in the mouse visual system. Neuron, 33 (2002), pp. 219-232
64. Rebsam, T.J. Petros, C.A. Mason. Switching retinogeniculate axon laterality leads to normal targeting but abnormal eye-specific segregation that is activity dependent. J. Neurosci., 29 (2009), pp. 14855-14863
65. N. Schaeren-Wiemers, A. Gerfin-Moser. A single protocol to detect transcripts of various types and expression levels in neural tissue and cultured cells: in situ hybridization using digoxigenin-labelled cRNA probes. Histochemistry, 100 (1993), pp. 431-440